AD_____

Award Number: DAMD17-02-1-0039

TITLE: Investigation of SNARE-Mediated Membrane Trafficking in Prostate Cancer Cells

PRINCIPAL INVESTIGATOR: Xin Li, M.D., Ph.D.

CONTRACTING ORGANIZATION: The Cleveland Clinic Foundation
Cleveland, OH 44195

REPORT DATE: November 2003

TYPE OF REPORT: Annual Summary

PREPARED FOR: U.S. Army Medical Research and Materiel Command
Fort Detrick, Maryland 21702-5012

REPORT DOCUMENTATION PAGE

Form Approved
OMB No. 074-0188

1. AGENCY USE ONLY (Leave blank)	2. REPORT DATE	3. REPORT TYPE AND DATES COVERED
	November 2003	Annual Summary (1 Feb 2002 - 31 Jan 2004)

4. TITLE AND SUBTITLE

Investigation of SNARE-Mediated Membrane Trafficking in Prostate Cancer Cells

5. FUNDING NUMBERS

DAMD17-02-1-0039

6. AUTHOR(S)

Xin Li, M.D., Ph.D.

7. PERFORMING ORGANIZATION NAME(S) AND ADDRESS(ES)

The Cleveland Clinic Foundation
Cleveland, OH 44195

E-Mail: lix2@ccf.org

8. PERFORMING ORGANIZATION REPORT NUMBER

9. SPONSORING / MONITORING AGENCY NAME(S) AND ADDRESS(ES)

U.S. Army Medical Research and Materiel Command
Fort Detrick, Maryland 21702-5012

10. SPONSORING / MONITORING AGENCY REPORT NUMBER

11. SUPPLEMENTARY NOTES

Original contains color plates: ALL DTIC reproductions will be in black and white

12a. DISTRIBUTION / AVAILABILITY STATEMENT

Approved for Public Release; Distribution Unlimited

12b. DISTRIBUTION CODE

13. ABSTRACT (Maximum 200 Words)

In order to better understand how polarized membrane trafficking pathways change during the loss of epithelial cell polarity during cancer progression we have studied syntaxins 3 and 4 in prostate cancer. Tumors of different stages from a TRAMP mice, human prostate cancers, and human prostate cancer cell lines were investigated for the expression and subcellular localization of syntaxins 3 and 4 by confocal microscopy and Western blot analysis. Like in renal epithelial cells, syntaxins 3 and 4 are strictly localized to the apical and basolateral plasma membrane, respectively, in normal human and mouse prostate epithelial cells. The expression of syntaxin 3 and syntaxin 4 in the plasma membrane were down-regulated in the tumor cells of Tramp mice and human prostate cancers, although they were still localized apically, basolaterally, respectively in tumor cells, in which the cell polarity was preserved. In contrast, syntaxins 3 and 4 were mislocalized to intracellular vesicles in metastatic prostate cancer cells. The mislocalization was also observed in human prostate cancer cell line DU145 when the cell polarity lost when the cells were cultured in low calcium medium. These results suggest that loss of epithelial cell polarity during cancer progression involves major changes in polarized exocytic pathways.

14. SUBJECT TERMS

SNARE, cell polarity, prostate cancer

15. NUMBER OF PAGES

58

16. PRICE CODE

17. SECURITY CLASSIFICATION OF REPORT	18. SECURITY CLASSIFICATION OF THIS PAGE	19. SECURITY CLASSIFICATION OF ABSTRACT	20. LIMITATION OF ABSTRACT
Unclassified	Unclassified	Unclassified	Unlimited

Table of Contents

Final Report for "Investigation of SNARE-mediated Membrane Trafficking in Prostate Cancer Cells" -DAMD17-02-1-0039

Abstract

A hallmark of epithelial-derived tumors is the progressive loss of cell polarity. Epithelial cell polarity is maintained, in part, by polarized exocytosis towards the apical and basolateral plasma membrane domains. Syntaxin 3 and 4 have been identified as t-SNAREs, which localize specifically to the apical and basolateral domains of epithelial cells, respectively, where they mediate the fusion of post-Golgi transport carriers. We have previously shown that plasma membrane t-SNAREs are re-directed into two types of intracellular vacuoles upon loss of epithelial polarity in vitro. This is accompanied by the re-direction of several surface proteins into these vacuoles, and results in their intracellular accumulation. In order to better understand how polarized membrane trafficking pathways change during the loss of epithelial cell polarity during cancer progression we have studied syntaxins 3 and 4 in prostate cancer. Tumors of different stages from a mouse model of prostate cancer (TRAMP), human prostate cancers, and human prostate cancer cell lines were investigated for the expression and subcellular localization of syntaxins 3 and 4 by confocal microscopy and Western blot analysis. Like in renal epithelial cells, syntaxins 3 and 4 are strictly localized to the apical and basolateral plasma membrane, respectively, in normal human and mouse prostate epithelial cells. The expression of syntaxin 3 and syntaxin 4 in the plasma membrane were down-regulated in the tumor cells of Tramp mice and human prostate cancers, although they were still localized apically, basolaterally, respectively in tumor cells, in which the cell polarity was preserved. In contrast, syntaxins 3 and 4 were mislocalized to intracellular vesicles in metastatic prostate cancer cells. The mislocalization was also observed in human prostate cancer cell line DU145 when the cell polarity lost when the cells were cultured in low calcium medium. These results suggest that loss of epithelial cell polarity during cancer progression involves major changes in polarized exocytic pathways.

Scientific trainings and publications under the support of this award

Although I have worked on cancer research for more than 10 years, this award let me switch to the prostate cancer research. During this study, I have had a great opportunity to collaborate with many scientists who work in the field of prostate cancer, especially the researchers in Dr. Heston's Lab, Department of Cancer Biology, CCF. I have learnt how to dissect the mouse prostate, and to identify the histological structures of different lobes of mouse prostate. I attended the monthly research update on the urological research in the Cleveland Clinic Foundation. Last year I attended "Retreat of Cell Biology between the Cleveland Clinic Foundation and Case Western Reserve University", and "42nd Annual Meeting of American Society of Cell Biology in San Francisco". One paper "Differential SNARE expression and localization in renal epithelial cells suggests mechanism for establishment of distinct trafficking phenotypes" was published as the first author in ***American Journal of Physiology*** 283: F1111–F1122 under the support of

this award (see attached). Four papers were published as a co-author (see attached). An abstract from this work was accepted as a poster presentation at **43rd Annual Meeting of American Society of Cell Biology** in San Francisco (see attached abstract).

Five papers were published as follows:

Li, X., Low, S.H., Miura, M. and Weimbs, T. (2002)
Differential SNARE Expression and Localization in Renal Epithelial Cells suggests mechanism for establishment of distinct trafficking phenotypes.
American Journal of Physiology 283: F1111–F1122

Low, S.H., Marmorstein, L.Y, Miura, M., **Li, X.**, Kudo, N., Marmorstein, A.D. and Weimbs, T. (2002)
Retinal pigment epithelial cells exhibit unique expression and localization of plasma membrane syntaxins which may contribute to their trafficking phenotype.
Journal of Cell Science 115, 4545-4553

Low, S.H., **Li, X.**, Miura, M., Kudo, N., Quinones, B. and Weimbs, T. (2003) Syntaxin 2 and Endobrevin are Required the Terminal Step of Cytokinesis.***Developmental Cell*** 4, 753-759

Kreitzer, G., Schmoranzer, J., Low, S.H., **Li, X.,** Gan, Y., Weimbs, T., Simon, S.M. and Rodriguez-Boulan, E. (2003)
Three-dimensional Analysis of Post-Golgi Carrier Exocytosis in Epithelial Cells.
Nature Cell Biology 5, 126-136

Weimbs, T., Low, S.H. and **Li, X.** and G Kreitzer (2003)
SNAREs and epithelial cells
Methods 30:191-197

Research Accomplishments

The first part of this project is to investigate the expression and localization of SNARE proteins in human prostate cancer tissues and transgenic mouse of prostate cancers (Tramp). 23 Tramp mice were obtained from Dr. Heston's Lab in the Department of Cancer Biology, Cleveland Clinic Foundation. By histology, these mice showed different stages of carcinogenesis of prostate cancer, with a metastatic lesion in the kidney in one mouse, lymphatic metastasis in two mice, a big abdominal tumor fused together in one mouse, and 9 mice accompanying tumors in the seminal vesicle. 5 cases of human prostatic carcinomas were obtained from the Department of Surgical Pathology, Cleveland Clinic Foundation. All of these cases were moderately differentiated adenocarcinomas without metastasis. The second part of this study is to investigate the effect of loss of cell polarity on the expression and localization in vitro. Five human prostatic cancer cell lines, including C4.2, CWR22, DU145, PC3, and LNCap were screened for the expression and localization of syntaxin 3 and 4. An in vitro model was

established by culturing DU145 cells in low calcium medium. The major accomplishments in this study are as follows.

1. **Plasma membrane t-SNAREs (i.e. syntaxin 3 and syntaxin 4) are expressed in human and mouse prostate gland**
2. **The expression of syntaxin 3 and 4 in the plasma membrane is down-regulated in poorly-differentiated areas of tumors in Tramp mice and in human prostate cancers compared to well-differentiated areas**
3. **Syntaxin 3 and 4 is mislocalized to intracellular vesicles in metastatic prostate cancer cells**
4. **Syntaxin 3 and 4 were mislocalized to the intracellular vesicles when the cells lost cell polarity by cultured in low calcium medium in vitro**

- **Plasma membrane t-SNAREs (i.e. syntaxin 3 and syntaxin 4) are expressed in human and mouse prostate gland**

Plasma membrane t-SNAREs, i. e. syntaxin 3 and syntaxin 4 in this study, which were found to mislocalize to the intracellular vacuoles upon the loss of cell polarity in our previous study, were expressed in prostate gland and prostate cancer in mouse and human by immunofluorescence (Fig. 1) and Western blot. Syntaxin 3 is localized to the apical plasma membrane, and syntaxin 4 is localized to the basolateral plasma membrane under a confocal microscope.

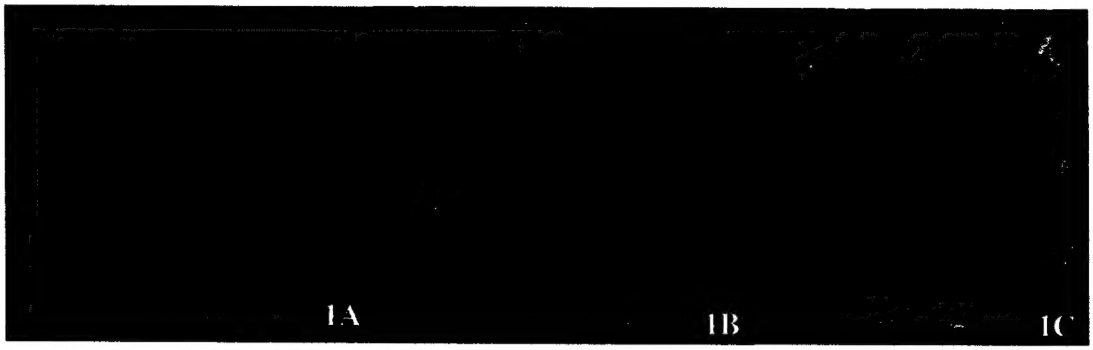

Fig. 1 Localization of syntaxin3 (1A) and 4 (1B) in normal mouse prostate gland and human prostate gland (1C). Syntaxin 3 and 4 are localized to the apical and basolateral membrane of normal prostate epithelial cells, respectively. Syntaxin 3 (1A and 1C) and 4 (1B) are labeled with green color, whereas E-cadherin (1A and 1C) and p27 (1B) are labeled with red color.

Syntaxin3 and 4 were also expressed in all human prostate cancer cell lines we observed (Fig. 2).

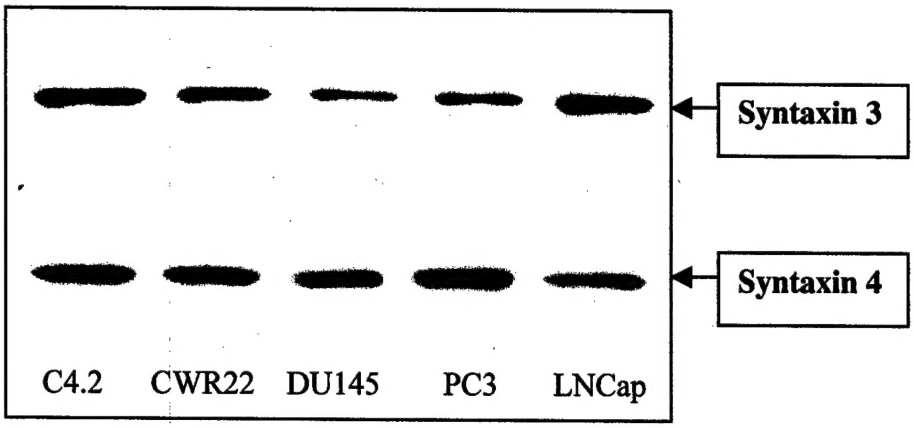

Fig. 2. Western blot analysis of syntaxins in human prostatic cancer cell lines. Total lysates were run on a 10% SDS gel, and immunoblotted with anti-syntaxin 3 (upper lanes), or syntaxin 4 (lower lanes) antibodies.

- **The expression of syntaxin 3 and 4 in the plasma membrane is down-regulated in poorly-differentiated areas of tumors in Tramp mice and in human prostate cancers compared to well-differentiated areas.**

Our preliminary results showed mistargeting of syntaxin 3 and 4 in renal cell carcinoma, and down-regulation of syntaxin 3 in Tramp mice. 23 Tramp mice prostate tissues and 5 human prostate cancers were investigated to see if this was a common feature of prostate cancer, and its relationship to the cell polarity, tumor differentiation and proliferation. Cell polarity was evaluated by basolateral marker E-cadherin. The cell proliferative status was estimated by cell cycle protein p27, which is a negative regulator of cell proliferation. Syntaxin 3 was found to be down-regulated in 15 of 23 Tramp mice, and in 4 of 5 human prostate cancers (Fig. 3). But this down-regulation was only observed in the poorly-differentiated lesions, not in the prostatic intraepithelial neoplasia (PIN). In the case of syntaxin 4, the same phenomenon was also observed in some lesions but not obvious in some of the Tramp mice and human samples (data not shown).

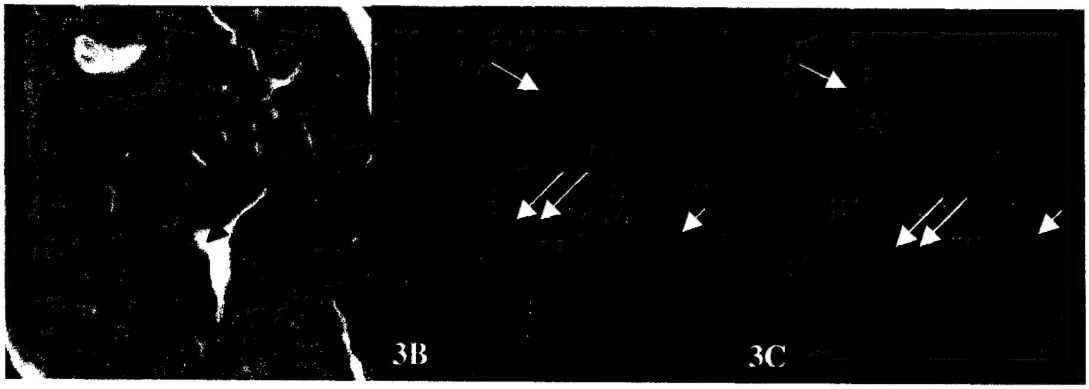

Fig.3 Expression of syntaxin 3 ansd 4 in Tramp mice. Lower expression of syntaxin3 and 4 in the plasma membrane was detected in the poorly-differentiated lesions of prostate cancer in human and Tramp mice (arrow), compared to well-differentiated acinus (double arrow). 3A is stained by H&E.

- **Syntaxin 3 and 4 is mislocalized to intracellular vesicles in metastatic prostate cancer cells**

Two Tramp mice had lymph metastases, one Tramp mouse exhibited a metastatic cancer in the right kidney (the left kidney was normal). The histology showed similar structures to the primary carcinomas in the prostate, but with less-differentiation (Fig. 4A and B). The localization of syntaxin 3 and 4 was in intracellular structures instead of plasma membrane. The same localization was found in a human prostatic cancer cell line (originated from metastatic cancer to the lymph node), LNCap cells (data showed before). But we could not detect the intracellular syntaxin3 and 4 in human prostate cancer. The likely reason is that the available cases used were moderately differentiated adenocarcinomas, which still retain the cell polarity, as shown by basolateral E-cadherin, although we did detect the down-regulated syntaxin 3 and E-cadherin. This suggests that intracellular syntaxin 3 and 4 may be related to the complete loss of cell polarity.

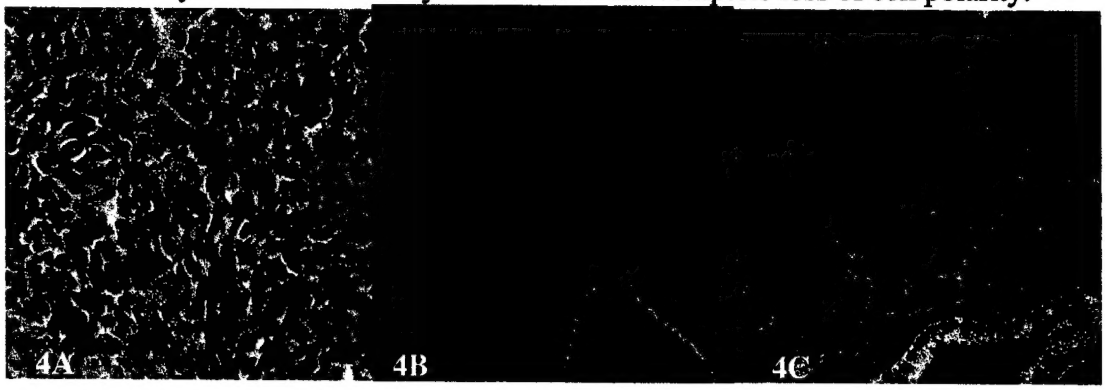

Fig. 4. Localization of syntaxin 3 (4B) and 4 (4C) in the lesions of lymphatic metastasis. Syntaxin 3 and 4 were found to be intracellular (labeled with green color). E-cadherin (4B) and p27 (4C) were labeled with red color. 4A is H&E staining.

The downregulation of syntaxin 3 and 4 were confirmed by Western Blot analysis.

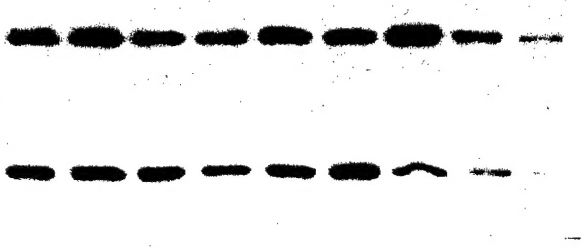

Fig. 5 Expression of syntaxin 3 (upper panel) and 4 (lower panel) in different cases of Tramp mice. The last two lanes on the right are the protein extracts from lymphatic metastasis. The other lanes are protein extracts from prostate.

- **Syntaxin 3 and 4 were mislocalized to the intracellular vesicles when the cells lost cell polarity by cultured in low calcium medium in vitro**

Our previous discovery have shown that plasma membrane t-SNAREs are re-localized into novel intracellular organelles called "vacuolar apical compartment (VAC) and vacuolar basolateral compartment (VBC), respectively when MDCK cells were cultured under conditions to prevent the development of cell polarity. In addition, membrane trafficking pathways that normally reach the apical and basolateral surface are re-directed into these organelles. This is also the true for prostate cancer cells. In a human prostate

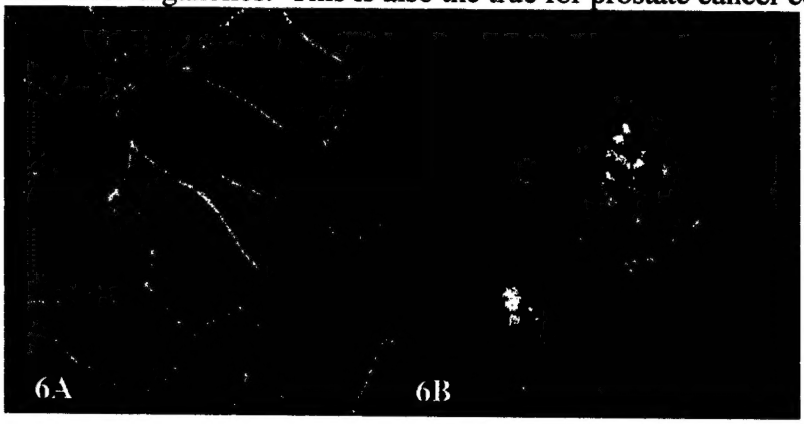

Fig. 6 Mistargeting of syntaxin 4 into intracellular organelles after losing cell polarity (6B), otherwise it localized to the basolateral plasma membrane (6A). Green,syntaxin 4, red, β-catenin.

cancer cell line DU145, syntaxin 3 and 4 were localized to the apical and basolateral plasma membrane, respectively. But when the cells were cultured in a low calcium medium, in which the cell polarity was lost, syntaxin 3 (data not shown) and 4 were mislocalized to the intracellular organelles (Fig. 6B). As a result, our results indicate that down-regulation and mislocalization of t-SNARE protein (e. g. syntaxin 3 and 4) play a role in the progression of prostate cancer.

Appendix (Articles and Abstracts published under this award)

1. **Li X**. Harsh K, Heston W, Weimbs T (2003) Down-regulation and mis-localization of plasma membrane-t-SNARE in prostate cancer cells. 43rd Annual Meeting of American Society for Cell Biology, San Francisco.
2. **Li, X.,** Low, S.H., Miura, M. and Weimbs, T. (2002) Differential SNARE Expression and Localization in Renal Epithelial Cells suggests mechanism for establishment of distinct trafficking phenotypes. ***American Journal of Physiology*** 283: F1111–F1122
3. Low, S.H., Marmorstein, L.Y, Miura, M., **Li, X**., Kudo, N., Marmorstein, A.D. and Weimbs, T. (2002)Retinal pigment epithelial cells exhibit unique expression and localization of plasma membrane syntaxins which may contribute to their trafficking phenotype. ***Journal of Cell Science*** 115, 4545-4553
4. Low, S.H., **Li, X**., Miura, M., Kudo, N., Quinones, B. and Weimbs, T. (2003) Syntaxin 2 and Endobrevin are Required the Terminal Step of Cytokinesis.***Developmental Cell*** 4, 753-759
5. Kreitzer, G., Schmoranzer, J., Low, S.H., **Li, X.,** Gan, Y., Weimbs, T., Simon, S.M. and Rodriguez-Boulan, E. (2003) Three-dimensional Analysis of Post-Golgi Carrier Exocytosis in Epithelial Cells. ***Nature Cell Biology*** 5, 126-136
6. Weimbs, T., Low, S.H. and **Li, X**. and G Kreitzer (2003) SNAREs and epithelial cells

Print this Page for Your Records Close Window

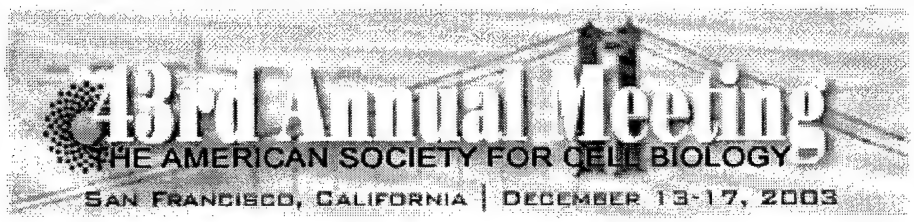

Control/Tracking Number : 03-A-2442-ASCB
Activity : Abstract Submission
Current Date/Time : 7/31/2003 1:05:33 PM

Down-regulation and mis-localization of plasma membrane t-SNAREs in prostate cancer cells

X. Li,[1] K. Harsch,[2] W. Heston,[2] T. Weimbs[1] ; [1] Cell Biology, Cleveland Clinic Foundation, Cleveland, OH, [2] Cancer Biology, Cleveland Clinic Foundation, Cleveland, OH

A hallmark of epithelial-derived tumors is the progressive loss of cell polarity. Epithelial cell polarity is maintained, in part, by polarized exocytosis towards the apical and basolateral plasma membrane domains. Syntaxin 3 and 4 have been identified as t-SNAREs which localize specifically to the apical and basolateral domains of epithelial cells, respectively, where they mediate the fusion of post-Golgi transport carriers. We have previously shown that plasma membrane t-SNAREs are re-directed into two types of intracellular vacuoles upon loss of epithelial polarity in vitro. This is accompanied by the re-direction of several surface proteins into these vacuoles, and results in their intracellular accumulation. In order to better understand how polarized membrane trafficking pathways change during the loss of epithelial cell polarity during cancer progression we have studied syntaxins 3 and 4 in prostate cancer which is epithelial-derived. Tumors of different stages from a mouse model of prostate cancer (TRAMP), human prostate cancers, and several human prostate cancer cell lines were investigated for the expression and subcellular localization of syntaxins 3 and 4 by confocal microscopy and Western blot analysis. Like in renal epithelial cells, syntaxins 3 and 4 are strictly localized to the apical and basolateral plasma membrane, respectively, in normal human and mouse prostate epithelial cells. Syntaxin 3, but not syntaxin 4, was down-regulated in the tumor cells of Tramp mice and human prostate cancers, although it was still localized apically in tumor cells in which cell polarity was preserved. In contrast, in metastatic prostate cancer cells syntaxins 3 and 4 are mislocalized to intracellular vesicles. These results suggest that loss of epithelial cell polarity during cancer progression involves major changes in polarized exocytic pathways, and particularly the inactivation of apical pathways which depend on syntaxin 3.
Author Disclosure Block: X. Li, None.

General Info (Complete):
ASCB Member : Yes – I am a current ASCB member or applicant
Presentation Preference : Poster Only
Student : No

To: Xin Li, Ph.D.
From: "ASCB Abstracts" <abstracts@ascb.org>
Subject: ASCB Poster Assignment/Confirmation - Control #03-A-2442
CC:
Date Sent: Friday, September 26, 2003 9:15 AM

YOUR SUBMITTED ABSTRACT FOR THE 43RD AMERICAN SOCIETY FOR CELL BIOLOGY ANNUAL MEETING IN SAN FRANCISCO, CA, DECEMBER 13-17, 2003 HAS BEEN SCHEDULED IN A POSTER SESSION AS FOLLOWS:
(Please advise co-authors of time and place as they will not receive notification.)

Original Abstract Control Number: 03-A-2442-ASCB
Title*: Down-regulation and mis-localization of plasma membrane t-SNAREs in prostate cancer cells
Corresponding Author: Li, Xin
Poster Session Title: Membrane Domains and Polarity I
Day/Date of Presentation: Sun, 12/14/2003
Time of Presentation: 1:30 PM - 3:00 PM
Place: Moscone Convention Center, Halls A/B/C
Program #: 453
Board #: B414

Note Board assignment above. All posters must be placed on the assigned board between 6:00 PM and 6:30 PM on the evening prior to the session (except those assigned to Sunday should place their poster on the assigned board between 5:30 PM and 6:00 PM on Saturday) and should remain in place until the session ends at 5:00 PM at which time the poster material should be removed. Authors must be at their posters at 12 Noon or 1:30 PM for presentation. There will be no major competing scientific symposia during poster presentations.
PLEASE NOTE: If the poster presentation time is on Wednesday, December 17, the poster material must be removed from your board at 3:00 PM. The ASCB is not responsible for poster materials left in Halls A/B/C after 3:00 PM on Wednesday.

Please remember to bring your own pushpins.

Reminders:
The advance registration deadline for the 43rd American Society for Cell Biology Annual Meeting in San Francisco, CA is October 14, 2003. If you have not yet registered, you may register online at http://www.ascb.org

You can also book your hotel online at http://www.ascb.org/meetings/am2003/main03mtg.htm through the housing bureau as rooms sell fast. The sooner you book a hotel, the better your chances of getting the hotel of your choice at pre-negotiated ASCB convention rates from $98!

* If your title contains Greek characters or HTML codes they may not appear correctly in this e-mail. Don't worry, they will be correct in the final publication.

Am J Physiol Renal Physiol 283: F1111–F1122, 2002;
10.1152/ajprenal.00185.2002.

SNARE expression and localization in renal epithelial cells suggest mechanism for variability of trafficking phenotypes

XIN LI, SENG HUI LOW, MASUMI MIURA, AND THOMAS WEIMBS
Department of Cell Biology, Lerner Research Institute, and Urological Institute, The Cleveland Clinic, Cleveland, Ohio 44195

Received 22 May 2002; accepted in final form 18 June 2002

Li, Xin, Seng Hui Low, Masumi Miura, and Thomas Weimbs. SNARE expression and localization in renal epithelial cells suggest mechanism for variability of trafficking phenotypes. *Am J Physiol Renal Physiol* 283: F1111–F1122, 2002; 10.1152/ajprenal.00185.2002.—The apical- and basolateral-specific distribution of target soluble *N*-ethylmaleimide-sensitive factor attachment protein receptors (t-SNAREs) of the syntaxin family appear to be critical for polarity in epithelial cells. To test whether differential SNARE expression and/or subcellular localization may contribute to the known diversity of trafficking phenotypes of epithelial cell types in vivo, we have investigated the distribution of syntaxins 2, 3, and 4 in epithelial cells along the renal tubule. Syntaxins 3 and 4 are restricted to the apical and basolateral domains, respectively, in all cell types, indicating that their mutually exclusive localizations are important for cell polarity. The expression level of syntaxin 3 is highly variable, depending on the cell type, suggesting that it is regulated in concert with the cellular requirement for apical exocytic pathways. While syntaxin 4 localizes all along the basal and lateral plasma membrane domains in vivo, it is restricted to the lateral membrane in Madin-Darby canine kidney (MDCK) cells in two-dimensional monolayer culture. When cultured as cysts in collagen, however, MDCK cells target syntaxin 4 correctly to the basal and lateral membranes. Unexpectedly, the polarity of syntaxin 2 is inverted between different tubule cell types, suggesting a role in establishing plasticity of targeting. The vesicle-associated (v)-SNARE endobrevin is highly expressed in intercalated cells and colocalizes with the H^+-ATPase in α- but not β-intercalated cells, suggesting its involvement in H^+-ATPase trafficking in the former cell type. These results suggest that epithelial membrane trafficking phenotypes in vivo are highly variable and that different cell types express or localize SNARE proteins differentially as a mechanism to achieve this variability.

syntaxin; endobrevin; membrane traffic; cell polarity; membrane fusion

THE VAST MAJORITY OF HUMAN cell types are polarized, i.e., they exhibit asymmetry, which is essential to their function. This includes epithelial cells, which form barriers between the outside world and the underlying basement membrane and connective tissue and make up most major human organs. Establishment and maintenance of epithelial cell polarity depend on the precise targeting of proteins to the apical and basolateral plasma membrane domains using vesicular transport pathways (41, 44). The underlying mechanisms of polarized trafficking in epithelial cells have been intensively studied in vitro using model cell lines, most frequently in the Madin-Darby canine kidney (MDCK) cell line derived from the distal renal tubule (62).

The soluble *N*-ethylmaleimide-sensitive factor attachment protein receptor (SNARE) membrane fusion machinery is essential for all membrane trafficking pathways investigated to date (10, 24). Target (t)-SNAREs of the syntaxin family generally localize to distinct compartments and organelles, where they mediate the fusion of specific incoming trafficking pathways. Membrane fusion can only occur with matching combinations of vesicle-associated (v)- and t-SNAREs (38, 56), suggesting that SNAREs contribute to the specificity of membrane traffic.

In MDCK cells, syntaxins 3 and 4 are mutually exclusively localized to the apical and basolateral plasma membrane, respectively (30). Syntaxin 3 is involved in apical recycling and in biosynthetic traffic from the *trans*-Golgi network (TGN) to the apical surface (31). In contrast, syntaxin 4 is involved in TGN-to-basolateral trafficking (26). In addition, MDCK cells express syntaxins 2 and 11, the functions of which have remained unknown, and both of which are localized to the plasma membrane in a nonpolarized fashion (30, 32). These results suggest that the correct localization of syntaxins is critical for the fidelity of polarized membrane traffic in epithelial cells.

Higher animal organisms consist of a multitude of epithelial cell types, each of which has specific functions. They vary not only in their proteome of plasma membrane proteins but also in the way they sort and target them to their final destination. Identical proteins can be localized to opposite surfaces in different epithelial cell types. A classic example is the H^+-ATPase, which is apically localized in α-intercalated cells of the renal distal tubule, whereas it is basolateral in β-intercalated cells (1, 7). The final polarity of a given protein may also be identical between two cell types, but the route by which the proteins reach their

Address for reprint requests and other correspondence: T. Weimbs, Dept. of Cell Biology, Lerner Research Institute, NC10, The Cleveland Clinic, 9500 Euclid Ave., Cleveland, OH 44195 (E-mail: weimbst@lerner.ccf.org).

The costs of publication of this article were defrayed in part by the payment of page charges. The article must therefore be hereby marked "*advertisement*" in accordance with 18 U.S.C. Section 1734 solely to indicate this fact.

surface differs. For example, MDCK cells target almost all newly synthesized apical proteins (including the influenza virus hemagglutinin) directly from the TGN to the apical surface. In contrast, the retinal pigment epithelium targets the influenza virus hemagglutinin to the apical plasma membrane indirectly by transcytosis via the basolateral domain (4). Hepatocytes are an extreme case and transport virtually all apical proteins by transcytosis (23). The epithelial sorting phenotype can also change during the development of a polarized monolayer (66). Therefore, great variability exists in the protein-targeting phenotypes among epithelial cell types.

It is unclear whether results obtained from MDCK cells are necessarily valid for all epithelial cell types in vivo. Moreover, it is unknown how the observed differences in targeting phenotypes between epithelial cell types are achieved mechanistically. We sought to investigate whether differences in the expression and/or subcellular localization of syntaxins may be part of this mechanism. We tested this by investigating syntaxins in epithelial cells along the renal tubule. There are 14 recognizably different epithelial cell types in the kidney (1), which play specific roles such as absorption of proteins and the maintenance of water, ions, and acid-base balance. Differences in membrane trafficking phenotypes between renal epithelial cell types are well known (1, 8, 9). MDCK cells are likely derived from the collecting duct (39), but they also have characteristics of other tubule segments (9). Investigating SNAREs along the renal tubule makes it possible to compare different epithelial cell types side by side and to relate results to the most widely used model system, MDCK cells.

Here, we report similarities and differences between renal epithelial cells in vivo and MDCK cells. Cell types along the renal tubule differ in the expressed complement of SNAREs as well as in their subcellular localization. Altogether, our results suggest that the modulation of SNARE expression and localization is used by epithelial cells as a mechanism to achieve the known plasticity of sorting phenotypes.

MATERIALS AND METHODS

Antibodies. Rabbit polyclonal antibodies against rat syntaxins 2, 3, and 4 were generated against bacterially expressed glutathione-*S*-transferase (GST) fusion proteins of the cytoplasmic domains of the respective syntaxin isoforms as described previously (32). In addition, polyclonal antibodies against the ~100 NH_2-terminal amino acids of human syntaxins 3 and 4 were raised. All antibodies were affinity purified using the respective syntaxin cytoplasmic domains that were separated from GST by thrombin cleavage and coupled to Affigel (Bio-Rad, Richmond, CA). Rabbit antiserum was raised against a GST fusion protein of the cytoplasmic domain of rat endobrevin. The expression plasmid was a gift from Wanjin Hong (Institute for Molecular and Cell Biology, Singapore). The endobrevin antibody was affinity purified as described above. As confirmatory controls, the following antibodies were used: affinity-purified polyclonal rabbit antibodies against rat syntaxins 2, 3, and 4 (described in Ref. 30; kindly provided by Mark Bennett and Beatriz Quiñones, University of California Berkeley); a monoclonal antibody against human syntaxin 4 (Transduction Laboratories); and a polyclonal antibody against the cytoplasmic domain of rat syntaxin 2 (Synaptic Systems, Göttingen, Germany). Rabbit antibodies against the 33- and 70-kDa subunits of the vacuolar H^+-ATPase (51) were kindly provided by Xiao-Song Xie (University of Texas, Southwestern Medical Center). Mouse monoclonal anti-band 3 antibody was kindly provided by Michael Jennings (University of Arkansas for Medical Sciences). Rabbit polyclonal anti-aquaporin-1 was obtained from Chemicon (Temecula, CA). Mouse monoclonal anti-calbindin D28 was from Sigma (St. Louis, MO). Rhodamine-labeled lectin *Dolichos biflorus* agglutinin was from Vector Labs (Burlingame, CA). Sheep polyclonal anti-Tamm-Horsfall glycoprotein was purchased from Biogenesis (Brentwood, NH).

Immunoblot analysis. Male Sprague-Dawley rats were euthanized by decapitation, and the kidneys were removed. Cortex and medulla were microdissected under a microscope and finely minced with a razor blade. Tissue was homogenized in ice-cold PBS with protease inhibitors (phenylmethylsulfonyl fluoride, leupeptin pepstatin, chymostatin, antipain, benzamidine, trasylol) using a Dounce homogenizer. The homogenates were first spun at 500 *g* for 2 min to pellet nuclei. The supernatants were then centrifuged at 13,000 *g* for 20 min to obtain the membrane fractions. Membrane fractions and supernatants (equal protein amounts) were separated by 15% SDS-PAGE. The proteins were transferred to polyvinylidene difluoride membranes and analyzed using the affinity-purified polyclonal anti-syntaxins 2, 3, or 4 antibodies, horseradish peroxidase-conjugated secondary antibodies (Jackson ImmunoResearch, West Grove, PA), and ECL (Pierce, Rockford, IL).

Immunolocalization in tissue sections. Sprague-Dawley male rats (230–250 g) were anesthetized by intraperitoneal administration of pentobarbital sodium, systemically heparinized, and perfused via the left ventricle with 4% paraformaldehyde in PBS with 1 mM calcium and 1 mM magnesium for 20 min. The kidneys were removed and cut into small blocks, which were further fixed in the same fixative overnight at 4°C. The blocks were dehydrated through serial ethanol and xylene and embedded in paraffin. Immunostaining was carried out on 5-μm sections. After deparaffinization and rehydration to PBS, the sections were pressure-cooked in 10 mM citric acid buffer, pH 6.0, for antigen retrieval. The sections were blocked with 3% BSA, 2% Triton X-100 in PBS and incubated with the indicated antibodies overnight at 4°C. To identify different tubule segments and cell types, double immunofluorescence staining of the same or serial sections was performed with the following: mouse anti-calbindin for the principal cells of connecting tubules and collecting ducts in the cortex (42); anti-H^+-ATPase polyclonal antibodies and anti-band 3 monoclonal antibody for intercalated cells (2); rabbit anti-aquaporin-1 polyclonal antibody for proximal tubule and descending limb of the loop of Henle (45); sheep anti-Tamm-Horsfall glycoprotein for thick ascending limb of the loop Henle (65); and rhodamine-labeled *D. biflorus* agglutinin for proximal tubules and collecting ducts (65). The reactions were visualized by fluorescein- or Texas red-labeled secondary antibodies (Jackson ImmunoResearch). Signals for syntaxins 3 and 4 were amplified by incubating with Alexa 488-labeled rabbit anti-FITC antibody (Molecular Probes, Eugene, OR) subsequent to the FITC-labeled secondary antibodies. Syntaxin 2 signals were amplified by tyramide signal amplification (TSA-Direct, NEN Life Science Products, Boston, MA). For simultaneously localizing two proteins recognized by rabbit primary antibodies, FITC-

or rhodamine-labeled Fab fragments of the secondary antibody (Jackson ImmunoResearch) were used after incubation with the first rabbit primary antibody. The sections were shortly fixed with 4% paraformaldehyde, then incubated with the second rabbit primary antibody, followed by Texas red- or FITC-labeled secondary antibody.

To eliminate cross-reactivity of syntaxin antibodies against related syntaxins, primary antibodies were preincubated with 2% native and 2% heat/SDS-denatured total lysates of *Escherichia coli*-expressing GST fusion proteins of the nonrelevant syntaxins. For example, bacterial lysates of syntaxins 2 and 3 were added to anti-syntaxin 4 antibody incubations. The fluorescent staining was analyzed using a confocal laser scanning microscope (TCS-NT, Leica, Bensheim, Germany).

Expression levels of syntaxins and endobrevin in different tubule segments were estimated as follows. Fluorescent images of multiple fields were acquired using identical exposure settings, ensuring that the regions of brightest signals did not exceed the maximal intensity of the eight-bit signal. The background was subtracted using Adobe Photoshop. Pixel values of each tubule type were integrated using National Institutes of Health IMAGE 1.61 software. For each type of tubule, at least three tubules were counted. The intensity values were divided by the number of cells in each tubule and averaged.

Cell culture, transfection, and immunolocalization in cultured cells. MDCK strain II cells were cultured in MEM containing Earle's salts and supplemented with 10% FBS, 100 U/ml penicillin, and 100 μg/ml streptomycin in 5% CO_2. Cells were cultured on Transwell polycarbonate filters (12 mm, 0.4-μm pore size, Corning Costar, Cambridge, MA) for 4–5 days (polarized) or for 1 day (semipolarized). For expression of COOH-terminal epitope-tagged syntaxin 4, human syntaxin 4 cDNA was cloned into a modified pcDNA4/TO vector (Invitrogen) to add two COOH-terminal myc epitope tags in tandem and one hexahistidine tag to the COOH terminus. MDCK cells were transfected, and stable clones were isolated by Zeocin selection. The additional epitope tags did not interfere with the correct polarized targeting of syntaxin 4 and allowed detection at the plasma membrane by surface immunolabeling.

For surface staining of epitope-tagged syntaxin 4, cells on Transwell filters were incubated with anti-myc antibody (9E10) antibody for 2 h on ice. After several washes, cells were fixed with 4% paraformaldehyde in PBS and incubated with FITC-labeled secondary antibody. The culture and immunostaining of MDCK cells in collagen gels have been described previously (52).

RESULTS

Only membrane-bound isoforms of syntaxins 2, 3, and 4 are expressed in rat kidney. Polyclonal antibodies were raised against GST fusion proteins of the full-length cytoplasmic domains of rat syntaxins 2, 3, and 4. The antibodies were affinity purified using the immobilized, thrombin-cleaved syntaxin domains and tested for their isoform specificity by Western blot analysis. A low degree of cross-reactivity was observed, which could be completely eliminated by preincubating each syntaxin antibody with the GST fusion proteins of the others, resulting in specific signals. Therefore, preincubation was used for all subsequent experiments.

Isoforms of syntaxins 2 and 3, derived from alternative RNA splicing, have been identified previously (20, 22, 53, 55). They all differ only in the COOH-terminal parts of the molecules, and our antibodies are predicted to react with all of them. Some of these isoforms lack COOH-terminal transmembrane anchors, and previous results indicated that some of the syntaxin 2 isoforms are not membrane bound and purify in soluble cytoplasmic fractions (53). To investigate whether soluble syntaxin isoforms may be expressed in rat kidney, medulla and cortex were dissected, and total membrane and cytosol fractions were analyzed by immunoblotting. Figure 1 shows that all syntaxins are detected exclusively in the membrane fractions. Only single bands of the expected size of the full-length proteins are detected, except for syntaxin 2, which shows a faint additional band of slightly higher molecular weight. No significant differences were detected between renal cortex and medulla. These results indicate that the majority of syntaxins 2, 3, and 4 in rat kidney are membrane-associated isoforms.

The apical and basolateral localization of syntaxins 3 and 4 are conserved in all renal epithelial cell types. In MDCK cells, syntaxins 3 and 4 are mutually exclusively localized at the apical and basolateral plasma membrane domains, respectively, where they function

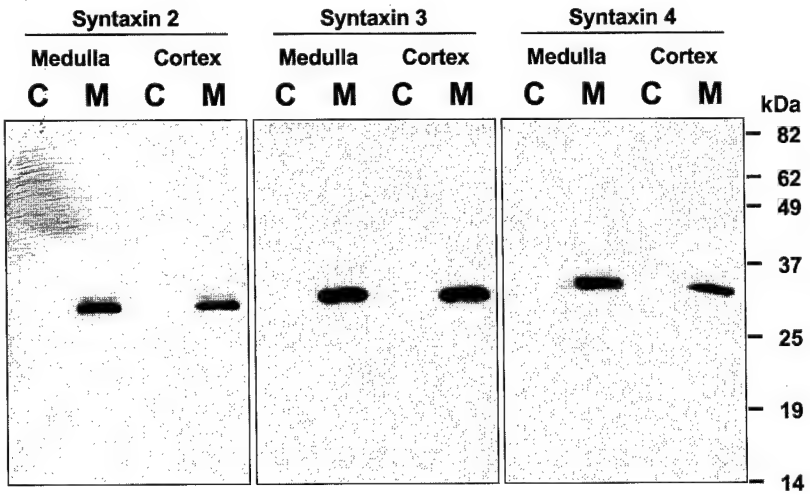

Fig. 1. Western blot analysis of syntaxins 2, 3, and 4 in rat kidney. Cortex and medulla were dissected under a microscope. Cytosolic (C) and membrane (M) protein fractions were isolated (see MATERIALS AND METHODS). Using affinity-purified antibodies against syntaxins 2, 3, and 4, 5 μg for syntaxins 2 and 3 or 20 μg for syntaxin 4 of total protein/lane were investigated by immunoblotting. Note that all syntaxins fractionate with total membranes and that their abundance is similar between renal cortex and medulla.

in polarized pathways (30, 31). To determine whether this is a general feature of all epithelial cell types along the renal tubule, we investigated their expression and localization by confocal immunofluorescence microscopy on rat kidney tissue sections. Individual tubule segments and cell types were identified by colabeling with lectins or antibodies against well-characterized marker proteins (see MATERIALS AND METHODS). Figure 2 shows that without exception, syntaxins 3 and 4 are restricted to the apical and basolateral plasma membrane domains, respectively, in all renal epithelial cell types.

The expression level of syntaxin 3 varies significantly between different cell types (for semiquantitative analysis, see Fig. 7). It is most highly expressed in proximal convoluted tubules, in which it localizes to

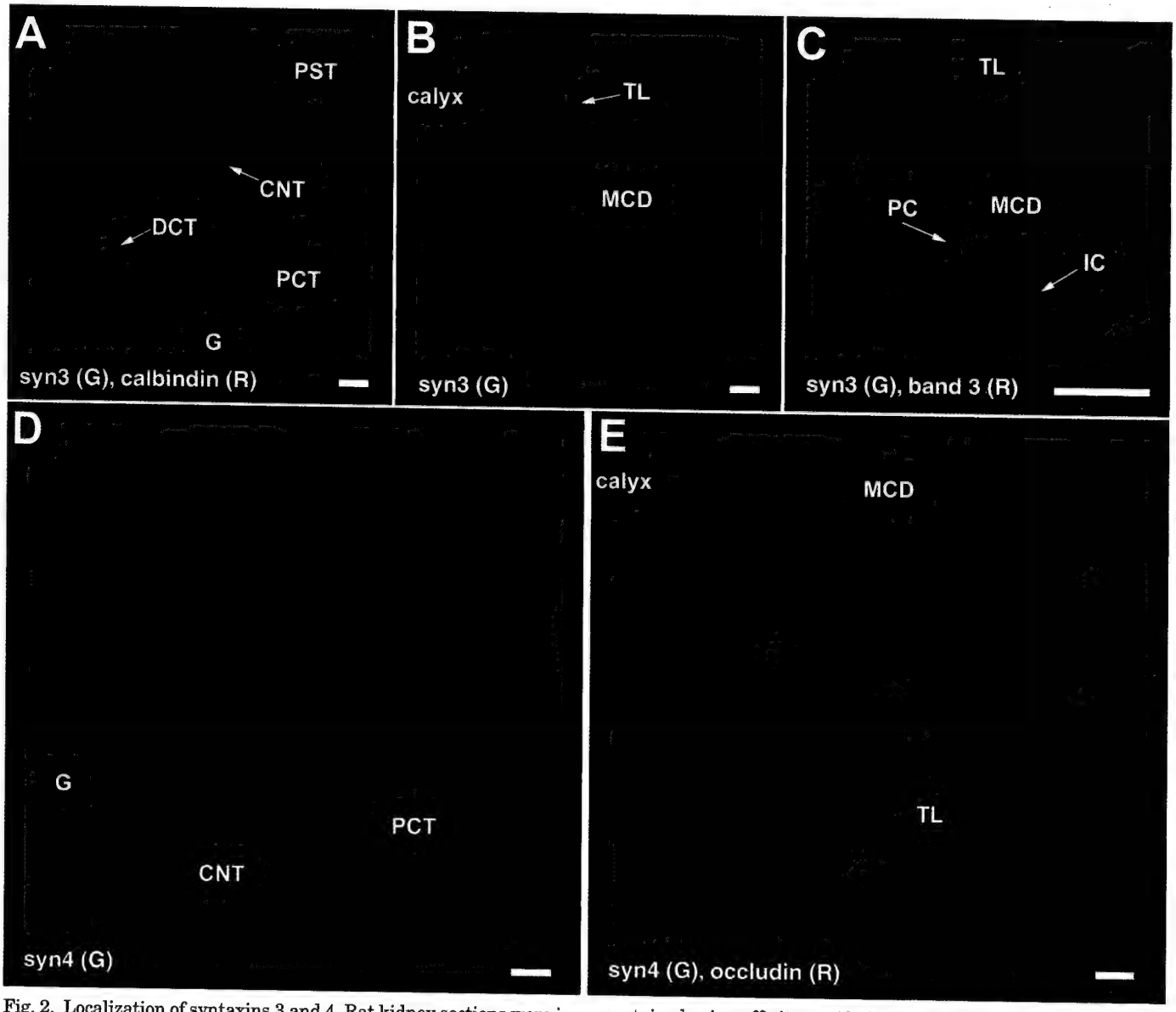

Fig. 2. Localization of syntaxins 3 and 4. Rat kidney sections were immunostained using affinity-purified syntaxin antibodies and colabeled with various segment-specific markers. Representative examples are shown. *A*, *B*, and *C*: syntaxin 3 labels in green (G). *D* and *E*: syntaxin 4 labels in green. Colabeling in red (R) is for calbindin (*A*), band 3 (*C*), and occludin (*E*). *A* and *D* show representative fields of renal cortex, whereas *B*, *C*, and *E* show medullary fields. Note that the subcellular localizations of syntaxins 3 and 4 are always restricted to the apical or basolateral plasma membrane, respectively. The intensity of staining is variable for syntaxin 3, with the highest level in the convoluted part of proximal tubules. Syntaxin 3 expression is weakest in the thick ascending limb of the loop of Henle. Syntaxin 4 is more uniformly expressed with the highest level in proximal tubules (*D*). Note that syntaxin 4 localizes to both the lateral and the basal membranes of all epithelial cell types. Abbreviations for this and subsequent figures are syn3 and syn4, Syntaxins 3 and 4, respectively; ATL, ascending thin limb of the loop of Henle; CCD, cortical collecting duct; CNT, cortical connecting tubule; DCT, distal convoluted tubule; DTL, descending thin limb of the loop of Henle; G, glomerulus; IC, intercalated cell; MCD, medullary collecting duct; PC, principal cell; PCT, proximal convoluted tubule; PST, proximal straight tubule; TAL, thick ascending limb of the loop of Henle; TL, thin loop of Henle. Bars, 20 μm.

the apical brush border (Fig. 2*A*). The expression level per cell is at least 10-fold lower in the thick ascending loop of Henle. Expression levels in other tubule segments are intermediate (Fig. 2, *B* and *C*).

In contrast to syntaxin 3, the expression level of syntaxin 4 is more uniform along the renal tubule. It is evenly distributed along the basal and lateral plasma membrane domains of all cell types. Syntaxin 4 also prominently localizes to the basal infoldings in cell types that possess them, such as proximal tubule cells (Fig. 2*D*).

All immunostaining results were confirmed using independently raised antibodies against rat syntaxins 3 and 4 (see MATERIALS AND METHODS). Furthermore, poly- and monoclonal antibodies against human syntaxins 3 and 4 were used in human kidney. In all cases, identical results were obtained (data not shown). Together, these results indicate that the mutually exclusive localizations of syntaxins 3 and 4 are highly conserved, suggesting that their apical- and basolateral-specific functions, respectively, are critical for the maintenance of epithelial cell polarity. The finding that the expression level of syntaxin 3 is highly cell type dependent indicates that syntaxin 3-dependent apical trafficking pathways vary among cell types and that renal epithelial cells have the ability to regulate its expression level, depending on their trafficking phenotype.

The polarity of syntaxin 2 is reversed between renal epithelial cell types. Investigation of syntaxin 2 localization revealed an unexpected pattern (Fig. 3). Expression is highest in medullary collecting ducts and the loop of Henle, where syntaxin 2 is restricted to the apical domain (Fig. 3, *B* and *C*). In contrast, most cortical tubule segments do not express detectable levels of syntaxin 2, except for the principal cells of connecting tubules and collecting ducts (Fig. 3*A*). In these cells, syntaxin 2 is localized to the basolateral domain. Therefore, the localization of syntaxin 2 is inverted between cortical and medullary principal cells. This suggests that localizing syntaxin 2 to different plasma membrane domains may be part of a mechanism to modulate epithelial sorting phenotypes. Again, the results could be confirmed with two independently raised anti-syntaxin 2 antibodies, resulting in identical staining patterns in rat and mouse kidney (not shown).

Syntaxins in intercalated cells. A striking example of the plasticity of epithelial sorting phenotypes are intercalated cells of the cortical connecting tubules and collecting ducts. One of their main functions is the maintenance of acid-base homeostasis. They exist in two varieties: α-cells, which secrete protons and target the H^+-ATPase apically, and β-cells, which secrete bicarbonate and target the H^+-ATPase basolaterally (1, 9). In addition, a bicarbonate exchanger and other proteins are differentially targeted in these two cell types. It has been suggested that α-cells can convert into β-cells and vice versa, depending on the acid-base status of the organism (8). Therefore, it is thought that the conversion between α- and β-cells involves an inversion of cell polarity, which implies that the molecular machineries for vesicle targeting would be inverted. If this were the case, we would expect that one or more plasma membrane syntaxins would be differently localized between α- and β-cells. To test this theory, cortical α- and β-cells were identified by immunostaining with an antibody against the 70-kDa subunit of H^+-ATPase. The localizations of syntaxins 2, 3, and 4 were defined by colabeling. Figure 4 shows that the apical and basolateral localization, respectively, of syntaxins 3 (Fig. 4*B*) and 4 (Fig. 4*C*) do not change between α- and β-intercalated cells. Syntaxin 2 is expressed and basolaterally localized in the neighboring principal cells as described above but is undetectable in

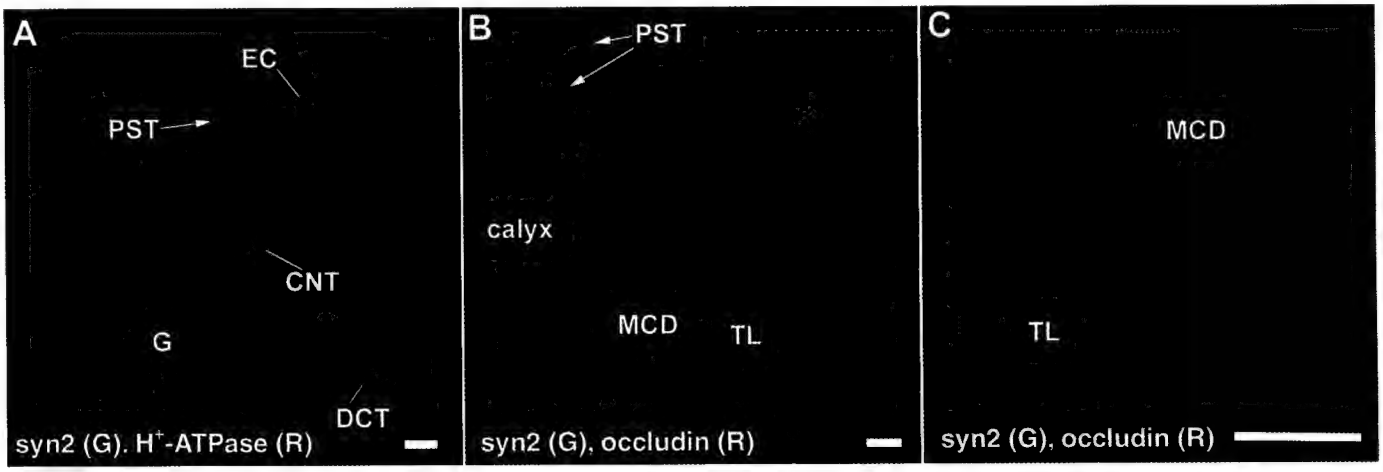

Fig. 3. Localization of syntaxin 2. Rat kidney sections were immunostained for syntaxin 2 (syn2; *A–C*, green) and vacuolar H^+-ATPase (*A*, red), or the tight junction protein occludin (*B* and *C*, red). *A*: representative field of kidney cortex. *B*: cortex (*top left*) and medulla (*bottom right*). *C*: higher magnification of medullary tubules. Syntaxin 2 is expressed in endothelial cells (EC) of the glomeruli (G) and between the tubules. Of the cortical epithelial cells, syntaxin 2 is only expressed in the principal cells of the connecting tubules and collecting ducts (*A*), in which it is basolaterally localized. In contrast, in the medulla, syntaxin 2 is apically localized in the thin limb of the loop of Henle and principal cells of collecting ducts (*B* and *C*). Bars, 20 μm.

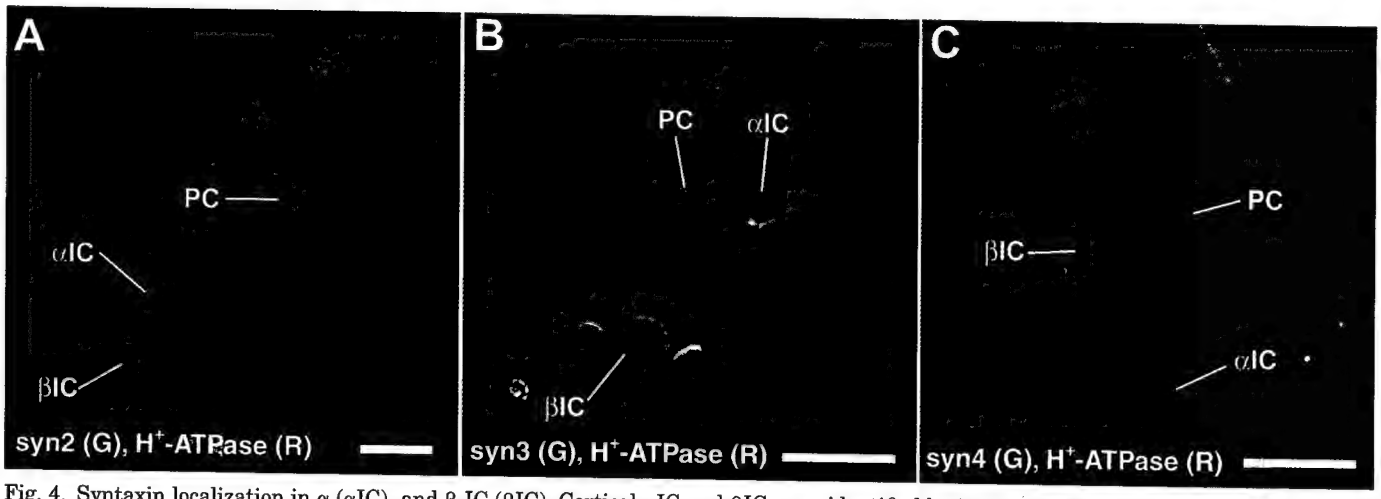

Fig. 4. Syntaxin localization in α (αIC)- and β-IC (βIC). Cortical αIC and βIC were identified by immunolocalization of the vacuolar H^+-ATPase (red), which is apical in αIC and basolateral in βIC. PC are negative for the H^+-ATPase. Syntaxin 2 (*A*) is only expressed in PC but not in intercalated cells. Syntaxin 3 (*B*) is expressed and apically localized in all 3 cell types. Similarly, syntaxin 4 (*C*) is basolaterally localized in all 3 cell types. Bars, 20 μm.

intercalated cells (Fig. 4*A*). The differential sorting phenotypes of α- and β-intercalated cells can therefore not be explained by differential localization of these plasma membrane syntaxins. These results make it unlikely that polarized membrane trafficking in general is inverted between these cell types.

Endobrevin is highly expressed in apical endosomes in proximal tubules and intercalated cells. Endobrevin/vesicle-associated membrane protein-8 is a member of the synaptobrevin family of v-SNAREs and implicated in early and/or late endosome fusion in nonpolarized cells (3). In polarized MDCK cells, green fluorescent protein (GFP)-tagged endobrevin has been reported to cycle between endosomes and the apical plasma membrane, indicating that it may be involved in an apical endocytic/recycling pathway in epithelial cells (58). We found that proximal tubule cells exhibit the highest expression levels of endobrevin. In these cells, endobrevin localizes to a narrow band of vesicles clustered underneath the apical brush border (Fig. 5*A*). Costaining for endobrevin and syntaxin 3 reveals no overlap (Fig. 5*B*). This is the characteristic localization of the extensive endocytic apparatus of proximal tubules involved in reabsorption of proteins from the ultrafiltrate (9, 37). The prominent localization of endobrevin on these apical endosomes, together with the previous finding of cycling of GST fusion protein-endobrevin through the apical plasma membrane of MDCK cells suggests that this protein may function as a v-SNARE on vesicles that recycle back to the apical brush border of proximal tubule cells.

Endobrevin is also highly expressed in intercalated cells of the connecting tubules and collecting ducts (Fig. 5, *C* and *D*). In α-intercalated cells, endobrevin colocalizes with the vacuolar H^+-ATPase in the apical cytoplasm. In contrast, in β-intercalated cells endobrevin is distributed throughout the cytoplasm and shows no colocalization with the H^+-ATPase. The vacuolar H^+-ATPase is known to cycle between endosomes and either apical or basolateral plasma membrane in α- and β-intercalated cells, respectively (1, 9). This result therefore suggests that endobrevin is involved in the apical recycling pathway of the H^+-ATPase in α-intercalated cells, whereas a different v-SNARE is likely involved in basolateral recycling in β-intercalated cells. Lower amounts of endobrevin are expressed in all other tubule epithelial cells in intracellular vesicles (see Fig. 7).

The in vivo localization of syntaxin 4 differs from that in cultured MDCK cells. The subcellular localization of syntaxin 4 in vivo, as described above, differs from its localization in cultured MDCK cells. Endogenous syntaxin 4 is concentrated at the lateral plasma membrane domain in polarized MDCK cells cultured on Transwell filters (Fig. 6*A*). In contrast, very little if any syntaxin 4 is detectable at the basal domain. This result could be confirmed in stably transfected MDCK cells expressing COOH-terminal myc-tagged syntaxin 4. The epitope tags are designed to protrude out of the cells, allowing surface labeling of live, intact cells. The subcellular localization of myc-tagged syntaxin 4 is identical to the endogenous protein (Fig. 6*B*).

In contrast, in subconfluent, semipolarized MDCK cells, syntaxin 4 localizes to the basal membrane that is in contact with the substratum (Fig. 6*C*). Therefore, during the development of a polarized monolayer, syntaxin 4 relocalizes from the basal to the lateral domain. The absence of a basal syntaxin 4 signal in polarized MDCK cells is not an artifact of the acquisition of confocal optical sections in the *X-Z* direction because the basal signal is clearly detectable in subconfluent cells under the same conditions. This result predicts that the majority of basolateral vesicle traffic in MDCK cells will be toward the lateral, not the basal, plasma membrane domain. This is in excellent agreement with our recent experiments in which basolateral trafficking of post-Golgi transport vesicles in MDCK cells was monitored by time-lapse fluorescence microscopy (Kre-

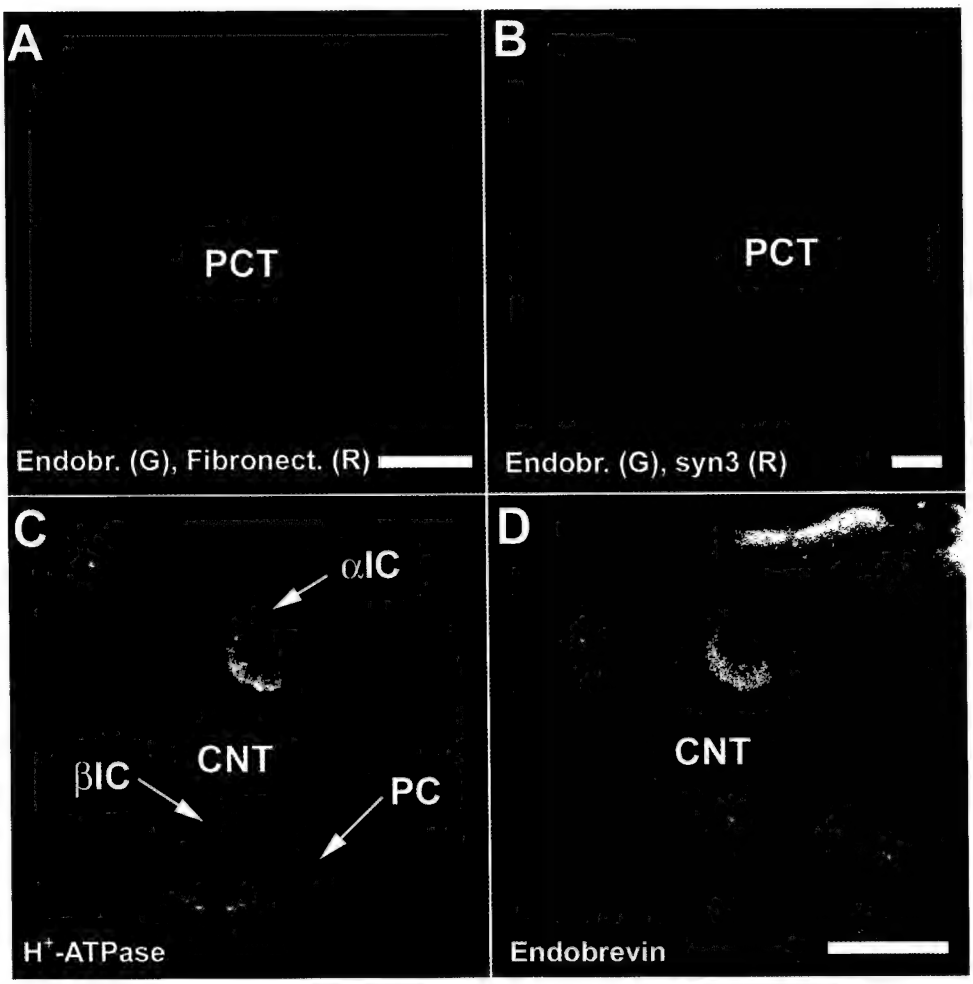

Fig. 5. Localization of endobrevin. Endobrevin is expressed in all epithelial cell types of the renal tubule, where it localizes to intracellular vesicles. It is most highly expressed in the convoluted proximal tubule [endobrevin (Endobr) is green, fibronectin is red, and nuclei are blue; *A*], in which it localizes to the prominent endosomes underneath the apical brush border. *C* and *D*: cortical connecting tubule costained for the vacuolar H^+-ATPase and endobrevin, respectively. In αIC, endobrevin is highly expressed and colocalizes with the H^+-ATPase in the apical region of the cells. In contrast, the expression level of endobrevin is lower in βIC and distributed throughout the cytoplasm. Expression is lowest in the PC. Bars, 10 μm.

itzer G, Schmoranzer J, Low SH, Li X, Gan Y, Weimbs T, Simon SM, and Rodriguez-Boulan E, unpublished observations). All "basolateral" fusion events occurred at the lateral domain, whereas no fusion was detected at the basal domain. In contrast, basolateral vesicles can fuse efficiently with the basal membrane of nonpolarized MDCK cells. Together, these results suggest that the subcellular localization of syntaxin 4 can serve as an indicator of the location of fusion sites in the trafficking pathways that depend on this SNARE.

In contrast to polarized MDCK cells, collecting duct cells in vivo, those from which MDCK cells are derived, exhibit very prominent basal staining of syntaxin 4 in addition to the lateral signal (Fig. 2). The same is the case for all other renal epithelial cell types in vivo. This suggests that the entire basolateral plasma membrane of renal epithelial cells in vivo is fusion competent for basolateral trafficking. Therefore, these results indicate that MDCK cells cultured on Transwell filters do not correctly reproduce the in vivo phenotype with respect to the localization of syntaxin 4 and basolateral trafficking. We investigated whether a culture system that more closely approximates the renal tubule may yield different results. MDCK cells can be cultured in gels of type I collagen, in which they form hollow spherical cysts that are lined by a monolayer of polarized cells. Under these conditions, syntaxin 4 localized all along the basal and lateral plasma membrane domains identically to native collecting duct cells in vivo. This suggests that MDCK cell culture in three-dimensional cysts more closely approximates the in vivo situation than does two-dimensional culture on Transwell filters and that vesicle fusion may occur all along the basolateral membrane.

DISCUSSION

Here, we report differences and similarities in the in vivo localization of plasma membrane syntaxins in the renal epithelium compared with the most widely studied in vitro epithelial model system, the MDCK cell line. One important finding is that the mutually exclusive localizations of syntaxins 3 and 4 are strictly conserved in all epithelial cell types. Without exception, syntaxin 3 localizes to the apical and syntaxin 4 to the basolateral domain. Syntaxin 3 has also previously been found to be apical specific in the Caco-2 colon epithelial cell line (6, 12, 17, 54) and in hepatocytes (15). Syntaxin 4 has been found on the basolateral plasma membrane of pancreatic acinar cells (16). Collectively, these results indicate that the polarized apical or basolateral localization, respectively, of syntaxins 3 and 4 is a common feature of

epithelial cells. This suggests that the strict separation of these two syntaxins is necessary for the establishment of distinct sites of polarized vesicle exocytosis and hence for the development and integrity of cell polarity.

We were unable to confirm previous results by another group that reported opposite polarities of syntaxins 3 and 4 in rat kidney (5, 35, 36). However, our results are in agreement with data by Lehtonen et al. (28), who used an independently raised antibody to investigate the localization of syntaxin 3 in developing mouse kidney and observed identical expression and subcellular localization, as presented here. We could confirm our immunolocalization data with several independent antibodies against syntaxins 3 and 4 in rat, mouse, and human kidney sections. In all cases, identical results were obtained. The cause for the aforementioned contradictory results remains unknown.

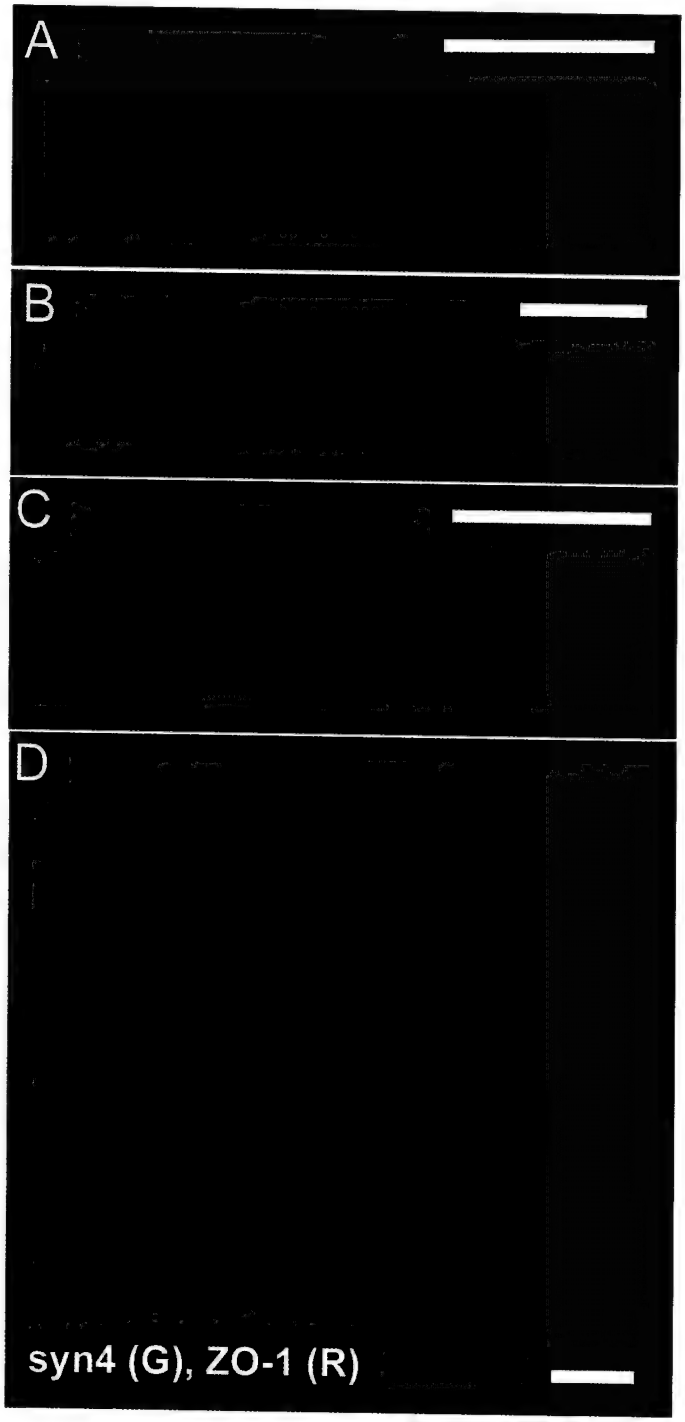

Fig. 6. Localization of syntaxin 4 in Madin-Darby canine kidney (MDCK) cell changes, depending on the degree of cell polarity and the culture system. *A*: MDCK cells were cultured on Transwell filters for 5 days and colabeled for endogenous syntaxin 4 (green) and the tight junction marker zonula occludens-1 (ZO-1; red). Shown is a confocal *X-Z* optical section with the apical plasma membrane at the *top*. Note the exclusively lateral localization of syntaxin 4. *B*: MDCK cells stably expressing COOH-terminal myc-tagged syntaxin 4 were cultured as above and subjected to surface labeling using anti-myc antibody. Note that the localization of recombinant syntaxin 4 is identical to that of the endogenous protein. *C*: the same cells as in *B* were cultured for 1 day to yield semipolarized cells. Surface immunolabeling revealed that under these conditions syntaxin 4 localizes to both the lateral and basal plasma membrane domains. *D*: MDCK cells were cultured in type-I collagen for the development of 3-dimensional cysts. Endogenous syntaxin 4 (green) and ZO-1 (red) were stained by coimmunolabeling and imaged by confocal fluorescence microscopy. Note that under these conditions syntaxin 4 localizes to both the basal and the lateral plasma membrane domains, resembling its localization in renal epithelial cells in vivo. Bars, 20 μm.

It is plausible that the cellular expression level of a given SNARE is at least a rough measure of the amount of traffic that depends on this SNARE and occurs in a given cell. For example, neurons express very high quantities of syntaxin 1, SNAP-25, and synaptobrevin, which are involved in synaptic vesicle exocytosis. Even a modest decrease in protein expression of syntaxin 1 and SNAP-25 results in decreased insulin secretion from pancreatic β-cells from islets in a rodent model of type 2 diabetes (43). Similarly, a 50% reduction in the expression level of syntaxin 4 in a heterozygous knockout mouse causes inhibition of GLUT4 transport to the plasma membrane in skeletal muscle cells (63). This suggests that the expression levels of SNAREs must be tightly regulated in concert with the cellular requirements for trafficking pathways that involve a given SNARE. Our results show that the expression level of syntaxin 4 is relatively uniform in all renal epithelial cell types (Fig. 7). This suggests that it performs a function that is required by all cell types. In nonepithelial cells, syntaxin 4 has been implicated in granule exocytosis in mast cells (50) and platelets (13) and insulin-stimulated GLUT4 translocation in skeletal muscle (63) and adipocytes (34, 40, 49, 60). In MDCK cells, syntaxin 4 is required for basolateral delivery of newly synthesized vesicular stomatitis virus G protein (26). This variety of trafficking pathways together with the uniform expression in renal epithelial cells suggest that syntaxin 4 functions as a "housekeeping" plasma membrane t-SNARE in many or all mammalian cells and that the "housekeeping trafficking pathways" in nonepithelial cell types correspond to pathways that lead to the basolateral domain of epithelial cells. Conceptually, the basolateral surfaces of virtually all epithelial cells face a similar environment, i.e., the underlying basement membrane and endothelial or connective tissue cells. It is there-

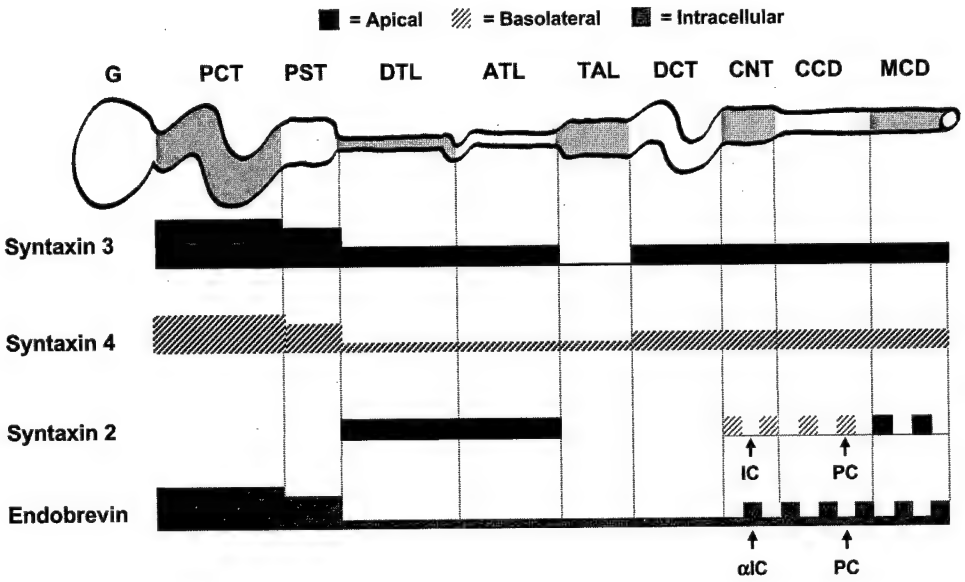

Fig. 7. Summary of expression and subcellular localization of syntaxins 2, 3, and 4 and endobrevin in different segments of the renal tubule. Shown is a schematic representation of the renal tubule with the segments indicated. The expression levels per cell of the SNAREs were estimated by integrating the pixel values of each tubule type as described in MATERIALS AND METHODS. The heights of the bars represent the relative expression levels for each SNARE. For abbreviations, see legend to Fig. 2.

fore likely that most epithelial cell types have similarly abundant common basolateral trafficking pathways that depend on syntaxin 4. Plausible examples are the secretion of extracellular matrix proteins, the recycling of membranes after endocytosis of growth factor receptors, etc.

In contrast, trafficking toward the apical surface of epithelial cells is expected to be highly cell type dependent because the environment that an epithelial cell faces apically can differ dramatically. This agrees well with our finding that the expression level of syntaxin 3 varies significantly among the renal tubule cell types. We have previously shown that syntaxin 3 is involved in two pathways in MDCK cells: apical delivery of newly synthesized membrane proteins and the apical recycling of apically internalized membranes (31). In a typical mammalian cell, the volume of recycling far outweighs that of biosynthetic traffic to the plasma membrane (57, 59). This difference is expected to be even more pronounced in nonproliferative, nonsecretory cell types such as renal tubule cells. Therefore, a high expression level of syntaxin 3 would be mostly indicative of a highly active apical recycling pathway. Indeed, we find the highest level of syntaxin 3 expression in the convoluted proximal tubule. This cell type exhibits a very high apical endocytosis rate for the absorption of proteins from the ultrafiltrate (11, 29, 47) and consequently recycles large amounts of membrane back to the apical plasma membrane. Interestingly, the highest expression level of the v-SNARE endobrevin is also found in the convoluted proximal tubule, and it localizes on apical endosomes underneath the brush border. GFP-tagged endobrevin has been reported to cycle through the apical plasma membrane of MDCK cells (58). We therefore suggest that in renal epithelial cells endobrevin functions as the v-SNARE on recycling vesicles that fuse with the apical plasma membrane utilizing syntaxin 3.

Whereas the polarities of syntaxins 3 and 4 are conserved throughout the renal tubule, the polarity of syntaxin 2 changes, depending on the cell type. Syntaxin 2 localizes to the basolateral plasma membrane in cortical principal cells, while it is apical in the principal cells of the medulla and in the thin loop of Henle. No expression is detectable in the other cell types. This suggests that syntaxin 2 is involved in a specialized trafficking pathway and that this pathway differs between cortical and medullary principal cells. We are unaware of a trafficking pathway whose polarity is known to be reversed in these two cell types. However, differences between medullary and cortical collecting duct principal cells have been reported previously. The apical renal urea transporter is expressed in medullary principal cells but absent in cortical principal cells (46). Also, medullary, but not cortical, principal cells exhibit prominent cytoplasmic fodrin staining (14). To date, syntaxin 2 has been implicated in two fusion events: zymogen granule exocytosis in pancreatic acinar cells (19) and the fusion of the acrosome with the plasma membrane of spermatozoa (25). Because these cell types differ significantly from renal epithelial cells, it is impossible to predict in which pathways syntaxin 2 may be involved, and functional studies will be required.

α- and β-Intercalated cells are classic examples of inversed sorting phenotypes between different epithelial cell types. They differ in their targeting of the vacuolar H^+-ATPase and other proteins (1, 9), which has led to the idea that cell polarity may be generally inversed between α- and β-intercalated cells. However, our finding that both cell types exhibit identical polarities of syntaxins 3 and 4 makes this very unlikely. Syntaxin 2 is not expressed in intercalated cells and can therefore play no role in differential H^+-ATPase targeting. It is possible that other, unidentified syntaxins may be differentially expressed at the plasma membranes of intercalated cells, but these would likely serve a very specialized trafficking pathway. We consider it more likely that the H^+-ATPase is differentially sorted into "conventional" apical or basolateral

trafficking pathways in α- and β-intercalated cells, respectively, which utilize syntaxin 3 or 4. This would predict that different classes of Golgi- or endosome-derived transport vesicles would be utilized for H^+-ATPase trafficking in α- and β-intercalated cells, which would likely contain different v-SNAREs. Interestingly, we found that endobrevin is highly expressed in intercalated cells and colocalizes with the H^+-ATPase in α- but not β-intercalated cells. This suggests that endobrevin is involved in apical H^+-ATPase trafficking in α-intercalated cells, whereas another v-SNARE would perform the equivalent function in β-intercalated cells.

Cultured MDCK cells are widely used as a model system for studying membrane trafficking. Recent attention has focused on the question of whether exocytic events occur all along the apical or basolateral plasma membrane domains or whether there are localized regions of vesicle fusion. It has been proposed that fusion events occur at the region of the tight junctions. This is based on the finding that several proteins implicated in membrane fusion localize there. These include rab8 (21), rab3b (61), rab13 (64), the sec6/8 complex or exocyst (18), and VAP-A (27). It had seemed odd that syntaxins apparently did not specifically localize to the tight junctions in MDCK cells. Recently, for the first time, the sites of fusion of post-Golgi transport vesicles in polarized MDCK cells could be identified by time-lapse fluorescence microscopy using GFP-tagged apical and basolateral marker proteins (Kreitzer G, Schmoranzer J, Low SH, Li X, Gan Y, Weimbs T, Simon SM, and Rodriguez-Boulan E, unpublished observations). These experiments demonstrated that basolateral transport vesicles fuse all along the lateral membrane, not just at the tight junctions. However, no fusion events were observed at the basal membrane. These findings agree well with the localization of syntaxin 4 in these cells, which is present along the lateral, but not basal, membrane. In contrast, syntaxin 4 does localize to the basal membrane of subconfluent, not fully polarized, MDCK cells, which agrees well with the observation of basal fusion events under these conditions (Kreitzer G, Schmoranzer J, Low SH, Li X, Gan Y, Weimbs T, Simon SM, and Rodriguez-Boulan E, unpublished observations). Altogether, these results suggest that the subcellular localization of syntaxins identifies the corresponding fusion sites. Because we find that syntaxin 4 localizes to both the lateral and basal domains of renal epithelial cells in vivo, this in turn suggests that vesicle fusion occurs all along the basolateral plasma membrane in vivo. Therefore, MDCK cells cultured on Transwell filters (the usual culture method) do not appear to faithfully reproduce the in vivo phenotype with respect to basolateral vesicle fusion. MDCK cells cultured as three-dimensional cysts in type-I collagen, however, target syntaxin 4 correctly to both domains.

In conclusion, we have shown that the expression levels of SNAREs and their subcellular localizations can differ very significantly among the epithelial cell types along the renal tubule. This agrees well with the known differences in epithelial trafficking phenotypes and suggests that regulation of SNARE expression and localization serves as a cellular mechanism to achieve, at least in part, these distinct phenotypes. In turn, the dysregulation of SNARE expression or localization may lead to abnormal intracellular trafficking and disease. Well-known examples of diseases involving epithelial cells and defects in polarized trafficking include polycystic kidney disease and microvillus inclusion disease (48).

We appreciate the gifts of reagents by Drs. Mark Bennett and Beatriz Quiñones (University of California Berkeley), Wanjin Hong (Institute for Molecular and Cell Biology, Singapore), Michael Jennings (University of Arkansas for Medical Sciences) and Xiao-Song Xie (University of Texas, Southwestern Medical Center). Elizabeth Loh and Zhizhou Zhang contributed to the construction of the expression vector for epitope-tagged human syntaxin 4.

This work was supported by a Jerry and Martha Jarrett Grant for Research on Polycystic Kidney Disease, National Institute of Diabetes and Digestive and Kidney Diseases Grant DK-62338, and Department of Defense Prostate Cancer Research Program Grant DAMD17-02-1-0039.

REFERENCES

1. **Al-Awqati Q, Vijayakumar S, Hikita C, Chen J, and Takito J.** Phenotypic plasticity in the intercalated cell: the hensin pathway. *Am J Physiol Renal Physiol* 275: F183–F190, 1998.
2. **Alper SL, Natale J, Gluck S, Lodish HF, and Brown D.** Subtypes of intercalated cells in rat kidney collecting duct defined by antibodies against erythroid band 3 and renal vacuolar H^+-ATPase. *Proc Natl Acad Sci USA* 86: 5429–5433, 1989.
3. **Antonin W, Holroyd C, Tikkanen R, Honing S, and Jahn R.** The R-SNARE endobrevin/VAMP-8 mediates homotypic fusion of early endosomes and late endosomes. *Mol Biol Cell* 11: 3289–3298, 2000.
4. **Bonilha VL, Marmorstein AD, Cohen-Gould L, and Rodriguez-Boulan E.** Apical sorting of influenza hemagglutinin by transcytosis in retinal pigment epithelium. *J Cell Sci* 110: 1717–1727, 1997.
5. **Breton S, Inoue T, Knepper MA, and Brown D.** Antigen retrieval reveals widespread basolateral expression of syntaxin 3 in renal epithelia. *Am J Physiol Renal Physiol* 282: F523–F529, 2002.
6. **Breuza L, Fransen J, and Le Bivic A.** Transport and function of syntaxin 3 in human epithelial intestinal cells. *Am J Physiol Cell Physiol* 279: C1239–C1248, 2000.
7. **Brown D.** Targeting of membrane transporters in renal epithelia: when cell biology meets physiology. *Am J Physiol Renal Physiol* 278: F192–F201, 2000.
8. **Brown D, Hirsch S, and Gluck S.** An H^+-ATPase in opposite plasma membrane domains in kidney epithelial cell subpopulations. *Nature* 331: 622–624, 1988.
9. **Brown D and Stow JL.** Protein trafficking and polarity in kidney epithelium: from cell biology to physiology. *Physiol Rev* 76: 245–297, 1996.
10. **Chen YA and Scheller RH.** SNARE-mediated membrane fusion. *Nat Rev Mol Cell Biol* 2: 98–106, 2001.
11. **Christensen EI, Nielsen S, Moestrup SK, Borre C, Maunsbach AB, de Heer E, Ronco P, Hammond TG, and Verroust P.** Segmental distribution of the endocytosis receptor gp330 in renal proximal tubules. *Eur J Cell Biol* 66: 349–364, 1995.
12. **Delgrossi MH, Breuza L, Mirre C, Chavrier P, and Le Bivic A.** Human syntaxin 3 is localized apically in human intestinal cells. *J Cell Sci* 110: 2207–2214, 1997.
13. **Flaumenhaft R, Croce K, Chen E, Furie B, and Furie BC.** Proteins of the exocytotic core complex mediate platelet alpha-granule secretion. Roles of vesicle-associated membrane protein, SNAP-23, and syntaxin 4. *J Biol Chem* 274: 2492–2501, 1999.

14. **Fujimoto T and Ogawa K.** Immunoelectron microscopy of fodrin in the rat uriniferous and collecting tubular epithelium. *J Histochem Cytochem* 37: 1345–1352, 1989.
15. **Fujita H, Tuma PL, Finnegan CM, Locco L, and Hubbard AL.** Endogenous syntaxins 2, 3 and 4 exhibit distinct but overlapping patterns of expression at the hepatocyte plasma membrane. *Biochem J* 329: 527–538, 1998.
16. **Gaisano HY, Ghai M, Malkus PN, Sheu L, Bouquillon A, Bennett MK, and Trimble WS.** Distinct cellular locations and protein-protein interactions of the syntaxin family of proteins in rat pancreatic acinar cells. *Mol Biol Cell* 7: 2019–2027, 1996.
17. **Galli T, Zahraoui A, Vaidyanathan VV, Raposo G, Tian JM, Karin M, Niemann H, and Louvard D.** A novel tetanus neurotoxin-insensitive vesicle-associated membrane protein in SNARE complexes of the apical plasma membrane of epithelial cells. *Mol Biol Cell* 9: 1437–1448, 1998.
18. **Grindstaff KK, Yeaman C, Anandasabapathy N, Hsu SC, Rodriguez-Boulan E, Scheller RH, and Nelson WJ.** Sec6/8 complex is recruited to cell-cell contacts and specifies transport vesicle delivery to the basal-lateral membrane in epithelial cells. *Cell* 93: 731–740, 1998.
19. **Hansen NJ, Antonin W, and Edwardson JM.** Identification of SNAREs involved in regulated exocytosis in the pancreatic acinar cell. *J Biol Chem* 274: 22871–22876, 1999.
20. **Hirai Y, Lochter A, Galosy S, Koshida S, Niwa S, and Bissell MJ.** Epimorphin functions as a key morphoregulator for mammary epithelial cells. *J Cell Biol* 140: 159–169, 1998.
21. **Huber LA, Pimplikar S, Parton RG, Virta H, Zerial M, and Simons K.** Rab8, a small GTPase involved in vesicular traffic between the TGN and the basolateral plasma membrane. *J Cell Biol* 123: 35–45, 1993.
22. **Ibaraki K, Horikawa HP, Morita T, Mori H, Sakimura K, Mishina M, Saisu H, and Abe T.** Identification of four different forms of syntaxin 3. *Biochem Biophys Res Commun* 211: 997–1005, 1995.
23. **Ihrke G and Hubbard AL.** Control of vesicle traffic in hepatocytes. *Prog Liver Dis* 13: 63–99, 1995.
24. **Jahn R and Sudhof TC.** Membrane fusion and exocytosis. *Annu Rev Biochem* 68: 863–911, 1999.
25. **Katafuchi K, Mori T, Toshimori K, and Iida H.** Localization of a syntaxin isoform, syntaxin 2, to the acrosomal region of rodent spermatozoa. *Mol Reprod Dev* 57: 375–383, 2000.
26. **Lafont F, Verkade P, Galli T, Wimmer C, Louvard D, and Simons K.** Raft association of SNAP receptors acting in apical trafficking in Madin-Darby canine kidney cells. *Proc Natl Acad Sci USA* 96: 3734–3738, 1999.
27. **Lapierre LA, Tuma PL, Navarre J, Goldenring JR, and Anderson JM.** VAP-33 localizes to both an intracellular vesicle population and with occludin at the tight junction. *J Cell Sci* 112: 3723–3732, 1999.
28. **Lehtonen S, Riento K, Olkkonen VM, and Lehtonen E.** Syntaxin 3 and Munc-18–2 in epithelial cells during kidney development. *Kidney Int* 56: 815–826, 1999.
29. **Lencer WI, Weyer P, Verkman AS, Ausiello DA, and Brown D.** FITC-dextran as a probe for endosome function and localization in kidney. *Am J Physiol Cell Physiol* 258: C309–C317, 1990.
30. **Low SH, Chapin SJ, Weimbs T, Kömüves LG, Bennett MK, and Mostov KE.** Differential localization of syntaxin isoforms in polarized MDCK cells. *Mol Biol Cell* 7: 2007–2018, 1996.
31. **Low SH, Chapin SJ, Wimmer C, Whiteheart SW, Kömüves LK, Mostov KE, and Weimbs T.** The SNARE machinery is involved in apical plasma membrane trafficking in MDCK cells. *J Cell Biol* 141: 1503–1513, 1998.
32. **Low SH, Miura M, Roche PA, Valdez AC, Mostov KE, and Weimbs T.** Intracellular redirection of plasma membrane trafficking after loss of epithelial cell polarity. *Mol Biol Cell* 11: 3045–3060, 2000.
33. **Low SH, Roche PA, Anderson HA, van Ijzendoorn SCD, Zhang M, Mostov KE, and Weimbs T.** Targeting of SNAP-23 and SNAP-25 in polarized epithelial cells. *J Biol Chem* 273: 3422–3430, 1998.
34. **Macaulay SL, Hewish DR, Gough KH, Stoichevska V, MacPherson SF, Jagadish M, and Ward CW.** Functional studies in 3T3L1 cells support a role for SNARE proteins in insulin stimulation of GLUT4 translocation. *Biochem J* 324: 217–224, 1997.
35. **Mandon B, Chou CL, Nielsen S, and Knepper MA.** Syntaxin-4 is localized to the apical plasma membrane of rat renal collecting duct cells: possible role in aquaporin-2 trafficking. *J Clin Invest* 98: 906–913, 1996.
36. **Mandon B, Nielsen S, Kishore BK, and Knepper MA.** Expression of syntaxins in rat kidney. *Am J Physiol Renal Physiol* 273: F718–F730, 1997.
37. **Maranda B, Brown D, Bourgoin S, Casanova JE, Vinay P, Ausiello DA, and Marshansky V.** Intra-endosomal pH-sensitive recruitment of the Arf-nucleotide exchange factor ARNO and Arf6 from cytoplasm to proximal tubule endosomes. *J Biol Chem* 276: 18540–18550, 2001.
38. **McNew JA, Parlati F, Fukuda R, Johnston RJ, Paz K, Paumet F, Sollner TH, and Rothman JE.** Compartmental specificity of cellular membrane fusion encoded in SNARE proteins. *Nature* 407: 153–159, 2000.
39. **Meier KE and Insel PA.** Hormone receptors and response in cultured renal epithelial cell lines. In: *Tissue Culture of Epithelial Cells*, edited by Taub M. New York: Plenum, 1985, p. 145–178.
40. **Min J, Okada S, Kanzaki M, Elmendorf JS, Coker KJ, Ceresa BP, Syu LJ, Noda Y, Saltiel AR, and Pessin JE.** Synip: a novel insulin-regulated syntaxin 4-binding protein mediating GLUT4 translocation in adipocytes. *Mol Cell* 3: 751–760, 1999.
41. **Mostov KE, Verges M, and Altschuler Y.** Membrane traffic in polarized epithelial cells. *Curr Opin Cell Biol* 12: 483–490, 2000.
42. **Moutairou K, Hayez N, Pohl V, Pattyn G, and Pochet R.** Calbindin localization in African giant rat kidney (*Cricetomys gambianus*). *Biochim Biophys Acta* 1313: 187–193, 1996.
43. **Nagamatsu S, Nakamichi Y, Yamamura C, Matsushima S, Watanabe T, Ozawa S, Furukawa H, and Ishida H.** Decreased expression of t-SNARE, syntaxin 1, and SNAP-25 in pancreatic beta-cells is involved in impaired insulin secretion from diabetic GK rat islets: restoration of decreased t-SNARE proteins improves impaired insulin secretion. *Diabetes* 48: 2367–2373, 1999.
44. **Nelson WJ and Yeaman C.** Protein trafficking in the exocytic pathway of polarized epithelial cells. *Trends Cell Biol* 11: 483–486, 2001.
45. **Nielsen S, DiGiovanni SR, Christensen EI, Knepper MA, and Harris HW.** Cellular and subcellular immunolocalization of vasopressin-regulated water channel in rat kidney. *Proc Natl Acad Sci USA* 90: 11663–11667, 1993.
46. **Nielsen S, Terris J, Smith CP, Hediger MA, Ecelbarger CA, and Knepper MA.** Cellular and subcellular localization of the vasopressin-regulated urea transporter in rat kidney. *Proc Natl Acad Sci USA* 93: 5495–5500, 1996.
47. **Obermuller N, Kranzlin B, Blum WF, Gretz N, and Witzgall R.** An endocytosis defect as a possible cause of proteinuria in polycystic kidney disease. *Am J Physiol Renal Physiol* 280: F244–F253, 2001.
48. **Olkkonen VM and Ikonen E.** Genetic defects of intracellular-membrane transport. *N Engl J Med* 343: 1095–1104, 2000.
49. **Olson AL, Knight JB, and Pessin JE.** Syntaxin 4, VAMP2, and/or VAMP3/cellubrevin are functional target membrane and vesicle SNAP receptors for insulin-stimulated GLUT4 translocation in adipocytes. *Mol Cell Biol* 17: 2425–2435, 1997.
50. **Paumet F, Le Mao J, Martin S, Galli T, David B, Blank U, and Roa M.** Soluble NSF attachment protein receptors (SNAREs) in RBL-2H3 mast cells: functional role of syntaxin 4 in exocytosis and identification of a vesicle-associated membrane protein 8-containing secretory compartment. *J Immunol* 164: 5850–5857, 2000.
51. **Peng SB, Crider BP, Tsai SJ, Xie XS, and Stone DK.** Identification of a 14-kDa subunit associated with the catalytic sector of clathrin-coated vesicle H^+-ATPase. *J Biol Chem* 271: 3324–3327, 1996.
52. **Pollack AL, Runyan RB, and Mostov KE.** Morphogenetic mechanisms of epithelial tubulogenesis: MDCK cell polarity is transiently rearranged without loss of cell-cell contact during

scatter factor/hepatocyte growth factor-induced tubulogenesis. *Dev Biol* 204: 64–79, 1998.

53. **Quinones B, Riento K, Olkkonen VM, Hardy S, and Bennett MK.** Syntaxin 2 splice variants exhibit differential expression patterns, biochemical properties and subcellular localizations. *J Cell Sci* 112: 4291–4304, 1999.
54. **Riento K, Galli T, Jansson S, Ehnholm C, Lehtonen E, and Olkkonen VM.** Interaction of munc-18–2 with syntaxin 3 controls the association of apical SNAREs in epithelial cells. *J Cell Sci* 111: 2681–2688, 1998.
55. **Rodger J, Davis S, Laroche S, Mallet J, and Hicks A.** Induction of long-term potentiation in vivo regulates alternate splicing to alter syntaxin 3 isoform expression in rat dentate gyrus. *J Neurochem* 71: 666–675, 1998.
56. **Scales SJ, Chen YA, Yoo BY, Patel SM, Doung YC, and Scheller RH.** SNAREs contribute to the specificity of membrane fusion. *Neuron* 26: 457–464, 2000.
57. **Snider MD and Rogers OC.** Membrane traffic in animal cells: cellular glycoproteins return to the site of Golgi mannosidase I. *J Cell Biol* 103: 265–275, 1986.
58. **Steegmaier M, Lee KC, Prekeris R, and Scheller RH.** SNARE protein trafficking in polarized MDCK cells. *Traffic* 1: 553–560, 2000.
59. **Steinman RM, Mellman IS, Muller WA, and Cohn ZA.** Endocytosis and the recycling of plasma membrane. *J Cell Biol* 96: 1–27, 1983.
60. **Tellam JT, Macaulay SL, McIntosh S, Hewish DR, Ward CW, and James DE.** Characterization of Munc-18c and syntaxin-4 in 3T3-L1 adipocytes. Putative role in insulin-dependent movement of GLUT-4. *J Biol Chem* 272: 6179–6186, 1997.
61. **Weber E, Berta G, Tousson A, St. John P, Green MW, Gopalokrishnan U, Jilling T, Sorscher EJ, Elton TS, Abrahamson DR, and Kirk KL.** Expression and polarized targeting of a rab3 isoform in epithelial cells. *J Cell Biol* 125: 583–594, 1994.
62. **Weimbs T, Low SH, Chapin SJ, and Mostov KE.** Apical targeting in polarized epithelial cells: there's more afloat than rafts. *Trends Cell Biol* 7: 393–399, 1997.
63. **Yang C, Coker KJ, Kim JK, Mora S, Thurmond DC, Davis AC, Yang B, Williamson RA, Shulman GI, and Pessin JE.** Syntaxin 4 heterozygous knockout mice develop muscle insulin resistance. *J Clin Invest* 107: 1311–1318, 2001.
64. **Zahraoui A, Joberty G, Arpin M, Fontaine JJ, Hellio R, Tavitian A, and Louvard D.** A small rab GTPase is distributed in cytoplasmic vesicles in non polarized cells but colocalizes with the tight junction marker ZO-1 in polarized epithelial cells. *J Cell Biol* 124: 101–115, 1994.
65. **Zolotnitskaya A and Satlin LM.** Developmental expression of ROMK in rat kidney. *Am J Physiol Renal Physiol* 276: F825–F836, 1999.
66. **Zurzolo C, Le Bivic A, Quaroni A, Nitsch L, and Rodriguez-Boulan E.** Modulation of transcytotic and direct targeting pathways in a polarized thyroid cell line. *Embo J* 11: 2337–2344, 1992.

Retinal pigment epithelial cells exhibit unique expression and localization of plasma membrane syntaxins which may contribute to their trafficking phenotype

Seng Hui Low[1], Lihua Y. Marmorstein[3], Masumi Miura[1], Xin Li[1], Noriko Kudo[1], Alan D. Marmorstein[1,3] and Thomas Weimbs[1,2,*]

[1]Department of Cell Biology, Lerner Research Institute, Cleveland, Ohio 44195, USA
[2]Urological Institute, [3]Department of Ophthalmic Research, Cleveland Clinic Foundation, Cleveland, Ohio 44195, USA
*Author for correspondence (e-mail: weimbst@lerner.ccf.org)

Accepted 21 August 2002
Journal of Cell Science 115, 4545-4553 © 2002 The Company of Biologists Ltd
doi:10.1242/jcs.00116

Summary

The SNARE membrane fusion machinery controls the fusion of transport vesicles with the apical and basolateral plasma-membrane domains of epithelial cells and is implicated in the specificity of polarized trafficking. To test the hypothesis that differential expression and localization of SNAREs may be a mechanism that contributes to cell-type-specific polarity of different proteins, we studied the expression and distribution of plasma-membrane SNAREs in the retinal pigment epithelium (RPE), an epithelium in which the targeting and steady-state polarity of several plasma membrane proteins differs from most other epithelia. We show here that retinal pigment epithelial cells both in vitro and in vivo differ significantly from MDCK cells and other epithelial cells in their complement of expressed t-SNAREs that are known – or suggested – to be involved in plasma membrane trafficking. Retinal pigment epithelial cells lack expression of the normally apical-specific syntaxin 3. Instead, they express syntaxins 1A and 1B, which are normally restricted to neurons and neuroendocrine cells, on their apical plasma membrane. The polarity of syntaxin 2 is reversed in retinal pigment epithelial cells, and it localizes to a narrow band on the lateral plasma membrane adjacent to the tight junctions. In addition, syntaxin 4 and the v-SNARE endobrevin/VAMP-8 localize to this sub-tight junctional domain, which suggests that this is a region of preferred vesicle exocytosis. Altogether, these data suggest that the unique polarity of many retinal pigment epithelial proteins results from differential expression and distribution of SNAREs at the plasma membrane. We propose that regulation of the expression and subcellular localization of plasma membrane SNAREs may be a general mechanism that contributes to the establishment of distinct sorting phenotypes among epithelial cell types.

Key words: Epithelial polarity, Membrane traffic, SNARE

Introduction

Epithelial cells exhibit characteristic polarized distribution patterns of proteins and lipids on their apical and basolateral plasma-membrane domains (Mostov et al., 2000; Yeaman et al., 1999). This polarity is essential for proper epithelial function. Polarized protein transport to the plasma membrane of epithelial cells depends on highly specific vesicular membrane traffic pathways that recognize sorting signals encoded in the cargo proteins.

In higher metazoan organisms a large variety of epithelial cell types perform a multitude of different functions. The apical surfaces of these cell types can face dramatically different environments. Extreme examples are epithelial cells lining the stomach, colon, bile duct, urinary tract, and the retinal pigment epithelium (RPE). Correspondingly, different epithelial cell types require different sets of apical and basolateral surface proteins to perform their unique roles in the body.

In many cases, apical and basolateral sorting signals are recognized and interpreted identically between different epithelial cell types. In other cases, identical proteins can be sorted to different plasma-membrane domains in different epithelial cell types. One example is the Na^+/K^+-ATPase, which is localized to the basolateral domain in the vast majority of epithelial cells types. However, in a few epithelia, such as the RPE and the choroid plexus epithelium, the Na^+/K^+-ATPase localizes apically (Marmorstein, 2001; Marrs et al., 1995). Proteins can also be ultimately targeted to the same domain but the pathway that they take to reach this domain differs between cell types. For example, in the Madin Darby canine kidney (MDCK) cell line, newly synthesized influenza virus hemagglutinin (HA) is directly targeted from the Golgi to the apical plasma membrane (Matlin and Simons, 1984; Misek et al., 1984). By contrast, in the RPE it is first transported to the basolateral plasma membrane and subsequently endocytosed and transcytosed to the apical surface (Bonilha et al., 1997). It is currently unknown how the variability in sorting phenotypes between different epithelial cell types is accomplished.

The RPE has long been recognized to differ from many other epithelia in the polarity of a number of proteins (Marmorstein, 2001). A unique characteristic of RPE cells is that their apical plasma membrane is in contact with the extracellular matrix (the interphotoreceptor matrix) whereas almost all other epithelia face an apical lumen devoid of matrix. Other proteins that are sorted differently in RPE compared with most epithelia include the extracellular matrix metalloproteinase inducer (EMMPRIN; apical) (Marmorstein et al., 1998), N-CAM (apical) (Marmorstein et al., 1998), αvβ5 integrin (apical) (Finnemann et al., 1997), and possibly CFTR, which is thought to be basolateral in RPE cells but is apically localized in other epithelia (Gallemore et al., 1998). Furthermore, physiological experiments have demonstrated that Ca^{2+}-sensitive chloride channels, which are typically present on the apical membrane of epithelial cells, are basolaterally polarized in RPE cells (Gallemore et al., 1998).

It is unknown whether the establishment of different epithelial sorting phenotypes involves major changes in the machineries involved in polarized targeting or simply the rerouting of proteins into different sorting pathways. SNARE-mediated membrane fusion is the final step in all vesicle trafficking pathways (Chen and Scheller, 2001; Jahn and Sudhof, 1999). SNAREs belong to several related protein families (Weimbs et al., 1997; Weimbs et al., 1998), and different family members usually exhibit a distinct subcellular localization and function only in specific trafficking pathways. Only 'matching' combinations of v- and t-SNAREs lead to successful membrane fusion (McNew et al., 2000; Scales et al., 2000), suggesting that the SNARE machinery plays a role not only in the mechanics of the fusion process but also in its specificity. Members of the syntaxin family of t-SNAREs appear to play a central role since syntaxins can interact with virtually all other components implicated in SNARE-mediated membrane fusion. It is reasonable to assume that the presence of a given syntaxin on a membrane domain determines which classes of transport vesicles will be able to fuse with that domain. We hypothesized that a feasible mechanism contributing to the known variety of epithelial trafficking phenotypes is for different epithelial cell types to express different sets of plasma membrane syntaxins and/or to localize them to different domains.

The best characterized epithelial model system to date is the MDCK cell line. We have previously shown that in these cells the t-SNAREs syntaxin 3 and 4 are specifically localized at the apical or basolateral plasma membrane domains, respectively (Low et al., 1996). Syntaxin 3 is functionally involved in trafficking from the TGN to the apical plasma membrane and in apical recycling (Low et al., 1998a). Syntaxin 4 is involved in TGN-to-basolateral trafficking (Lafont et al., 1999). Two other syntaxins, syntaxin 2 and 11, are also expressed at the plasma membrane in MDCK cells but they are present in both domains and their function is unknown (Low et al., 1996; Low et al., 2000). In general, the localization of these t-SNAREs appears to be well conserved in a number of other epithelial cell lines and tissues such as Caco-2 cells, HepG2 cells, hepatocytes, kidney epithelium and intestinal epithelium (Delgrossi et al., 1997; Fujita et al., 1998; Galli et al., 1998; Lehtonen et al., 1999; Li et al., 2002; Low et al., 1998b; Riento et al., 1998). Syntaxin 3, however, has been found to deviate from its normal apical plasma membrane localization in two specialized epithelial cell types. It localizes to zymogen granules in pancreatic acinar cells (Gaisano et al., 1996) and to H^+/K^+-ATPase-containing tubulovesicles in non-stimulated gastric parietal cells (Peng et al., 1997). Moreover, syntaxin 2 localizes to the apical plasma-membrane domain in pancreatic acinar cells (Gaisano et al., 1996) in contrast to its non-polarized distribution in MDCK cells.

We hypothesized that changes in SNARE expression and/or subcellular localization may contribute to the differential sorting phenotypes of specialized epithelial cell types. To test this, we investigated the expression and localization of the plasma membrane SNARE machinery in RPE cells in vitro and in vivo. We report here that RPE cells in vitro and in vivo differ significantly from MDCK cells and other epithelial cells in the expressed complement of SNARE proteins as well as in their subcellular localization. Altogether, our results suggest that the differential expression and subcellular localization of SNAREs is used as a general mechanism contributing to the modulation of epithelial sorting phenotypes and is at least in part responsible for the unique distribution of plasma membrane proteins in the RPE.

Materials and Methods

Materials

Cell culture media were from the Lerner Research Institute Cell Culture Facility. Fetal bovine serum was from ICN Biomedicals (Costa Mesa, CA). Transwell polycarbonate cell culture filters were purchased from Corning Costar Corporation (Massachusetts, MA). Affinity-purified polyclonal antibodies against the cytoplasmic domains rat syntaxins 2, 3 and 4 and against an C-terminal peptide of human SNAP-23 have been described previously (Low et al., 2000; Low et al., 1998b). Rabbit antiserum was raised against a GST fusion protein of the cytoplasmic domain of rat endobrevin. The expression plasmid was a gift from Wanjin Hong (Institute for Molecular and Cell Biology, Singapore). The endobrevin antibody was affinity-purified against the immobilized cytoplasmic domain of endobrevin without GST. In addition, a similarly raised and affinity-purified rabbit antibody against endobrevin was a gift from Wanjin Hong. Affinity-purified polyclonal antibodies against rat syntaxins 1A, 1B, 2, 3 and 4 were gifts from Mark Bennett and Beatriz Quinones (UC Berkeley). A polyclonal antibody against a peptide from syntaxin*1B (peptide sequence identical in mouse, rat, cow, human) was from Synaptic Systems GmbH (Göttingen, Germany). A mouse monoclonal antibody against occludin was from Zymed Laboratories (South San Francisco, CA). A rat monoclonal antibody against ZO-1 was from Chemicon International (Temacula, CA). Secondary antibodies, cross-absorbed against multiple species and conjugated to FITC, Texas Red or Cy5 were from Jackson Immunoresearch (West Grove, PA).

Cell culture

RPE-J cells were from ATCC (CRL-2240) and cultured in Dulbecco's Modified Eagle's medium containing 4 mM glutamine, 1.5 g/l sodium bicarbonate, 4.5 g/l glucose and 1 mM sodium pyruvate. This media was further supplemented with 4% FBS, non-essential amino acids and penicillin and streptomycin. The cells were maintained at 32°C and 5% CO_2. For polarized monolayers, the cells were plated at 300,000 cells/cm^2 on Matrigel-coated Transwell Filters (Corning, Acton, MA) in culture medium supplemented with 2.5 nM retinoic acid and cultured for 1 week at 32°C. The cells were then transferred to a 40°C incubator for another week. The media was changed every 3 days.

Tissue and cell extracts, SDS-PAGE and immunoblotting

Total protein fractions of RPE-J cells were prepared by directly lysing cells from confluent dishes by boiling in SDS-PAGE sample buffer.

DNA was sheared by passing lysates through a 22G needle. Rat kidney and brain lysates were prepared by dissecting out the tissues and finely mincing with a razor blade. The tissues were then Dounce-homogenized in PBS containing 10 mM EDTA, protease inhibitors and PMSF. SDS was added to a final concentration of 2% and the lysate was passed through a 22G needle to shear the DNA, and the sample was boiled for 5 minutes. Proteins were separated on 10% or 15% SDS-polyacrylamide gels followed by transfer to PVDF membrane and incubation with the indicated antibodies. Bands were visualized by enhanced chemiluminescence.

RT-PCR

Total RNA was isolated from RPE-J cells, rat kidney or rat brain by using Trizol (GIBCO) according to the manufacturer's instructions. 5 μg of total RNA were used for reverse transcription in a 25 μl total volume using random hexamers as primers. For the detection of syntaxin 2 isoforms, 1 μl of the reverse-transcribed samples were used for 50 μl PCR reactions using primers and conditions as described previously (Quinones et al., 1999). The following primer pairs were designed to recognize rat syntaxin 3A; 5′-GCTGAGATGTTAG-ATAACATAG-3′ and 5′-TTCAGCCCAACGGACAATCCAA-3′ or syntaxin 3B; 5′-CAGGGAGCCATGATTGACCGTA-3′ and 5′-AAATATGCCCCCAATGGTAGAA-3′, utilizing the same PCR conditions as for syntaxin 2. 10 μl of each PCR reaction were separated on 2% agarose gels.

Immunolocalization

Sprague-Dawley rats were anesthetized by intraperitoneal administration of sodium pentobarbital (50 mg/kg) and perfused via the left ventricle with 4% paraformaldehyde in PBS containing 1 mM calcium and 1 mM magnesium for 20 minutes. The eyes were enucleated, the anterior segments removed, and the eyecups stored in the same fixative overnight at 4°C. Fixed eyecups were then dehydrated and embedded in paraffin. Immunostaining was carried out on 5 μm sections. After deparaffinization and rehydration to PBS, the sections were subjected to heat-mediated antigen retrieval by pressure cooking in 10 mM citric acid buffer, pH 6.0. The sections were blocked with 3% BSA, 2% Triton X-100 in PBS, incubated with the indicated antibodies overnight at 4°C. The reactions were visualized with fluorescein- and Texas-Red-labeled secondary antibodies (Jackson ImmunoResearch, West Grove, PA). SNARE-signals were amplified by incubating with Alexa 488-labeled rabbit anti-FITC antibody (Molecular Probes) after FITC-labeled secondary antibodies. Nuclei were stained with DAPI. The fluorescent staining was analyzed using a confocal laser scanning microscope (TCS-NT, Leica, Benseim, Germany). Immunostaining for syntaxins 1B, 2, 3, 4 and endobrevin was verified using two independently raised antibodies each of which resulted in identical staining patterns. Only one antibody was available against syntaxin 1A.

For immunostaining of cultured RPE-J cells, cells were either fixed in methanol at –20°C or with 4% paraformaldehyde in PBS, permeabilized with 0.025% (wt/vol) saponin Sigma (St. Louis, MO) in PBS and blocked with 3% BSA followed by sequential incubations with primary antibodies and FITC- and Texas-red-conjugated secondary antibodies. Signal amplification and imaging were performed as described above.

Results

SNARE protein expression pattern in RPE-J cells

To investigate the expression pattern in RPE cells of t- and v-SNAREs that are normally involved in plasma membrane fusion in other cell types we made use of a cell line derived from rat RPE. These cells, RPE-J, were immortalized by infection with a temperature-sensitive SV40 virus (Nabi et al., 1993). RPE-J cells polarize in culture and have many of the attributes of native RPE, such as the ability to phagocytose photoreceptor outer segments (Finnemann et al., 1997). Total lysates of polarized RPE-J cells were separated by SDS-PAGE and probed by western blot using a panel of SNARE-specific antibodies. For comparison, equal amounts of total homogenate from rat kidney or 1/10 of the amount of total rat brain homogenate were investigated side-by-side. Among the SNAREs that are expressed in MDCK and other epithelial cells, the expression levels of syntaxins 2, 4 and SNAP-23 are roughly comparable between RPE-J cells and kidney (Fig. 1A). By contrast, syntaxin 3 was undetectable in RPE-J cells. The v-SNAREs cellubrevin and endobrevin are found in both kidney and RPE-J cells.

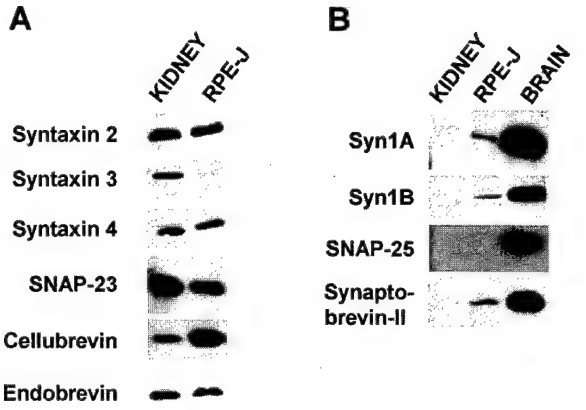

Fig. 1. Comparison of SNARE expression in RPE-J cells and rat kidney or brain by western blot analysis. Equal protein amounts of total homogenates of differentiated RPE-J cells, rat kidney or rat brain (1/10 of the protein) were separated by SDS-PAGE and analyzed by western blot with specific antibodies as indicated. Note that syntaxin 3 is virtually undetectable in RPE-J cells. By contrast, the expression levels of syntaxins 2 and 4 are roughly comparable between RPE-J and rat kidney. SNAP-23, cellubrevin and endobrevin are expressed in both kidney and RPE-J. RPE-J cells also express the 'neuron-specific' t-SNAREs syntaxin 1A and 1B but there is no detectable SNAP-25.

Next, we investigated the possible expression of SNAREs that are typically restricted to neurons and neuroendocrine cells. Brain tissue contains very large amounts of the t-SNAREs syntaxin 1A, syntaxin 1B, SNAP-25 and of the v-SNARE synaptobrevin-2, all of which are involved in calcium-regulated synaptic vesicle exocytosis. Surprisingly, RPE-J cells expressed significant quantities of syntaxins 1A, 1B and synaptobrevin-2 (Fig. 1B). However, no SNAP-25 was detectable even after prolonged exposure of the blot (data not shown). None of these SNAREs were detectable in kidney, with the exception of low amounts of synaptobrevin-2.

In summary, the SNARE expression pattern of RPE-J cells shows two unexpected features: the absence of the normally apical-specific syntaxin 3 and the presence of 'neuronal' SNAREs.

Expression of syntaxin 2 and 3 transcripts in RPE-J cells

Four syntaxin 2 isoforms derived from alternative RNA

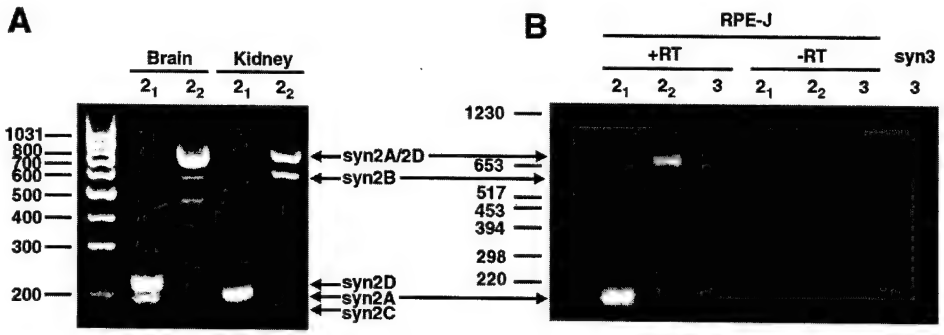

Fig. 2. RT-PCR analysis of syntaxin isoform expression in RPE-J cells. mRNA of syntaxin 3 and of different alternatively spliced isoforms of syntaxin 2 were amplified by RT-PCR. For syntaxin 2 isoform determination, two primer pairs were used that had been previously shown to distinguish between isoforms 2A, 2B, 2C and 2D (Quinones et al., 1999). Primer combination 2_1 generates the following PCR products: syntaxin 2A (200 bp), 2D (228 bp), no products for syntaxin 2B and 2C. Primer combination 2_2 generates the following PCR products: syntaxin 2A (700 bp), 2B (600 bp), 2C (170 bp), 2C 170 bp), 2D (728 bp). The respective positions of the different products are indicated by arrows. A shows that transcripts for syntaxin 2A, B and C can be detected in rat kidney. Rat brain expresses all four syntaxin 2 isoforms as previously reported. As shown in B, reaction products for syntaxins 2A and 2B were detected from RPE-J cells but not 2C, 2D. For the detection of syntaxin 3A transcripts, a single primer pair was used. B shows that syntaxin-3A-specific reaction product was detected in the positive control (lane 'syn3', rat syntaxin 3A cDNA as template), whereas no syntaxin 3A product could be detected from RPE-J cells. As a negative control, no products were detected in samples that were not reverse transcribed (-RT).

splicing have previously been identified in rat tissues. Syntaxins 2A and 2B are membrane anchored by hydrophobic domains, whereas syntaxin 2C and 2D lack hydrophobic domains and are only partially membrane bound (Quinones et al., 1999). All four syntaxin 2 isoforms differ only in their C-termini whereas the N-terminal bulk of their sequences are identical. Since our polyclonal syntaxin 2 antibodies react with all four isoforms (data not shown) and since the molecular weights of these isoforms are very similar, they can not be distinguished from each other by western blot analysis. In order to investigate which syntaxin 2 isoforms are expressed in RPE-J cells and to confirm the observed absence of syntaxin 3-expression, we analyzed total RNA by RT-PCR. We used two primer combinations that have previously been shown to distinguish between the four different rat syntaxin 2 isoforms (Quinones et al., 1999). Fig. 2A shows that all four syntaxin 2 isoforms could be detected in rat brain whereas rat kidney expressed syntaxins 2A, B and C as previously described. By contrast, in RPE-J cells, syntaxins 2A and a lesser amount of syntaxin 2B, but no transcripts for syntaxins 2C or 2D, could be detected (Fig. 2). No syntaxin 3 transcripts were detectable, confirming the lack of expression observed on the protein level.

SNARE localization in RPE-J cells

To determine the subcellular localization of the expressed t-SNAREs, RPE-J cells were cultured as polarized monolayers on Matrigel-coated polycarbonate filters, labeled with affinity-purified syntaxin antibodies and analyzed by confocal fluorescence microscopy. As expected, syntaxin 3 was undetectable (data not shown). Fig. 3 shows that both syntaxins 2 and 4 localize to the plasma membrane at the regions of cell-cell contact whereas no significant apical staining was detectable. Both syntaxins 2 and 4 colocalize with the basolateral marker EMMPRIN as well as with the tight junction protein ZO-1. Since RPE-J cells are typically flat (Marmorstein et al., 1998), it was not possible to determine by light microscopy whether syntaxin 2 and 4 are distributed all along the lateral membrane or whether they are concentrated close to the tight junctions. The expression levels of syntaxins 1A and 1B were below the detection limit.

In conclusion, syntaxin 4 localizes to the basolateral plasma membrane domain in RPE-J cells similar to all previously investigated epithelial cell types. However, syntaxin 2 localizes to the basolateral plasma membrane domain, which is in striking contrast to its apical localization in other epithelial cell types.

SNARE localization in RPE in situ

RPE-J cells and other cultured RPE cells have been found to differ in their protein-sorting phenotype from RPE cells in situ. Na^+/K^+-ATPase, N-CAM and EMMPRIN, which are apically polarized in RPE cells in the eye, are typically non-polar or basolateral in culture (Marmorstein, 2001). We therefore investigated SNARE expression and subcellular localization in rat retina. Sections of the posterior pole of rat eyes were fluorescently double-labeled using SNARE-specific antibodies and antibodies against various marker proteins and analyzed by confocal microscopy. Cryosections and paraffin sections yielded identical results. Fig. 4A shows that syntaxin 3 is abundantly expressed in photoreceptor cells but is not detectable above background in RPE cells, in agreement with our results on RPE-J cells.

As predicted from our studies on RPE-J cells, syntaxins 2, 4, 1A and 1B are all clearly detectable in RPE cells in situ. Syntaxins 2 and 4 exhibit a surprising subcellular localization. Syntaxin 2 is restricted to a narrow band that localizes closely with the tight junctional protein occludin. At higher magnification it was apparent that these two proteins do not exactly overlap but that syntaxin 2 localizes to a region of the lateral plasma membrane basal to the tight junctions (Fig. 4D). Since the tight junctions represent the border between the apical and basolateral plasma membrane domains in epithelial cells, syntaxin 2 is therefore a basolateral SNARE in RPE cells in contrast to its apical localization in other epithelial cells. This is in agreement with our results on RPE-J cells.

Syntaxin 4 also localizes to the same narrow band underneath the tight junctions. However, in contrast to syntaxin 2, it is also clearly present at the basal plasma membrane of RPE cells (Fig. 4E). Both syntaxin 1A (Fig. 4B) and syntaxin 1B (Fig. 4C) are localized throughout the apical plasma

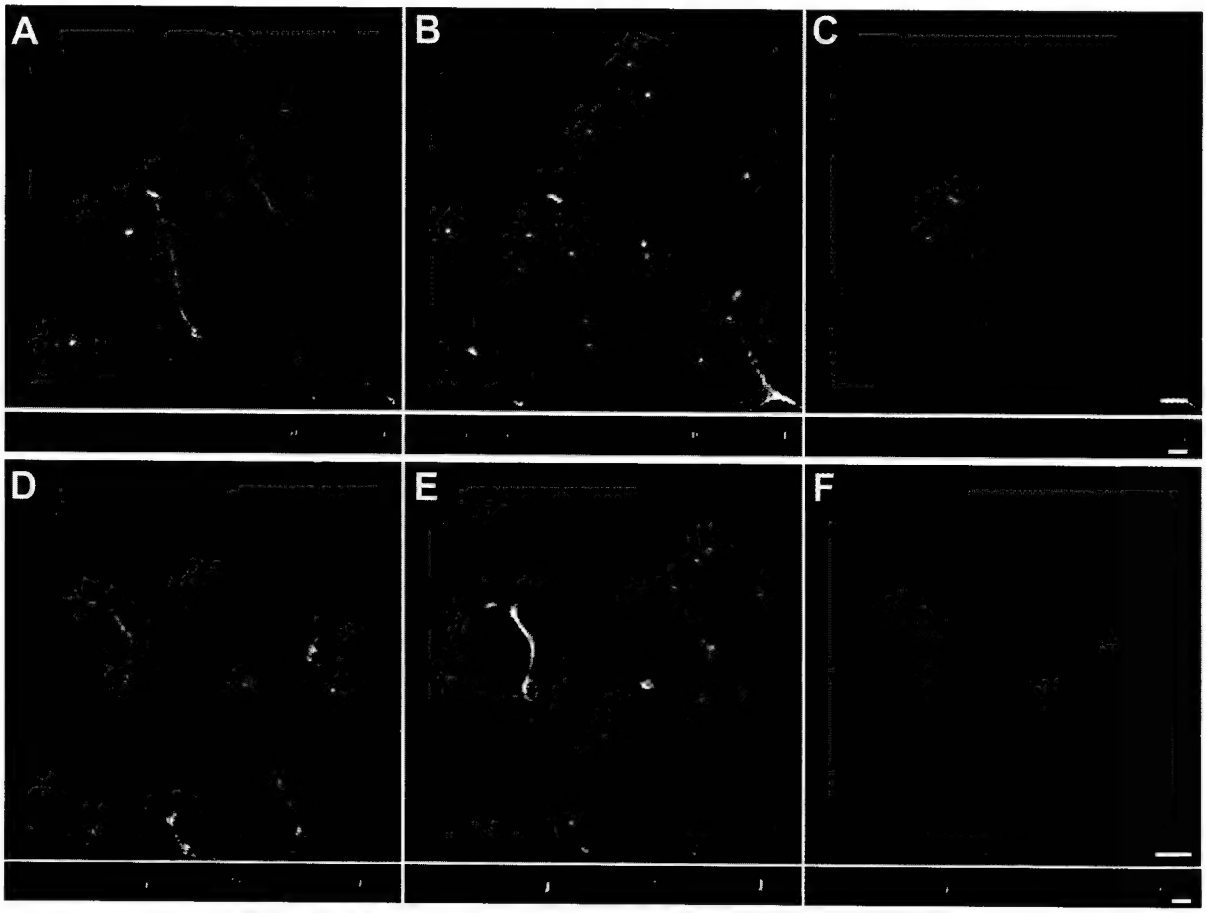

Fig. 3. Localization of syntaxins 2 and 4 in RPE-J cells. Polarized monolayers of RPE-J cells were cultured on Transwell filters, and syntaxin localizations were analyzed by double-label confocal immunofluorescence microscopy. Panels A-C and D-F, respectively, represent the same fields of xy confocal sections. Small panels underneath are xz confocal sections. A shows immunostaining for syntaxin 2, B for the tight junction protein ZO-1 and C the color-merged image. D shows immunostaining for syntaxin 4, E for the basolateral plasma membrane protein EMMPRIN and F the color-merged image. Note that syntaxin 2 and ZO-1 colocalize throughout most of the areas of cell-cell contact. However, the localization of ZO-1 at the tight junctions is more uniform. There are areas of intense syntaxin 2 staining, whereas others are nearly devoid of it. Syntaxin 4 and EMMPRIN both colocalize in a relatively uniform fashion at the areas of cell-cell contact. Bars, 5 μm.

membrane in RPE cells, which constitutes 75% of the total RPE plasma membrane owing to microvilli that interdigitate with the photoreceptor outer segments. The outer segments themselves are negative for both syntaxins.

Endobrevin is a v-SNARE that has been found to be most highly expressed in epithelial cells. It has been implicated in endosome fusion in non-epithelial cells (Antonin et al., 2000) but has also been shown to cycle through the apical plasma membrane in MDCK cells (Steegmaier et al., 2000). Fig. 4F shows that endobrevin was surprisingly also highly concentrated underneath the tight junctions in RPE cells similar to syntaxins 2 and 4. In addition, endobrevin localized to intracellular vesicles throughout the cytoplasm.

Immunostaining results for syntaxins 1B, 2, 3, 4 and endobrevin were confirmed using independently raised antibodies and yielded identical results (see Materials and Methods, data not shown).

Discussion

The retinal pigment epithelium is a prime example of an epithelial cell type exhibiting unique cell polarity and intracellular trafficking (Marmorstein, 2001). Other examples include the α- and β-intercalated cells of the renal connecting tubule (Al-Awqati et al., 1998), the choroid plexus epithelium, the Fischer rat thyroid (FRT) cell line and the renal LLC-PK_1 cell line. In these epithelial cells, the targeting of several plasma membrane proteins was found to differ from that of the MDCK cell line – the most frequently studied model system. So far, only in the case of LLC-PK_1 cells has a molecular cause of the different targeting phenotype been identified. This cell line lacks expression of the μ1B subunit of the epithelial-specific AP-1B adaptor, which results in the inability to recognize tyrosine-based basolateral targeting signals (Fölsch et al., 1999; Fölsch et al., 2001) in the endocytic pathway (Gan et al., 2002). Consequently, several normally basolateral proteins are apically mistargeted in LLC-PK_1 cells. It is, however, unclear whether the absence of μ1B expression represents a defect or may indeed be used by epithelial cell types in vivo to achieve a certain sorting phenotype. FRT cells are known to target most GPI-anchored proteins to the basolateral plasma membrane, whereas they are apically

targeted in MDCK and most other epithelial cells (Zurzolo et al., 1993). The relevance of the sorting phenotype in the FRT cell line is unclear, however, since GPI-anchored proteins are correctly apically targeted in primary thyroid epithelial cells (Kuliawat et al., 1995).

In the present work we tested our hypothesis that the expression of different sets of plasma membrane syntaxins and/or their localization to different domains is a mechanism contributing to the known variety of epithelial trafficking phenotypes. Our investigation of this possibility using RPE cells as an example of an epithelium with a polarity phenotype that diverges substantially from the prototypic MDCK cell is in agreement with this hypothesis. Fig. 5 shows a schematic summary of the results.

RPE cells both in vitro and in vivo lack expression of the normally apical-specific syntaxin 3. This may suggest that a trafficking pathway that normally involves syntaxin 3 is absent in this cell type. This finding is in excellent agreement with a known difference in the targeting of the influenza virus hemagglutinin (HA) in RPE cells. We have previously shown that syntaxin 3 functions in transport from the trans-Golgi network to the apical plasma membrane in MDCK cells (Low et al., 1998a) (route A in Fig. 5). This route is taken by newly synthesized HA in MDCK cells (Matlin and Simons, 1984; Misek et al., 1984), and indeed Lafont et al. could demonstrate that apical HA-trafficking in MDCK cells is syntaxin 3 dependent (Lafont et al., 1999). By contrast, newly synthesized HA is initially transported to the basolateral plasma membrane domain in RPE-J cells and in RPE cells in situ (Bonilha et al., 1997) (route B_1 or B_2) and is subsequently transcytosed to the apical domain (route T). HA therefore bypasses the direct TGN-to-apical route in this cell type. Importantly, our previous results indicated that syntaxin 3 is not involved in basolateral-to-apical transcytosis (route T) in MDCK cells, suggesting that this step requires another (unidentified) syntaxin. The absence of syntaxin 3 in RPE cells therefore agrees well with the itinerary of HA in this cell type, which avoids syntaxin-dependent trafficking routes.

A direct TGN-to-apical route does exist in RPE cells, however, and is taken by cargo proteins such as p75-NTR, VEGF-165, TGF-β, (Marmorstein et al., 2000; Marmorstein et al., 1998) and retinol binding protein and transthyreitin (Jaworowski et al., 1995). Since this occurs in the absence of syntaxin 3 we propose that an alternative route exists in RPE cells (route A_2) that utilizes a different syntaxin and may or may not exist in MDCK cells. Likely candidates are syntaxin 1A or 1B, which we found to be expressed at the apical plasma membrane in RPE cells. These two syntaxins are usually expressed in neurons and neuroendocrine cells and function in calcium-regulated exocytosis such as synaptic vesicle fusion with the presynaptic plasma membrane. An intriguing speculation is that apical vesicle fusion in RPE cells may be calcium regulated.

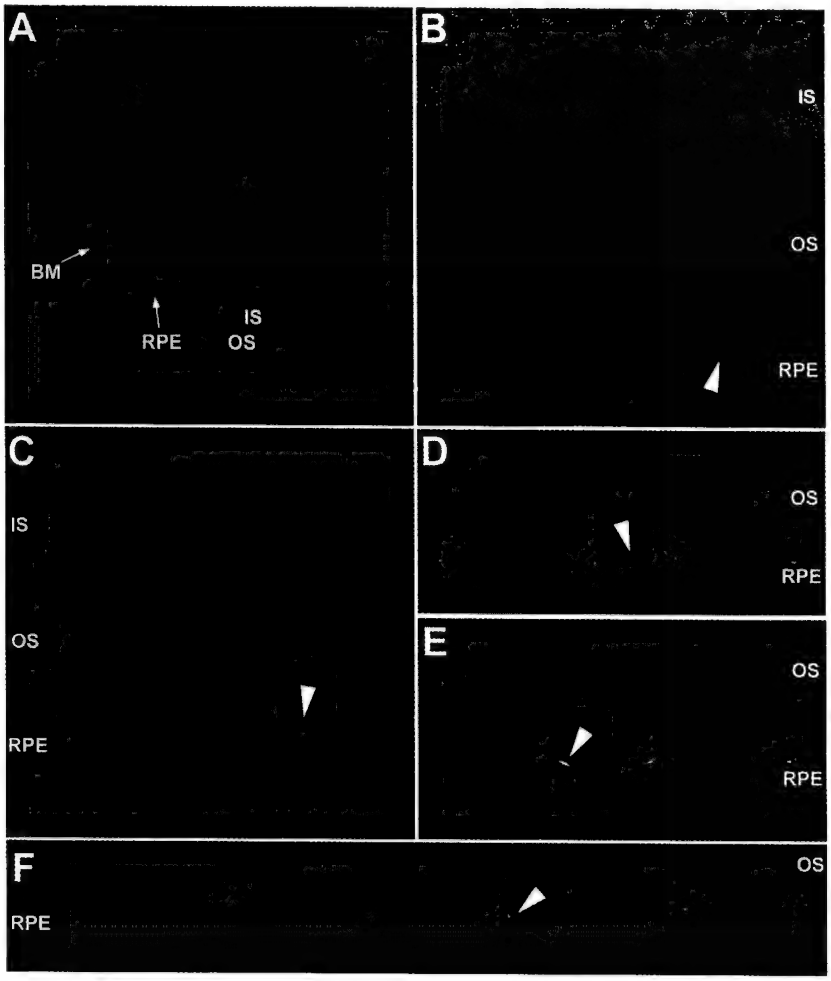

Fig. 4. Expression and subcellular localization of SNAREs in vivo. Rat eye tissue sections were double-labeled with specific antibodies and analyzed by confocal fluorescence microscopy. In all panels, the respective SNARE is in green, staining for the double-label is in red and the nuclear stain is in blue. (A) Syntaxin 3 (green), collagen-IV (red). Note that syntaxin 3 is expressed in the photoreceptor inner segments (IS) but is not detectable in the photoreceptor outer segments (OS) or the RPE cells. RPE cells are identified by the collagen-IV-positive basement membrane (BM). (B) Syntaxin 1A (green), collagen-IV (red). Note the expression of syntaxin 1A at the apical plasma membrane of RPE cells (arrowhead) that is in contact with the photoreceptor outer segments, which themselves are negative. (C) Syntaxin 1B (green), occludin (red). Note the syntaxin 1B signal on the apical plasma membrane of the RPE cells (arrowhead) above the tight junctions identified by occludin-staining. (D) Syntaxin 2 (green), occludin (red). Note that syntaxin 2 localizes to a narrow band just underneath the occludin-positive tight junctions. Syntaxin 2 does not overlap with occludin but is instead always towards the basolateral side of the cells, indicating that it localized to a region of the lateral plasma membrane that is adjacent to the tight junctions. (E) Syntaxin 4 (green), occludin (red). Similar to syntaxin 2, syntaxin 4 localizes to a narrow band underneath the occludin-positive tight junctions (arrowhead). In addition, syntaxin 4 staining is evident at the basal plasma membrane and in intracellular vesicles that are often perinuclear. (F) Endobrevin (green), occludin (red). Note that endobrevin localizes to narrow a band underneath the tight junctions (arrowhead) in addition to localizing in small vesicles that are diffusely distributed throughout the cytoplasm of RPE cells.

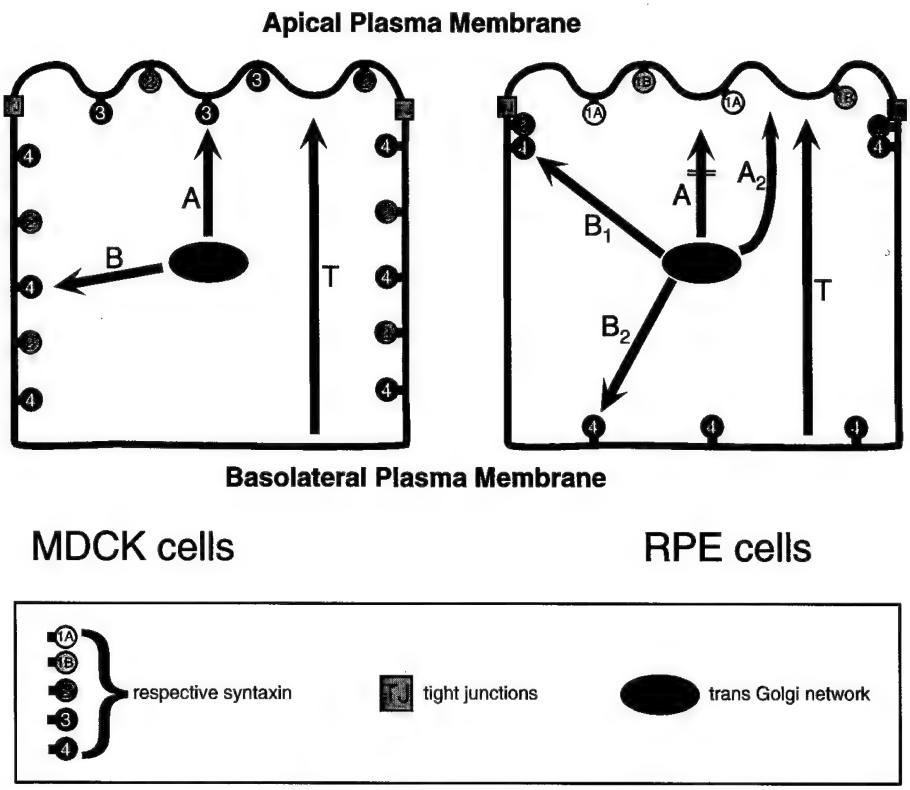

Fig. 5. Schematic models of syntaxin distribution and polarized trafficking pathways in MDCK and RPE cells. The subcellular localizations of syntaxins are indicated as reported previously in MDCK cells (Low et al., 1996) and in the present work in RPE cells. In MDCK cells, trafficking from the TGN to the apical plasma membrane (route A) was previously shown to involve syntaxin 3 (Low et al., 1998a), whereas trafficking from the TGN to the basolateral plasma membrane (route B) was shown to involve syntaxin 4 (Lafont et al., 1999). By contrast, basolateral-to-apical transcytosis is independent of syntaxin 3 in MDCK cells (Low et al., 1998a). The absence of syntaxin 3 in RPE cells suggests that route A does not exist in this cell type but that probably an alternative route designated A_2 exists. This alternative route may depend on syntaxin 1A and/or 1B, which are expressed in RPE cells and localize to the apical plasma membrane. In RPE cells, syntaxin 2 is exclusively localized to a region below the tight junctions, in contrast to its distribution along both plasma membrane domains in MDCK cells. Syntaxin 4 localizes all along the lateral membrane in MDCK cells, and post-Golgi transport vesicles carrying basolateral cargo can fuse along the entire lateral membrane (Kreitzer et al., submitted). By contrast, in RPE cells syntaxin 4 localizes to the same narrow band underneath the tight junctions as does syntaxin 2. In addition, syntaxin 4 localizes to the basal membrane. This suggests that syntaxin 4 may serve two different trafficking pathways that lead to either location (designated B_1 and B_2). These syntaxin-4-dependent routes may originate from the TGN and/or endosomes.

A surprising finding is that syntaxin 2 is localized to the basolateral plasma membrane domain in RPE cells. Of the four known syntaxin 2 splice isoforms, we found that only syntaxins 2A and 2B were expressed in RPE-J cells; these isoforms differ only in their C-terminal transmembrane domains (Quinones et al., 1999). In pancreatic acinar cells, syntaxin 2 localizes to the apical plasma membrane but it was not investigated which isoforms are expressed in these cells (Gaisano et al., 1996). Syntaxin 2 is therefore the first known syntaxin whose polarity can be reversed depending on the epithelial cell type. In MDCK cells, syntaxin 2A expressed by stable transfection localizes to both the apical and basolateral plasma membrane domains (Low et al., 1996). It is interesting to note that syntaxin 2A expressed by adenovirus-mediated transfection was found to be concentrated at the apical plasma membrane of MDCK cells whereas syntaxin 2B was more evenly distributed on both domains (Quinones et al., 1999). From these data it is unlikely that the reversed polarity of syntaxin 2 in RPE cells can be explained simply by the expression of alternative isoforms. Other mechanisms must be responsible for this differential targeting, for example, differential recognition of targeting signals within the amino-acid sequence of syntaxin 2. This mechanism remains to be identified. It also remains unknown which cargo proteins utilize a syntaxin-2-dependent fusion step. To date, syntaxin 2 has been implicated in only two fusion events, zymogen granule exocytosis in acinar cells (Hansen et al., 1999) and the fusion of the acrosome with the plasma membrane of spermatozoa (Katafuchi et al., 2000). Since the major contents of both zymogen granules and the acrosome are hydrolytic enzymes it is tempting to speculate that syntaxin 2 is used for the secretion of similar cargo in RPE and other epithelial cells.

Unexpectedly, we found that both syntaxins 2 and 4 localize to a narrow band just underneath the tight junctions in RPE cells in vivo. Confocal microscopy of double-stained sections showed that both syntaxins do not overlap with the tight junction protein occludin; instead they are immediately adjacent on the lateral membrane, indicating that both are involved in basolateral trafficking pathways. On the basis of the localization of other proteins implicated in vesicle fusion on the tight junctions of epithelial cells, it has been proposed that the tight junctions – or structures in close proximity – may be preferred sites of vesicle exocytosis. These proteins include rab8 (Huber et al., 1993), rab3b (Weber et al., 1994), rab13 (Zahraoui et al., 1994), the sec6/8 complex or exocyst (Grindstaff et al., 1998) and VAP-A (Lapierre et al., 1999). Direct evidence of vesicle fusion events at the tight junctions, however, has been lacking, and the fact that syntaxin 4 localizes all along the lateral membrane in MDCK and other epithelial cells seemed to be at odds with this hypothesis. Recently, fusion events of post-Golgi transport vesicles carrying GFP-tagged apical and basolateral marker proteins were monitored in polarized MDCK cells using time-lapse microscopy (G. Kreitzer, J. Schmoranzel, S.-H. Low, Y. Chen et al., unpublished). The results demonstrated that fusion of basolateral vesicles occurs all along the lateral plasma

membrane in agreement with the lateral localization of syntaxin 4. It is still possible that more specialized trafficking pathways may be directed towards the tight junctions in MDCK cells, but this remains to be investigated. Our striking finding that syntaxins 2 and 4 localize close to the tight junctions in RPE cells strongly suggests that a tight junctional 'fusion patch' indeed exists in this epithelial cell type and that exocytic pathways that depend on these syntaxins will be directed toward this site (route B_1 in Fig. 5). Syntaxin 4, but not syntaxin 2, was also present at the basal membrane in RPE cells, suggesting that basolateral fusion events occur either at the 'tight junctional fusion patch' or at the basal membrane (route B_2). It is possible that syntaxin 4 is not only involved in TGN-to-basolateral trafficking in epithelial cells but also in recycling pathways as could be deduced from its known involvement in GLUT-4 translocation from endosomes to the plasma membrane in adipocytes (Macaulay et al., 1997; Olson et al., 1997; Tellam et al., 1997). In this case, routes B_1 and B_2 may differ in that one of them originates from endosomes rather than the TGN.

In conclusion, we have shown that RPE cells differ in their complement of plasma membrane syntaxins and in the polarity of one syntaxin from other epithelial cell types. Furthermore, they exhibit the prominent localization of two syntaxins at a putative 'sub-tight junctional fusion patch'. These differences suggest that epithelial cell types can indeed differ in the molecular machineries controlling membrane trafficking. We consider it therefore unlikely that the known variability of epithelial trafficking phenotypes is solely due to re-routing of cargo proteins – for example, by differential recognition of sorting signals – into otherwise identical trafficking pathways. A more likely scenario may be that epithelial cells can regulate the presence/absence, preponderance and/or direction of entire trafficking pathways. This would include the expression and localization of plasma membrane syntaxins, which serve as 'end points' of all exocytic pathways. It is unlikely, however, that regulation of syntaxin expression/localization alone can accomplish the diversity of epithelial trafficking phenotypes. Membrane trafficking pathways consist of a succession of mechanisms – such as vesicle budding, transport along cytoskeletal elements etc. – many of which may need to be modulated depending on the epithelial cell type.

We gratefully acknowledge gifts of antibodies and cDNAs by Wanjin Hong (Institute for Molecular and Cell Biology, Singapore), Mark Bennett and Beatriz Quinones (UC Berkeley). Work in T.W.'s laboratory was supported by NIH-DK62338, a Jerry and Martha Jarrett Grant for Research on Polycystic Kidney Disease, a grant from the Department of Defense Prostate Cancer Research Program (DAMD17-02-1-0039) and a Beginning Grant-in-Aid by the American Heart Association. S.H.L. is supported by a Scientist Development Grant from the American Heart Association. Work in A.D.M.'s laboratory was supported by NIH-EY13160 and a Kirchgessner Foundation Research Grant. Work in L.Y.M.'s laboratory was supported by NIH-EY13847.

References

Al-Awqati, Q., Vijayakumar, S., Hikita, C., Chen, J. and Takito, J. (1998). Phenotypic plasticity in the intercalated cell: the hensin pathway. *Am. J. Physiol.* **275**, F183-F190.

Antonin, W., Holroyd, C., Tikkanen, R., Honing, S. and Jahn, R. (2000). The R-SNARE Endobrevin/VAMP-8 mediates homotypic fusion of early endosomes and late endosomes. *Mol. Biol. Cell* **11**, 3289-3298.

Bonilha, V. L., Marmorstein, A. D., Cohen-Gould, L. and Rodriguez-Boulan, E. (1997). Apical sorting of influenza hemagglutinin by transcytosis in retinal pigment epithelium. *J. Cell Sci.* **110**, 1717-1727.

Chen, Y. A. and Scheller, R. H. (2001). SNARE-mediated membrane fusion. *Nat. Rev. Mol. Cell Biol.* **2**, 98-106.

Delgrossi, M. H., Breuza, L., Mirre, C., Chavrier, P. and le Bivic, A. (1997). Human syntaxin 3 is localized apically in human intestinal cells. *J. Cell Sci.* **110**, 2207-2214.

Finnemann, S. C., Bonilha, V. L., Marmorstein, A. D. and Rodriguez-Boulan, E. (1997). Phagocytosis of rod outer segments by retinal pigment epithelial cells requires alpha(v)beta5 integrin for binding but not for internalization. *Proc. Natl. Acad. Sci. USA* **94**, 12932-12937.

Fölsch, H., Ohno, H., Bonifacino, J. S. and Mellman, I. (1999). A novel clathrin adaptor complex mediates basolateral targeting in polarized epithelial cells. *Cell* **99**, 189-198.

Fölsch, H., Pypaert, M., Schu, P. and Mellman, I. (2001). Distribution and function of AP-1 clathrin adaptor complexes in polarized epithelial cells. *J. Cell Biol.* **152**, 595-606.

Fujita, H., Tuma, P. L., Finnegan, C. M., Locco, L. and Hubbard, A. L. (1998). Endogenous syntaxins 2, 3 and 4 exhibit distinct but overlapping patterns of expression at the hepatocyte plasma membrane. *Biochem. J.* **329**, 527-538.

Gaisano, H. Y., Ghai, M., Malkus, P. N., Sheu, L., Bouquillon, A., Bennett, M. K. and Trimble, W. S. (1996). Distinct cellular locations and protein-protein interactions of the syntaxin family of proteins in rat pancreatic acinar cells. *Mol. Biol. Cell* **7**, 2019-2027.

Gallemore, R. P., Hughes, B. A. and Miller, S. S. (1998). Light induced responses of the retinal pigment epithelium. In *The Retinal Pigment Epithelium* (eds M. F. Marmor and T. J. Wolfensberger), pp. 175-198. New York: Oxford University Press.

Galli, T., Zahraoui, A., Vaidyanathan, V. V., Raposo, G., Tian, J. M., Karin, M., Niemann, H. and Louvard, D. (1998). A novel tetanus neurotoxin-insensitive vesicle-associated membrane protein in SNARE complexes of the apical plasma membrane of epithelial cells. *Mol. Biol. Cell* **9**, 1437-1448.

Gan, Y., McGraw, T. E. and Rodriguez-Boulan, E. (2002). The epithelial-specific adaptor AP1B mediates post-endocytic recycling to the basolateral membrane. *Nat. Cell Biol.* **4**, 605-609.

Grindstaff, K. K., Yeaman, C., Anandasabapathy, N., Hsu, S. C., Rodriguez-Boulan, E., Scheller, R. H. and Nelson, W. J. (1998). Sec6/8 complex is recruited to cell-cell contacts and specifies transport vesicle delivery to the basal-lateral membrane in epithelial cells. *Cell* **93**, 731-740.

Hansen, N. J., Antonin, W. and Edwardson, J. M. (1999). Identification of SNAREs involved in regulated exocytosis in the pancreatic acinar cell. *J. Biol. Chem.* **274**, 22871-22876.

Huber, L. A., Pimplikar, S., Parton, R. G., Virta, H., Zerial, M. and Simons, K. (1993). Rab8, a small GTPase involved in vesicular traffic between the TGN and the basolateral plasma membrane. *J. Cell Biol.* **123**, 35-45.

Jahn, R. and Sudhof, T. C. (1999). Membrane fusion and exocytosis. *Annu. Rev. Biochem.* **68**, 863-911.

Jaworowski, A., Fang, Z., Khong, T. F. and Augusteyn, R. C. (1995). Protein synthesis and secretion by cultured retinal pigment epithelia. *Biochim. Biophys. Acta* **1245**, 121-129.

Katafuchi, K., Mori, T., Toshimori, K. and Iida, H. (2000). Localization of a syntaxin isoform, syntaxin 2, to the acrosomal region of rodent spermatozoa. *Mol. Reprod. Dev.* **57**, 375-383.

Kuliawat, R., Lisanti, M. P. and Arvan, P. (1995). Polarized distribution and delivery of plasma membrane proteins in thyroid follicular epithelial cells. *J. Biol. Chem.* **270**, 2478-2482.

Lafont, F., Verkade, P., Galli, T., Wimmer, C., Louvard, D. and Simons, K. (1999). Raft association of SNAP receptors acting in apical trafficking in Madin-Darby canine kidney cells. *Proc. Natl. Acad. Sci. USA* **96**, 3734-3738.

Lapierre, L. A., Tuma, P. L., Navarre, J., Goldenring, J. R. and Anderson, J. M. (1999). VAP-33 localizes to both an intracellular vesicle population and with occludin at the tight junction. *J. Cell Sci.* **112**, 3723-3732.

Lehtonen, S., Riento, K., Olkkonen, V. M. and Lehtonen, E. (1999). Syntaxin 3 and Munc-18-2 in epithelial cells during kidney development. *Kidney Int.* **56**, 815-826.

Li, X., Low, S. H., Miura, M. and Weimbs, T. (2002). SNARE expression

and localization in renal epithelial cells suggests mechanism for variability of trafficking phenotypes. *Am. J. Physiol.* (in press).

Low, S. H., Chapin, S. J., Weimbs, T., Kömüves, L. G., Bennett, M. K. and Mostov, K. E. (1996). Differential localization of syntaxin isoforms in polarized MDCK cells. *Mol. Biol. Cell* **7**, 2007-2018.

Low, S. H., Chapin, S. J., Wimmer, C., Whiteheart, S. W., Kömüves, L. K., Mostov, K. E. and Weimbs, T. (1998a). The SNARE machinery is involved in apical plasma membrane trafficking in MDCK cells. *J. Cell Biol.* **141**, 1503-1513.

Low, S. H., Miura, M., Roche, P. A., Valdez, A. C., Mostov, K. E. and Weimbs, T. (2000). Intracellular redirection of plasma membrane trafficking after loss of epithelial cell polarity. *Mol. Biol. Cell* **11**, 3045-3060.

Low, S. H., Roche, P. A., Anderson, H. A., van IJzendoorn, S. C. D., Zhang, M., Mostov, K. E. and Weimbs, T. (1998b). Targeting of SNAP-23 and SNAP-25 in polarized epithelial Cells. *J. Biol. Chem.* **273**, 3422-3430.

Macaulay, S. L., Hewish, D. R., Gough, K. H., Stoichevska, V., MacPherson, S. F., Jagadish, M. and Ward, C. W. (1997). Functional studies in 3T3L1 cells support a role for SNARE proteins in insulin stimulation of GLUT4 translocation. *Biochem. J.* **324**, 217-224.

Marmorstein, A. D. (2001). The polarity of the retinal pigment epithelium. *Traffic* **2**, 867-872.

Marmorstein, A. D., Csaky, K. G., Baffi, J., Lam, L., Rahaal, F. and Rodriguez-Boulan, E. (2000). Saturation of, and competition for entry into, the apical secretory pathway. *Proc. Natl. Acad. Sci. USA* **97**, 3248-3253.

Marmorstein, A. D., Gan, Y. C., Bonilha, V. L., Finnemann, S. C., Csaky, K. G. and Rodriguez-Boulan, E. (1998). Apical polarity of N-CAM and EMMPRIN in retinal pigment epithelium resulting from suppression of basolateral signal recognition. *J. Cell Biol.* **142**, 697-710.

Marrs, J. A., Andersson-Fisone, C., Jeong, M. C., Cohen-Gould, L., Zurzolo, C., Nabi, I. R., Rodriguez-Boulan, E. and Nelson, W. J. (1995). Plasticity in epithelial cell phenotype: modulation by expression of different cadherin cell adhesion molecules. *J. Cell Biol.* **129**, 507-519.

Matlin, K. S. and Simons, K. (1984). Sorting of an apical plasma membrane glycoprotein occurs before it reaches the cell surface in cultured epithelial cells. *J. Cell Biol.* **99**, 2131-2139.

McNew, J. A., Parlati, F., Fukuda, R., Johnston, R. J., Paz, K., Paumet, F., Sollner, T. H. and Rothman, J. E. (2000). Compartmental specificity of cellular membrane fusion encoded in SNARE proteins. *Nature* **407**, 153-159.

Misek, D. E., Bard, E. and Rodriguez-Boulan, E. (1984). Biogenesis of epithelial cell polarity: intracellular sorting and vectorial exocytosis of an apical plasma membrane glycoprotein. *Cell* **39**, 537-546.

Mostov, K. E., Verges, M. and Altschuler, Y. (2000). Membrane traffic in polarized epithelial cells. *Curr. Opin. Cell Biol.* **12**, 483-490.

Nabi, I. R., Mathews, A. P., Cohen-Gould, L., Gundersen, D. and Rodriguez-Boulan, E. (1993). Immortalization of polarized rat retinal pigment epithelium. *J. Cell Sci.* **104**, 37-49.

Olson, A. L., Knight, J. B. and Pessin, J. E. (1997). Syntaxin 4, VAMP2, and/or VAMP3/cellubrevin are functional target membrane and vesicle SNAP receptors for insulin-stimulated GLUT4 translocation in adipocytes. *Mol. Cell Biol.* **17**, 2425-2435.

Peng, X.-R., Yao, X., Chow, D.-C., Forte, J. G. and Bennett, M. K. (1997). Association of syntaxin 3 and vesicle-associated membrane protein (VAMP) with H+/K+-ATPase-containing tubulovesicles in gastric parietal cells. *Mol. Biol. Cell* **8**, 399-407.

Quinones, B., Riento, K., Olkkonen, V. M., Hardy, S. and Bennett, M. K. (1999). Syntaxin 2 splice variants exhibit differential expression patterns, biochemical properties and subcellular localizations. *J. Cell Sci.* **112**, 4291-4304.

Riento, K., Galli, T., Jansson, S., Ehnholm, C., Lehtonen, E. and Olkkonen, V. M. (1998). Interaction of munc-18-2 with syntaxin 3 controls the association of apical SNAREs in epithelial cells. *J. Cell Sci.* **111**, 2681-2688.

Scales, S. J., Chen, Y. A., Yoo, B. Y., Patel, S. M., Doung, Y. C. and Scheller, R. H. (2000). SNAREs contribute to the specificity of membrane fusion. *Neuron* **26**, 457-464.

Steegmaier, M., Lee, K. C., Prekeris, R. and Scheller, R. H. (2000). SNARE protein trafficking in polarized MDCK cells. *Traffic* **1**, 553-560.

Tellam, J. T., Macaulay, S. L., McIntosh, S., Hewish, D. R., Ward, C. W. and James, D. E. (1997). Characterization of Munc-18c and syntaxin-4 in 3T3-L1 adipocytes. Putative role in insulin-dependent movement of GLUT-4. *J. Biol. Chem.* **272**, 6179-6186.

Weber, E., Berta, G., Tousson, A., St John, P., Green, M. W., Gopalokrishnan, U., Jilling, T., Sorscher, E. J., Elton, T. S., Abrahamson, D. R. et al. (1994). Expression and polarized targeting of a rab3 isoform in epithelial cells. *J. Cell Biol.* **125**, 583-594.

Weimbs, T., Low, S. H., Chapin, S. J., Mostov, K. E., Bucher, P. and Hofmann, K. (1997). A conserved domain is present in different families of vesicular fusion proteins: A new superfamily. *Proc. Natl. Acad. Sci. USA* **94**, 3046-3051.

Weimbs, T., Mostov, K. E., Low, S. H. and Hofmann, K. (1998). A model for structural similarity between different SNARE complexes based on sequence relationships. *Trends Cell Biol.* **8**, 260-262.

Yeaman, C., Grindstaff, K. K. and Nelson, W. J. (1999). New perspectives on mechanisms involved in generating epithelial cell polarity. *Physiol. Rev.* **79**, 73-98.

Zahraoui, A., Joberty, G., Arpin, M., Fontaine, J. J., Hellio, R., Tavitian, A. and Louvard, D. (1994). A small rab GTPase is distributed in cytoplasmic vesicles in non polarized cells but colocalizes with the tight junction marker ZO-1 in polarized epithelial cells. *J. Cell Biol.* **124**, 101-115.

Zurzolo, C., Lisanti, M. P., Caras, I. W., Nitsch, L. and Rodriguez-Boulan, E. (1993). Glycosylphosphatidylinositol-anchored proteins are preferentially targeted to the basolateral surface in Fischer rat thyroid epithelial cells. *J. Cell Biol.* **121**, 1031-1039.

Developmental Cell, Vol. 4, 753–759, May, 2003, Copyright ©2003 by Cell Press

Syntaxin 2 and Endobrevin Are Required for the Terminal Step of Cytokinesis in Mammalian Cells

Seng Hui Low,[1] Xin Li,[1] Masumi Miura,[1]
Noriko Kudo,[1] Beatriz Quiñones,[3]
and Thomas Weimbs*,[1,2]
[1]Department of Cell Biology
Lerner Research Institute and
[2]Glickman Urological Institute
The Cleveland Clinic
Cleveland, Ohio 44195
[3]Department of Plant and Microbial Biology
University of California, Berkeley
Berkekey, California 94720

Summary

The terminal step of cytokinesis in animal cells is the abscission of the midbody, a cytoplasmic bridge that connects the two prospective daughter cells. Here we show that two members of the SNARE membrane fusion machinery, syntaxin 2 and endobrevin/VAMP-8, specifically localize to the midbody during cytokinesis in mammalian cells. Inhibition of their function by overexpression of nonmembrane-anchored mutants causes failure of cytokinesis leading to the formation of binucleated cells. Time-lapse microscopy shows that only midbody abscission but not further upstream events, such as furrowing, are affected. These results indicate that successful completion of cytokinesis requires a SNARE-mediated membrane fusion event and that this requirement is distinct from exocytic events that may be involved in prior ingression of the plasma membrane.

Introduction

Cytokinesis, the division of a cell into two daughter cells, is a fundamental process in biology common to all organisms (Field et al., 1999; Finger and White, 2002; Glotzer, 2001; O'Halloran, 2000; Zeitlin and Sullivan, 2001). In animal cells, cytokinesis is a multistep process that involves the assembly of an actin/myosin-dependent contractile ring that guides the invagination of the plasma membrane leading to the formation of a cleavage furrow. Furrowing proceeds until the cytoplasm is constricted to a narrow bridge—termed the midbody—that contains the remnants of the spindle microtubules and connects the two prospective daughter cells. The terminal step of cytokinesis is the abscission of the midbody, which leads to completely separate daughter cells. The mechanism by which midbody abscission is achieved has remained unknown. However, this step would be expected to involve membrane fusion events. Otherwise, the plasma membranes of the newly generated daughter cells would be ruptured.

So far, requirements for membrane fusion events during cytokinesis have been identified only for stages that precede midbody abscission. For example, exocytosis is required to supply the necessary additional surface area required for furrow ingression during cytokinesis in *C. elegans* and sea urchin embryos (Jantsch-Plunger and Glotzer, 1999; Shuster and Burgess, 2002). In *C. elegans*, furrow ingression appears to require Syn-4, a syntaxin family member of the SNARE membrane fusion machinery (Jantsch-Plunger and Glotzer, 1999). The function of Syn-4 may not be restricted to furrow ingression, however, because its disruption also causes defects in nuclear envelope reformation. Rab3, a member of a family of proteins implicated in the regulation of SNARE function, has been implicated in furrow ingression in sea urchin embryos, but it may also act at earlier stages because its disruption also leads to failure of nuclear division (Conner and Wessel, 2000). SNARE proteins can also be involved in animal cytokinesis in an indirect fashion. For example, a syntaxin has been implicated previously in cell division in sea urchin embryos. Functional disruption of this syntaxin affects nuclear division, which subsequently appears to inhibit cytokinesis indirectly due to a halt of cell cycle progression (Conner and Wessel, 1999). The mechanism of cytokinesis in plant cells differs from that in animal cells in that no furrowing of the plasma membrane occurs, and no midbody-like bridge is formed. Instead, plant cells assemble a new plasma membrane and cell wall—termed the cell plate—in the middle of the dividing cells. The cell plate is assembled by the fusion of small vesicles with each other and with the growing cell plate in a process that requires the action of members of the SNARE membrane fusion machinery (Assaad et al., 2001; Heese et al., 2001; Lauber et al., 1997; Waizenegger et al., 2000).

While these studies have established that membrane fusion events are required for steps during cytokinesis prior to midbody abscission, the mechanism of this terminal step has remained unknown. Interestingly, recent experiments in *C. elegans* have indicated that midbody abscission can be inhibited using the fungal metabolite brefeldin A—a drug that disrupts several organelles and trafficking pathways—under conditions that do not affect furrow ingression (Skop et al., 2001). This suggested that different cellular machineries may control fusion events that facilitate furrow ingression and midbody abscission.

Here we report the identification of two members of the SNARE membrane fusion machinery, syntaxin 2 and endobrevin/VAMP-8, which specifically localize to the midbody region during cytokinesis in mammalian cells. Their functional inhibition causes failure of midbody abscission while earlier steps of cytokinesis are unaffected. These results indicate that the terminal step of cytokinesis is not a passive "ripping-apart" or "pinching-off" mechanism but is regulated by a SNARE-mediated membrane fusion event that is distinct from exocytic events that are involved in prior ingression of the plasma membrane.

Results and Discussion

Syntaxin 2 Localizes to the Midbody

Membrane fusion events in intracellular vesicle trafficking pathways are generally mediated by proteins of the

*Correspondence: weimbst@lerner.ccf.org

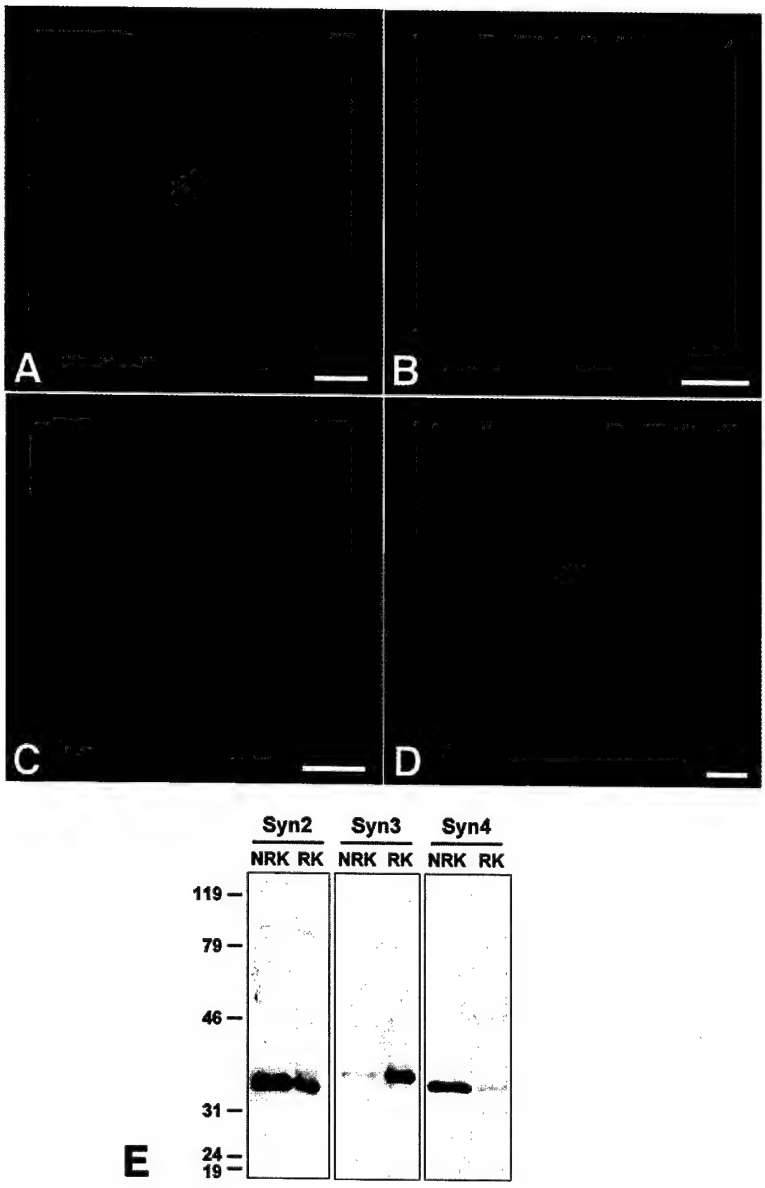

Figure 1. Syntaxin 2 Localizes to the Midbody during Cytokinesis

(A) Coimmunolocalization of syntaxin 2 (green) and β-tubulin (red) in NRK cells during the midbody stage of cytokinesis. Nuclei are stained with DAPI (blue).

(B) Competition with purified antigen eliminates syntaxin 2-specific staining.

(C and D) Neither syntaxin 3 (C) nor syntaxin 4 (D) localize to the midbody of dividing cells. Scale bars, 5 μm.

(E) Immunoblot analysis of NRK cell lysates shows that syntaxins 2 and 4 are abundantly expressed in NRK cells whereas the expression level of syntaxin 3 is relatively low. Equal amounts (15 μg protein) of total rat kidney (RK) lysates were used as controls. Molecular weight makers are indicated in kilodaltons.

SNARE superfamily, which consists of several subfamilies, including syntaxins (Chen and Scheller, 2001; Jahn and Sudhof, 1999; Weimbs et al., 1997). Our analysis of the localization of syntaxin 2 in cultured proliferating NRK (normal rat kidney) cells led to the following serendipitous finding. An affinity-purified antibody against syntaxin 2 strongly labeled small structures in a fraction of the cell population. Colabeling for β-tubulin identified these structures as midbodies. Syntaxin 2 immunoreactivity localized to distinct regions of ~1 μm apparent diameter on either side of the midbody (Figure 1A). These syntaxin 2 regions were intersected by microtubules. This staining pattern was consistently observed using two independently raised syntaxin 2 antibodies and could be eliminated by competing antigen, indicating that it is specific (Figure 1B). Identical staining patterns were also observed with several other mammalian cell lines including HEK293 and CHO cells (data not shown). It should be noted that a well-known apparent gap exists in the center of the midzone in which tightly packed matrix proteins prevent antibody staining to microtubules even though they are present (Mullins and McIntosh, 1982). By analogy, it is therefore possible that the localization of syntaxin 2 may extend further toward the midzone than can be demonstrated by immunostaining. In interphase cells, syntaxin 2 localized to the plasma membrane and intracellular vesicles (data not shown) as previously reported (Quinones et al., 1999).

Syntaxin 2 is a ubiquitously expressed t-SNARE (Bennett et al., 1993) that has been reported to be targeted to the plasma membrane in several cell types, including polarized Madin Darby canine kidney (MDCK) cells (Li et al., 2002; Low et al., 1996, 2000). Two other widely expressed plasma membrane t-SNAREs are syntaxins 3 and 4 (Li et al., 2002; Low et al., 1996). Western blot analysis showed that NRK cells express all three syntaxins (Figure 1E). However, neither syntaxin 3 nor syntaxin 4 exhibited the same midbody localization as syntaxin 2 during cytokinesis (Figures 1C and 1D).

The subcellular steady-state location of a given t-SNARE

generally corresponds to the site at which this t-SNARE functions. The localization of syntaxin 2 at the midbody therefore suggested that it may be involved in a fusion event required for cytokinesis. We considered two possibilities. First, syntaxin 2 may be involved in increasing the cell surface area during furrowing by mediating the fusion of vesicles with the plasma membrane close to the site of ingression. Second, syntaxin 2 may be directly involved in the final abscission of the midbody to result in completely separated daughter cells.

Syntaxin 2 Function Is Required for Cytokinesis

To investigate whether syntaxin 2 function is required for cytokinesis and to examine its mechanism of action, we employed a dominant-negative approach. The overall domain structure of syntaxins is highly conserved (Weimbs et al., 1997, 1998), and they are characterized by a C-terminal transmembrane anchor, while the rest of the molecule protrudes into the cytoplasm. Recombinant soluble SNAREs that lack the membrane anchors are known to inhibit membrane fusion by forming nonfunctional complexes with endogenous SNARE proteins (Hua and Scheller, 2001). A brain-specific, alternatively spliced isoform of syntaxin 2, termed syntaxin 2D, has previously been identified that lacks a transmembrane anchor, while the remainder of the cytoplasmic domain is identical to full-length syntaxin 2 (Quinones et al., 1999). The function of syntaxin 2D is unknown. However, it was reported to be a soluble cytoplasmic protein (Quinones et al., 1999) and would be predicted to act as a dominant-negative inhibitor of the function of membrane-anchored syntaxin 2.

We expressed syntaxin 2D in MDCK cells using an adenovirus vector with a tetracycline-regulatable promotor. Immunofluorescence analysis confirmed the cytoplasmic localization of syntaxin 2D (Figure 2A). Syntaxin 2D expression for 16 hr resulted in a high frequency of binucleated cells, indicating that the cells had undergone nuclear division in the absence of cytokinesis (Figures 2A and 2D). This effect could be prevented by suppressing syntaxin 2D expression by the addition of doxycycline, indicating that the observed block of cytokinesis is not due to the adenoviral infection. Furthermore, adenovirus-mediated expression of the membrane-anchored, full-length syntaxin 2A did not result in an increase in binucleated cells (Figure 2D). Given that only ~50% of the cells underwent mitosis during the course of these experiments, we estimate that cytokinesis failed in approximately 60% of the mitotic events in cells that expressed syntaxin 2D. These results indicate that syntaxin 2 function is required for cytokinesis.

Syntaxin 2 Function Is Required for Midbody Abscission

To distinguish whether syntaxin 2 inhibition prevents the ingression of the cleavage furrow or the abscission of the midbody, syntaxin 2D-expressing cells were investigated by time-lapse phase-contrast microscopy (see Supplemental Data, Movie S1 [http://www.developmentalcell.com/cgi/content/full/4/5/753/DC1]). Figure 2C shows representative frames. In six independent time-lapse experiments, 41 failed cytokinesis events were observed that resulted in the formation of binucleated cells. In all cases, nuclear division, cleavage furrow formation and ingression, and the formation of midbodies were indistinguishable from controls. However, the cells were unable to undergo midbody abscission. The average time that the syntaxin 2D-expressing cells remained in the midbody stage was 153 min (range 64–355 min, n = 41), after which midbody regression occurred to lead to binucleated cells.

In two additional independent time-lapse experiments, the fate of the cell population was quantified on a cell-by-cell basis. While approximately 60% of cells did not undergo mitosis during the recordings (14 hr), of those that did, 48 failed in cytokinesis (53%) and 43 completed it successfully (47%). The heterogeneity of expression levels of syntaxin 2D in the cell population and the fact that the expression level necessarily has to ramp up during the course of the experiment are likely reasons for the observed inhibition of cytokinesis in less than 100% of the cells. Furthermore, this suggests that a minimum threshold level of cellular syntaxin 2D is required for successful inhibition, compatible with a dominant-negative effect.

As a further control for the specificity of the dominant-negative inhibition of syntaxin 2 function, truncated versions of syntaxins 3 and 4—lacking the transmembrane anchors—were expressed in MDCK cells by transient transfection. This was compared to transient transfection of syntaxin 2A or 2D cDNAs. All cDNAs were inserted into the identical plasmid vector, and side-by-side transient expression resulted in comparable levels of expressed proteins. Similar to the adenoviral gene transfer above, expression of syntaxin 2D for 24 hr resulted in a high frequency of binucleated cells (Figure 2E). In contrast, neither expression of the membrane-anchored syntaxin 2A nor of the truncated syntaxins 3 or 4 had this effect. This result indicates that the dominant-negative inhibition by nonmembrane-anchored syntaxins is specific and that syntaxin 2 is specifically involved in cytokinesis.

To investigate whether syntaxin 2 inhibition might affect the reassembly of the nuclear envelope, the binucleated cells were immunostained with antibodies against the nuclear transport factor p97 (Figure 2B) or lamin B_2 (data not shown). The nuclear envelopes of the binucleated cells appeared to be complete and intact and were indistinguishable from those of control cells, indicating that syntaxin 2 inhibition has no effect on the nuclear envelope and that nuclear division was unperturbed. We also did not observe evidence for micronuclei or nuclear buds in the binucleated cells after syntaxin 2 inhibition. These defects would be indicators of loss or malsegregation of chromosomes as a result of defects in the spindle or centromeres or as a consequence of chromosome undercondensation (Fenech and Crott, 2002). Overall, these results indicate that syntaxin 2 is required specifically for midbody abscission but not for further upstream events of mitosis such as chromosome segregation, nuclear envelope reassembly, furrowing, etc. Furthermore, the results indicate for the first time that midbody abscission involves a SNARE-mediated fusion event and suggest that this event utilizes a fusion machinery that differs from that which is required for exocytosis for the delivery of new membrane to aid in furrow ingression. Finally, if midbody abscission is blocked by syntaxin 2 inhibition, cells cannot otherwise "rip apart" or "pinch off" to complete cytokinesis.

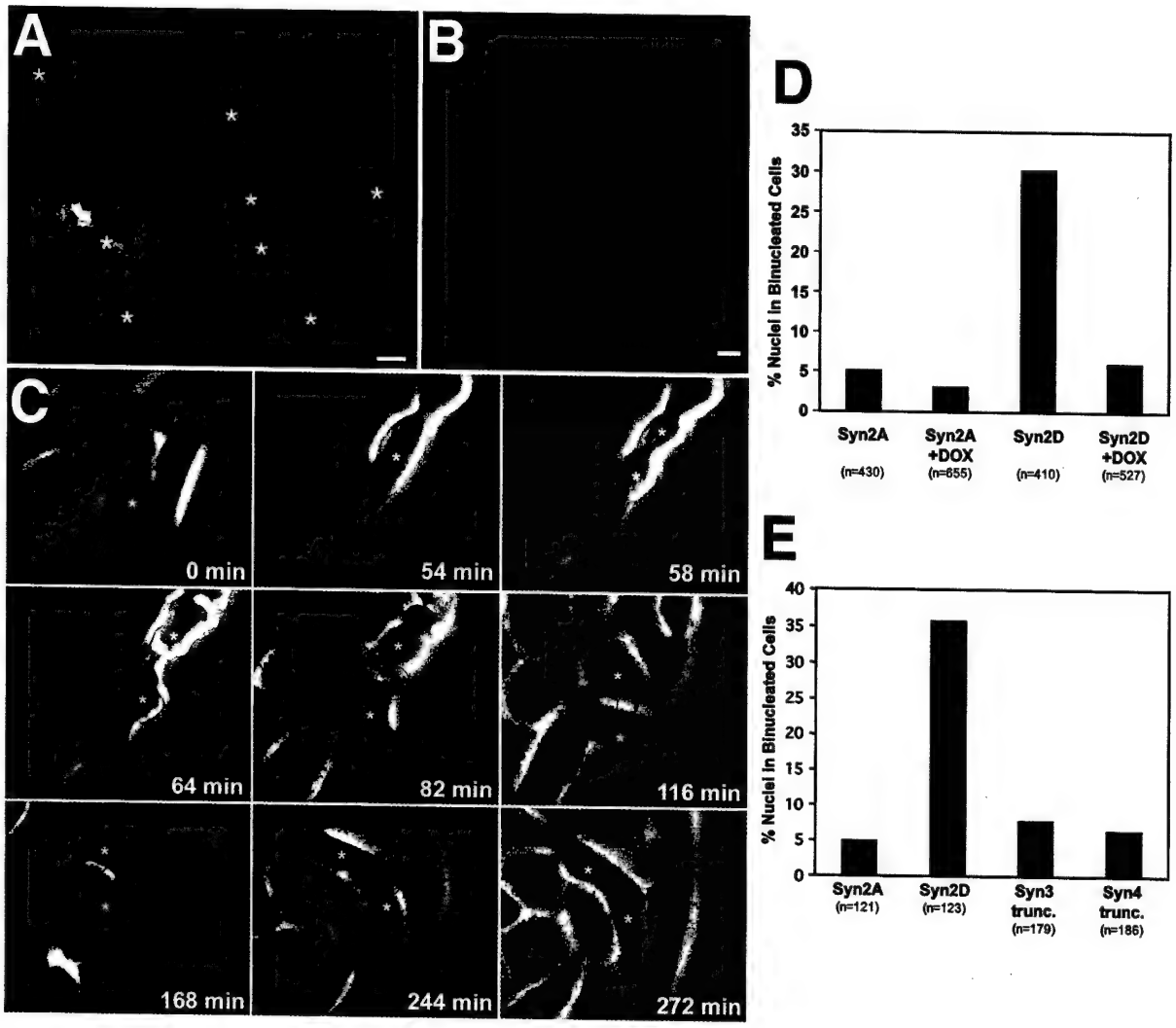

Figure 2. Expression of Soluble Syntaxin 2 Inhibits Midbody Abscission Resulting in Binucleated Cells

(A) Syntaxin 2D, a splice isoform lacking a transmembrane anchor, was expressed in MDCK cells. Immunostaining for syntaxin 2 (green) reveals expressing cells. Binucleated cells are denoted by asterisks. Scale bar, 5 μm.

(B) Binucleated cells formed after 16 hr expression of syntaxin 2D were subjected to double immunostaining for the nuclear transport factor p97 (green) and the tight junction protein ZO-1 (red). Note that the nuclei of binucleated cells exhibited normal p97 staining, indicating that nuclear division and reformation of the nuclear envelopes was unaffected.

(C) Frames of time-lapse phase contrast microscopy of MDCK cells expressing syntaxin 2D. For orientation, the cell if interest is highlighted by asterisks and the midbody is circled (see Supplemental Data, Movie S1 [http://www.developmentalcell.com/cgi/content/full/4/5/753/DC1]).

(D) Quantification of failed cytokinesis after 16 hr expression of the full-length syntaxin 2A or the truncated syntaxin 2D using adenovirus vectors calculated as the fraction of nuclei in binucleated cells as the percentage of the total nuclei. As negative controls, syntaxin expression was prevented by the addition of doxycycline (+DOX). The total numbers of nuclei counted for each condition are indicated.

(E) Failed cytokinesis after 24 hr expression of syntaxin 2A, syntaxin 2D, or truncated versions of syntaxins 3 or 4 lacking transmembrane anchors by plasmid-mediated transient transfection.

Endobrevin/VAMP-8 Functions Together with Syntaxin 2 during Midbody Abscission

If syntaxin 2 mediates a membrane fusion event that is required for the severing of the midbody, it would be predicted to involve other members of the SNARE machinery as well. In other intracellular fusion events, small v-SNAREs of the synaptobrevin/VAMP family mediate membrane fusion in concert with syntaxins. A v-SNARE involved in cytokinesis would be expected to exhibit a relatively ubiquitous tissue expression pattern. We investigated whether the two ubiquitously expressed v-SNAREs cellubrevin/VAMP-3 or endobrevin/VAMP-8 localize to the midbody region during cytokinesis. Figure 3A shows that cellubrevin is only found on intracellular vesicles but not at the midbody during cytokinesis. In contrast, endobrevin is highly concentrated at the midbody in a staining pattern very similar to that of syntaxin 2 (Figures 3B and 3D). Again, the immunosignal could be eliminated by competition with antigen (Figure 3C), and two independent endobrevin antibodies resulted in identical staining patterns (data not shown). Double immunofluorescence microscopy with antibodies against syntaxin 2 and endobrevin revealed nearly completely overlapping localizations (Figure 3E). During interphase,

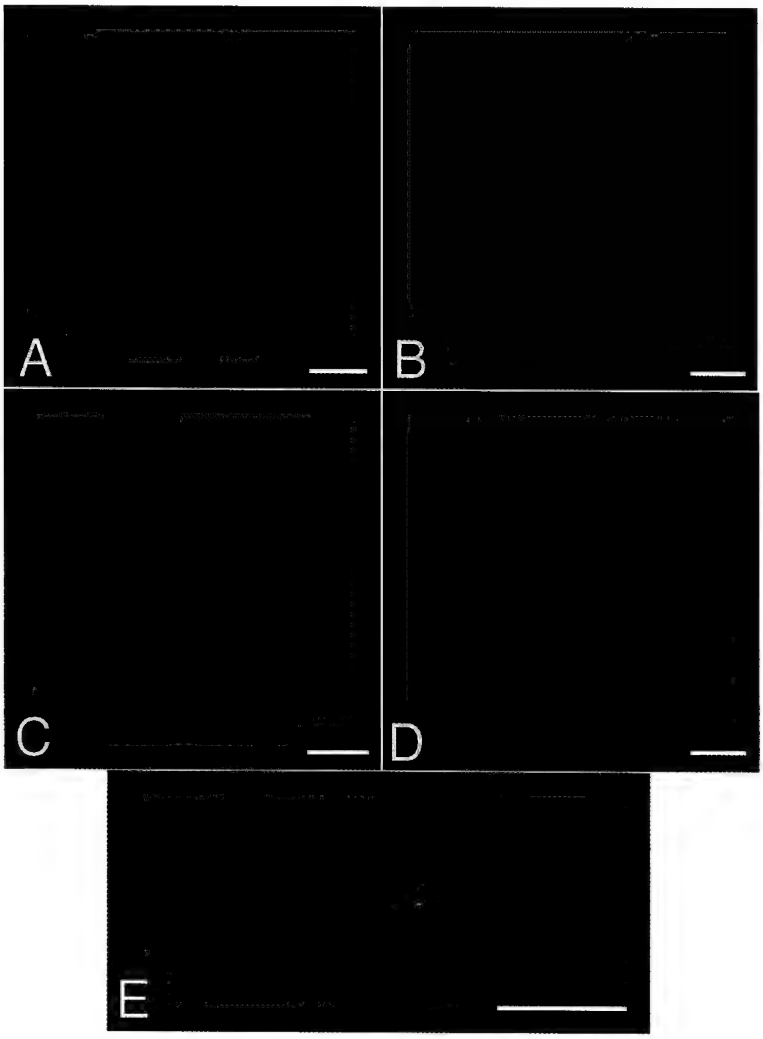

Figure 3. Endobrevin Colocalizes with Syntaxin 2 on the Midbody

(A) Cellubrevin (green) localizes to intracellular vesicles in late telophase NRK cells but not to the midbody, which is identified by immunostaining for β-tubulin (red).

(B–D) Endobrevin (green) localizes to midbody in NRK cells (B). The immunostaining for endobrevin is eliminated by competition with total bacterial lysate containing GST-endobrevin (C) but not by lysate containing GST (D).

(E) Coimmunostaining for syntaxin 2 (green) and endobrevin (red) reveals their colocalization on the midbody of NRK cells. Scale bars, 5 μm.

endobrevin localizes to several intracellular organelles, including tubulovesicular structures, small vesicles, multivesicular bodies, vacuolar endosomes, TGN, plasma membrane, and clathrin-coated pits in NRK cells and has been reported to mediate homotypic fusion of early endosomes and late endosomes (Antonin et al., 2000).

To investigate whether endobrevin is functionally involved in cytokinesis, we constructed a truncation mutant lacking the C-terminal transmembrane anchor and expressed it using a tetracycline-regulatable adenoviral vector as described above for syntaxin 2D. Figure 4A shows that expressed truncated endobrevin distributes throughout the cytoplasm and results in a high percentage of binucleated cells after 16 hr. As a control, when the expression of truncated endobrevin was prevented by the inclusion of doxycycline the formation of binucleated cells was suppressed (Figure 4B). These results indicate that truncated endobrevin acts as a dominant-negative inhibitor of membrane-anchored endobrevin resulting in inhibition of cytokinesis. Time-lapse microscopy revealed that endobrevin inhibition did not interfere with events upstream of midbody-formation but resulted in the inability to cleave the midbodies (see Supplemental Data, Movie S2 [http://www.developmentalcell.com/cgi/content/full/4/5/753/DC1]). The average time between midbody formation and regression into binucleated cells was 173 min (range 80–345 min, n = 45). This phenotype was indistinguishable from that of syntaxin 2 inhibition as described above, suggesting that syntaxin 2 and endobrevin act together at the same step during midbody abscission.

Collectively, these results show for the first time that midbody abscission requires the action of members of the SNARE membrane fusion machinery. Inhibition of syntaxin 2 or endobrevin had no apparent effect on cleavage furrow invagination, nuclear division, reformation of the nuclear envelope, or other mitotic events. It is therefore unlikely that these SNAREs are involved in any mitotic step prior to midbody abscission. Since cleavage furrow invagination is believed to require exocytosis for the insertion of additional plasma membrane, it is likely that other SNAREs are involved in this process in mammalian cells. A possible candidate is syntaxin 4, which we found to localize to the ingressed plasma membranes separating the prospective daughter cells prior to midbody abscission (see Figure 1D). This would be analogous to the proposed function of SYN-4 in *C. elegans* (Jantsch-Plunger and Glotzer, 1999). Note that

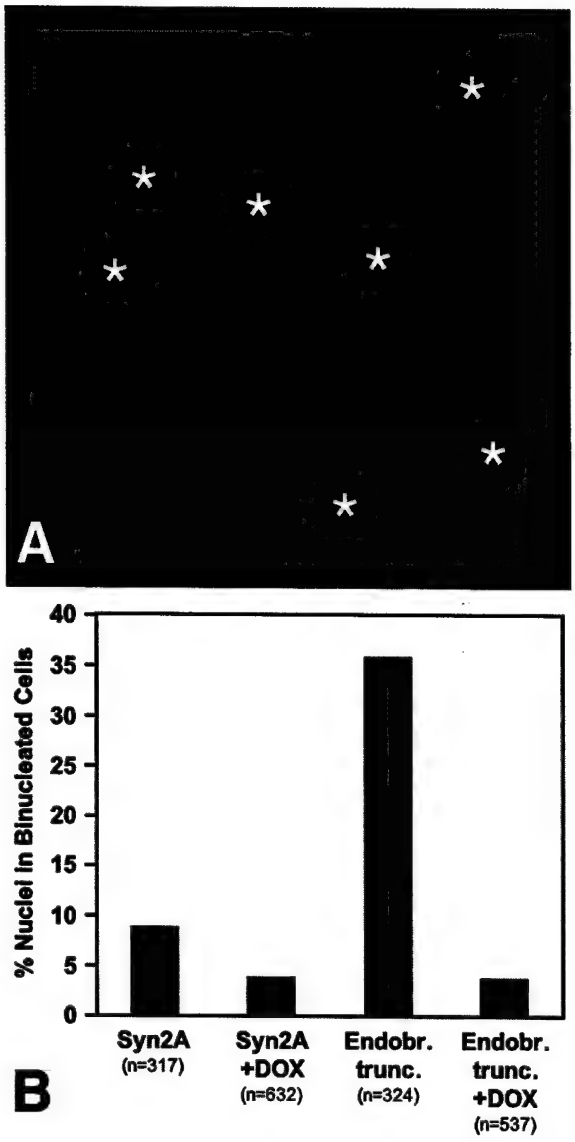

Figure 4. Endobrevin Function Is Required for Cytokinesis

(A) Expression of truncated endobrevin lacking its transmembrane anchor (green) in MDCK cells for 16 hr results in the formation of binucleated cells (denoted by asterisks).

(B) Quantification of failed cytokinesis after expression of truncated endobrevin or syntaxin 2A as a control for 16 hr. As a further control, expression was suppressed by doxycycline (DOX).

mammalian and *C. elegans* SNAREs are too divergent to allow assignment of orthologs by sequence comparison (Jantsch-Plunger and Glotzer, 1999; Weimbs et al., 1997). Therefore, despite the coincidental similarity of their names, it remains to be established whether the mammalian syntaxin 4 may have the equivalent role of the *C. elegans* SYN-4 in cleavage furrow ingression.

Most proteins involved in cytokinesis also have other functions in nondividing cells. This is likely the case for syntaxin 2 and endobrevin as well. Both are expressed in nondividing cells such as renal epithelial cells (Li et al., 2002) and the retinal pigment epithelium (Low et al., 2002). Syntaxin 2 is has previously been implicated in the sperm acrosome reaction (Katafuchi et al., 2000) as well as zymogen granule exocytosis in pancreatic acinar cells (Hansen et al., 1999), and endobrevin has been reported to be involved in endosome fusion (Antonin et al., 2000). Our finding that syntaxin 2 and endobrevin function in midbody abscission during cell division indicates that this terminal step of cytokinesis utilizes a SNARE machinery that is distinct from those involved in prior mitotic steps that require membrane fusion such as furrowing. If the function of syntaxin 2 or endobrevin is inhibited, cell division can not be completed, indicating that other SNAREs can not substitute their function. This suggests that midbody abscission is a highly regulated, active process, and that mammalian cells possess no alternative mechanisms that can accomplish the breakage of this narrow bridge.

Cell division is not only a fundamental biological process but is also of particular interest as a target for antitumor strategies. Currently used anti-tumor compounds target the cell cycle at various steps. The identification of molecules involved in the terminal step of cytokinesis may provide potential new targets that may be exploited for cancer therapy.

Experimental Procedures

Antibodies

Affinity-purified antibodies against the cytoplasmic domains of rat syntaxins 2, 3, and 4 have been described previously (Low et al., 2000). An antibody against the cytoplasmic domain of endobrevin was raised and affinity purified equivalently as described previously (Li et al., 2002). As confirmatory controls, independently raised affinity-purified antibodies against syntaxin 2 (Quinones et al., 1999) and endobrevin (gift from Wanjin Hong, IMCB, Singapore) were used. A monoclonal β-tubulin antibody developed by Michael Klymkowsky was obtained from the Developmental Studies Hybridoma Bank, The University of Iowa. Antibodies against the Nuclear Transport Factor p97 and ZO-1 were from ABR (Golden, CO) and Chemicon (Temecula, CA), respectively.

Cell Culture and Immunolocalization

NRK cells (from ATCC) were cultured in DMEM with sodium pyruvate, 10% FBS and penicillin and streptomycin. MDCK cells were cultured as described (Low et al., 2000). Cells were fixed in methanol and subjected to immunostaining and confocal fluorescence microscopy as described previously (Low et al., 2000). For localizing simultaneously two proteins recognized by rabbit primary antibodies (syntaxin 2 and endobrevin), fluorescein-labeled F_{ab} fragments of the secondary antibody (Jackson ImmunoResearch, West Grove, PA) were used after incubation with the first rabbit primary antibody. The cells were briefly fixed again with 4% paraformaldehyde and then incubated with the second rabbit primary antibody, followed by Texas red-labeled secondary antibody (Weimbs et al., 2003). Antibody concentrations were titered so that all negative controls were negative.

Expression of SNARE Cytoplasmic Domains

The adenovirus vectors for tetracycline-regulated expression of rat syntaxins 2A and 2D have been described previously (Quinones et al., 1999). The identical vector system was used for the expression of truncated endobrevin lacking its transmembrane domain. MDCK cells stably expressing the TET transactivator (Clontech, Palo Alto, CA) were infected with virus numbers titered to result in ~80%–90% of expressing cells after 16 hr. After fixation, double immunostaining for the respective truncated SNARE and the p58 endogenous plasma membrane marker (Low et al., 2000), and nuclear staining with DAPI, random fields were imaged by fluorescence microscopy, and the number of nuclei in mono- and binucleated cells were counted manually. The fraction of nuclei in binucleated cells as a percentage of the total nuclei was expressed as a measure for the failure in cytokinesis. For plasmid-mediated transient transfection

experiments, the cDNAs encoding syntaxin 2A or 2D or truncated versions of syntaxin 3 or 4 were inserted into the vector pcDNA4/TO and transfected into MDCK cells cultured on glass cover slips using the ExGen 500 transfection reagent (Fermentas, Hanover, MD). This resulted in comparable expression levels as assessed by fluorescence microscopy. After 24 hr, analysis of failed cytokinesis was carried out as described above.

Time-Lapse Microscopy

Truncated SNAREs were expressed in MDCK cells as described above. Approximately 8 hr postinfection, cells were subjected to time-lapse phase contrast microscopy (2 minutes/frame) using a fully motorized Leica DMIRB microscope equipped with a temperature-, CO_2-, and humidity-controlled environmental chamber. Images were processed using Metamorph, Adobe Photoshop, and QuickTime.

Acknowledgments

Wanjin Hong and Steve Hardy are gratefully acknowledged for gifts of reagents. We are grateful to Judith Drazba and Amit Vasanji for help with time-lapse microscopy. Work in T.W.'s laboratory was supported by NIH-DK62338 and NIH-GM066785, a Jerry and Martha Jarrett Grant for Research on Polycystic Kidney Disease, a grant from the Department of Defense Prostate Cancer Research Program (DAMD17-02-1-0039), and a Beginning Grant-in-Aid from the American Heart Association. S.H.L. was supported by a Scientist Development Grant from the American Heart Association.

Received: December 2, 2002
Revised: March 3, 2003
Accepted: March 3, 2003
Published: May 5, 2003

References

Antonin, W., Holroyd, C., Tikkanen, R., Honing, S., and Jahn, R. (2000). The R-SNARE endobrevin/VAMP-8 mediates homotypic fusion of early endosomes and late endosomes. Mol. Biol. Cell *11*, 3289–3298.

Assaad, F., Huet, Y., Mayer, U., and Jurgens, G. (2001). The cytokinesis gene keule encodes a sec1 protein that binds the syntaxin knolle. J. Cell Biol. *152*, 531–544.

Bennett, M.K., Garcia-Arraras, J.E., Elferink, L.A., Peterson, K., Fleming, A.M., Hazuka, C.D., and Scheller, R.H. (1993). The syntaxin family of vesicular transport receptors. Cell *74*, 863–873.

Chen, Y.A., and Scheller, R.H. (2001). SNARE-mediated membrane fusion. Nat. Rev. Mol. Cell Biol. *2*, 98–106.

Conner, S.D., and Wessel, G.M. (1999). Syntaxin is required for cell division. Mol. Biol. Cell *10*, 2735–2743.

Conner, S.D., and Wessel, G.M. (2000). A rab3 homolog in sea urchin functions in cell division. FASEB J. *14*, 1559–1566.

Fenech, M., and Crott, J.W. (2002). Micronuclei, nucleoplasmic bridges and nuclear buds induced in folic acid deficient human lymphocytes-evidence for breakage-fusion-bridge cycles in the cytokinesis-block micronucleus assay. Mutat. Res. *504*, 131–136.

Field, C., Li, R., and Oegema, K. (1999). Cytokinesis in eukaryotes: a mechanistic comparison. Curr. Opin. Cell Biol. *11*, 68–80.

Finger, F.P., and White, J.G. (2002). Fusion and fission: membrane trafficking in animal cytokinesis. Cell *108*, 727–730.

Glotzer, M. (2001). Animal cell cytokinesis. Annu. Rev. Cell Dev. Biol. *17*, 351–386.

Hansen, N.J., Antonin, W., and Edwardson, J.M. (1999). Identification of SNAREs involved in regulated exocytosis in the pancreatic acinar cell. J. Biol. Chem. *274*, 22871–22876.

Heese, M., Gansel, X., Sticher, L., Wick, P., Grebe, M., Granier, F., and Jurgens, G. (2001). Functional characterization of the KNOLLE-interacting t-SNARE AtSNAP33 and its role in plant cytokinesis. J. Cell Biol. *155*, 239–249.

Hua, Y., and Scheller, R.H. (2001). Three SNARE complexes cooperate to mediate membrane fusion. Proc. Natl. Acad. Sci. USA *98*, 8065–8070.

Jahn, R., and Sudhof, T.C. (1999). Membrane fusion and exocytosis. Annu. Rev. Biochem. *68*, 863–911.

Jantsch-Plunger, V., and Glotzer, M. (1999). Depletion of syntaxins in the early Caenorhabditis elegans embryo reveals a role for membrane fusion events in cytokinesis. Curr. Biol. *9*, 738–745.

Katafuchi, K., Mori, T., Toshimori, K., and Iida, H. (2000). Localization of a syntaxin isoform, syntaxin 2, to the acrosomal region of rodent spermatozoa. Mol. Reprod. Dev. *57*, 375–383.

Lauber, M.H., Waizenegger, I., Steinmann, T., Schwarz, H., Mayer, U., Hwang, I., Lukowitz, W., and Jurgens, G. (1997). The Arabidopsis KNOLLE protein is a cytokinesis-specific syntaxin. J. Cell Biol. *139*, 1485–1493.

Li, X., Low, S.H., Miura, M., and Weimbs, T. (2002). SNARE expression and localization in renal epithelial cells suggest mechanism for variability of trafficking phenotypes. Am. J. Physiol. Renal Physiol. *283*, F1111–F1122.

Low, S.H., Chapin, S.J., Weimbs, T., Kömüves, L.G., Bennett, M.K., and Mostov, K.E. (1996). Differential localization of syntaxin isoforms in polarized MDCK cells. Mol. Biol. Cell *7*, 2007–2018.

Low, S.H., Miura, M., Roche, P.A., Valdez, A.C., Mostov, K.E., and Weimbs, T. (2000). Intracellular redirection of plasma membrane trafficking after loss of epithelial cell polarity. Mol. Biol. Cell *11*, 3045–3060.

Low, S.H., Marmorstein, L.Y., Miura, M., Li, X., Kudo, N., Marmorstein, A.D., and Weimbs, T. (2002). Retinal pigment epithelial cells exhibit unique expression and localization of plasma membrane syntaxins which may contribute to their trafficking phenotype. J. Cell Sci. *115*, 4545–4553.

Mullins, J.M., and McIntosh, J.R. (1982). Isolation and initial characterization of the mammalian midbody. J. Cell Biol. *94*, 654–661.

O'Halloran, T.J. (2000). Membrane traffic and cytokinesis. Traffic *1*, 921–926.

Quinones, B., Riento, K., Olkkonen, V.M., Hardy, S., and Bennett, M.K. (1999). Syntaxin 2 splice variants exhibit differential expression patterns, biochemical properties and subcellular localizations. J. Cell Sci. *112*, 4291–4304.

Shuster, C.B., and Burgess, D.R. (2002). Targeted new membrane addition in the cleavage furrow is a late, separate event in cytokinesis. Proc. Natl. Acad. Sci. USA *99*, 3633–3638.

Skop, A.R., Bergmann, D., Mohler, W.A., and White, J.G. (2001). Completion of cytokinesis in C. elegans requires a brefeldin A-sensitive membrane accumulation at the cleavage furrow apex. Curr. Biol. *11*, 735–746.

Waizenegger, I., Lukowitz, W., Assaad, F., Schwarz, H., Jurgens, G., and Mayer, U. (2000). The Arabidopsis KNOLLE and KEULE genes interact to promote vesicle fusion during cytokinesis. Curr. Biol. *10*, 1371–1374.

Weimbs, T., Low, S.H., Chapin, S.J., Mostov, K.E., Bucher, P., and Hofmann, K. (1997). A conserved domain is present in different families of vesicular fusion proteins: a new superfamily. Proc. Natl. Acad. Sci. USA *94*, 3046–3051.

Weimbs, T., Mostov, K.E., Low, S.H., and Hofmann, K. (1998). A model for structural similarity between different SNARE complexes based on sequence relationships. Trends Cell Biol. *8*, 260–262.

Weimbs, T., Low, S.H., Li, X., and Kreitzer, G. (2003). SNAREs and epithelial cells. Methods, in press.

Zeitlin, S.G., and Sullivan, K.F. (2001). Animal cytokinesis: Breaking up is hard to do. Curr. Biol. *11*, R514–R516.

Three-dimensional analysis of post-Golgi carrier exocytosis in epithelial cells

Geri Kreitzer*#, Jan Schmoranzer‡§, Seng Hui Low¶, Xin Li¶, Yunbo Gan*, Thomas Weimbs¶, Sanford M Simon‡ and Enrique Rodriguez-Boulan*†**

*Margaret M. Dyson Vision Research Institute, Weill Medical College of Cornell University, New York, NY 10021, USA
†Department of Cell Biology, Weill Medical College of Cornell University, New York, NY 10021, USA
‡Laboratory of Cellular Biophysics, Rockefeller University, New York, NY 10021, USA
§Department of Biology, Chemistry, Pharmacology, Free University, Berlin 14195, Germany
¶Department of Cell Biology, Lerner Research Institute and the Glickman Urological Institute, The Cleveland Clinic, Cleveland, OH 44195, USA
e-mail: #ggurlan@med.cornell.edu or **boulan@med.cornell.edu

Published online: 27 January 2003; DOI: 10.1038/ncb917

Targeted delivery of proteins to distinct plasma membrane domains is critical to the development and maintenance of polarity in epithelial cells. We used confocal and time-lapse total internal reflection fluorescence microscopy (TIR-FM) to study changes in localization and exocytic sites of post-Golgi transport intermediates (PGTIs) carrying GFP-tagged apical or basolateral membrane proteins during epithelial polarization. In non-polarized Madin Darby Canine Kidney (MDCK) cells, apical and basolateral PGTIs were present throughout the cytoplasm and were observed to fuse with the basal domain of the plasma membrane. During polarization, apical and basolateral PGTIs were restricted to different regions of the cytoplasm and their fusion with the basal membrane was completely abrogated. Quantitative analysis suggested that basolateral, but not apical, PGTIs fused with the lateral membrane in polarized cells, correlating with the restricted localization of Syntaxins 4 and 3 to lateral and apical membrane domains, respectively. Microtubule disruption induced Syntaxin 3 depolarization and fusion of apical PGTIs with the basal membrane, but affected neither the lateral localization of Syntaxin 4 or Sec6, nor promoted fusion of basolateral PGTIs with the basal membrane.

Epithelial cells perform polarized transport and secretory functions that are essential for survival of the organism. To perform these vectorial functions, epithelial cells segregate their plasma membrane proteins into apical and basolateral domains, separated by tight junctions. Apical and basolateral membrane proteins are synthesized in the endoplasmic reticulum, transferred to the Golgi apparatus and segregated into different PGTIs for export to the cell surface[1–3]. Segregation is thought to occur in the *trans*-Golgi network (TGN) and is mediated by sorting signals embedded within the protein structure. Apical sorting signals include N- and O-linked glycans in the ectodomain, glycosyl phosphatidylinositol and transmembrane anchors, and amino-acid stretches in the cytoplasmic domain[4,5]. In contrast, basolateral sorting signals usually comprise amino acid stretches in the cytoplasmic domain that typically include tyrosine, dileucine and monoleucine motifs, as well as clusters of acidic amino acids[6,7]. Apical or basolateral membrane proteins can exit the Golgi in vesicular or tubular PGTIs[3,8,9]. The formation of PGTIs depends on the direct or indirect interaction of sorting signals with cytoplasmic adaptors and coat proteins[10–13]. Adaptors can also mediate binding of cargo to specific microtubule motors[14–16], which can modulate the transport and/or budding of Golgi-derived vesicles, as well as the emergence of tubular PGTIs[9].

Work in the past two decades has suggested that microtubules are important in establishing epithelial polarity, although exactly how they contribute to this process is still unknown. During epithelial polarization, microtubules re-organize from centrosomally nucleated, radial arrays into longitudinal bundles (minus-ends towards the apical surface) oriented in parallel with the lateral membrane, and into arrays of mixed polarity underlying the apical pole and overlying the basal membrane[17,18]. This microtubule reorganization is accompanied by relocation of the Golgi complex to the apical region of the cytoplasm[17,19]. Time-lapse studies in fibroblasts and sub-confluent epithelial cells have shown that vesicular and tubular PGTIs move through the cytoplasm along microtubules for delivery to the plasma membrane[3,8,20]. Injection of kinesin antibodies completely inhibits post-Golgi transport, indicating that microtubules are essential for post-Golgi trafficking under physiological conditions[9]. In polarized epithelial cells, biochemical assays have shown that disruption of microtubules slows the delivery of apical membrane proteins and often results in their mis-targeting to the basolateral surface[18,19,21–27]. In contrast, disruption of microtubules does not significantly affect delivery of basolateral membrane proteins[22,24,28], but does induce apical exocytosis of proteins normally secreted into the basolateral medium[29,30]. Although the effects of microtubule disruption on apical and basolateral protein targeting have been well characterized, it is unclear whether and how microtubules exert selective control over the intracellular distribution of PGTIs, as well as over their fusion with specific domains of the plasma membrane.

A key event in epithelial polarization is the establishment of polarized transport routes to apical and basolateral regions of the plasma membrane. The asymmetric distribution of docking and fusion machinery for PGTIs is probably involved in regulating polarized exocytosis in epithelial cells. Basolateral exocytosis seems to depend on an evolutionarily conserved 'tethering' complex known as the exocyst. In polarized MDCK cells, the exocyst localizes to the lateral membrane near the tight junction[31]. Antibodies against the exocyst components Sec6 and Sec8 block basolateral

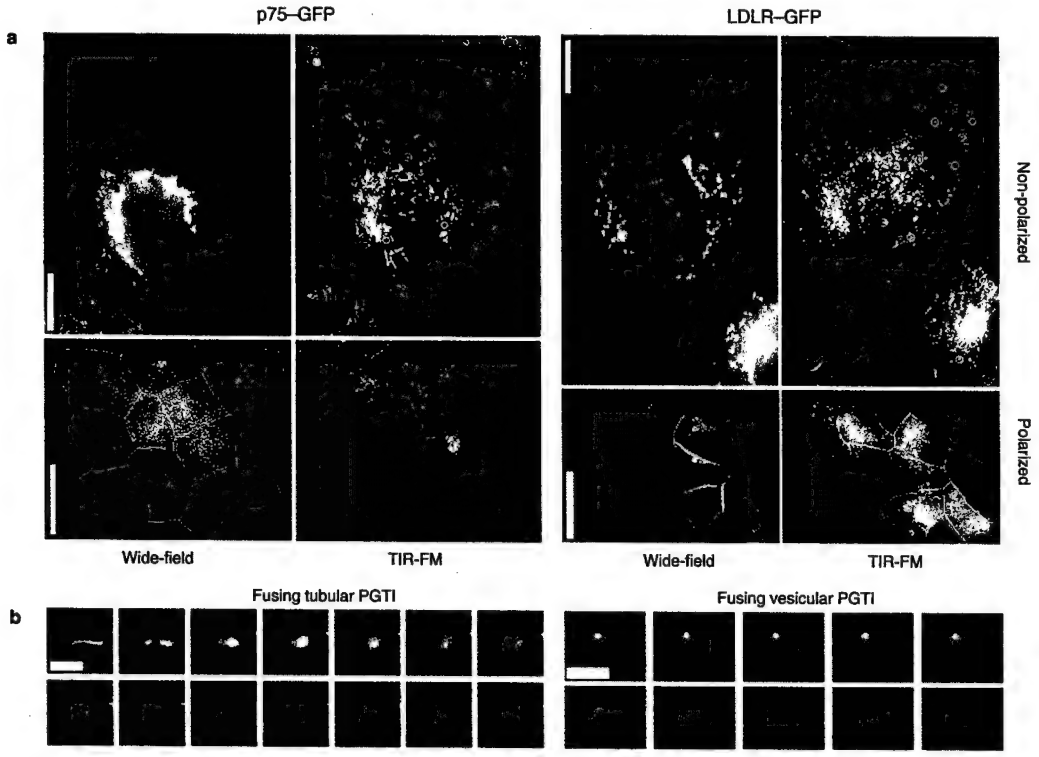

Figure 1 **Fusion of PGTIs with the basal membrane in MDCK cells.** Fusion of post-Golgi carriers with the basal plasma membrane was monitored by TIR-FM after release from a Golgi temperature block. 500-frame time-lapse sequences were acquired at 222-ms intervals, unless otherwise stated. **a**, Wide-field images of non-polarized cells show the total intracellular distribution of GFP-tagged membrane proteins just after release from the Golgi temperature block. TIR-FM images show time-lapse overlays (every 20 frames) from recordings made in cells expressing p75–GFP (21 min after release of the Golgi block; Supplementary Information, Movie 1) or LDLR–GFP (19 min after release of the Golgi block. Positions of fusion events mapped in Supplementary Information Movie 1 are circled in TIR-FM panels. In polarized cells, PGTIs containing p75–GFP or LDLR–GFP did not fuse with the basal membrane in polarized cells at any time after release of the Golgi block. Corresponding wide-field images of polarized cells show that although no fusion events were detected by TIR-FM, p75–GFP and LDLR–GFP emptied from the Golgi and localized to the apical and basolateral plasma membranes, respectively. **b**, Selected sequential frames from TIR-FM recordings showing examples of tubular or vesicular PGTIs fusing with the membrane are shown. Scale bars represent 15 μm in **a** and 2 μm in **b**. Accompanying movies can be found at http://www.boulan-lab.acomhosting.com.

transport[31], and overexpression of another exocyst component, Sec10, results in enhanced basolateral transport[32]. Components of the plasma membrane fusion machinery, the t-SNAREs Syntaxin 3 and 4, localize to apical and basolateral plasma membranes, respectively, in polarized MDCK cells[33]. In semi-intact MDCK cell transport assays, addition of α-SNAP antibodies or cleavage of the t-SNARE, SNAP23, with botulinum E toxin reduced surface delivery of apical and basolateral markers, whereas anti-Syntaxin 3 antibodies selectively inhibited apical transport[34,35]. In intact cells, overexpression of Syntaxin 3 results in decreased apical transport and a twofold accumulation of vesicles under the apical plasma membrane[34]. These data suggest that SNARE-mediated fusion events are essential to polarized exocytosis.

In this study, we used confocal microscopy and TIR-FM to analyse the three-dimensional distribution of apical and basolateral PGTIs, and to localize their sites of exocytosis in non-polarized and polarized MDCK cells. Additionally, we tested whether microtubules modulate the distribution of tethering or fusion complexes involved in generating polarized transport routes to the cell surface. Our results demonstrate that both apical and basolateral PGTIs fuse with the basal plasma membrane in non-polarized MDCK cells. After polarization, apical and basolateral PGTIs become spatially segregated in different regions of the apical cytoplasm; basolateral PGTIs were observed primarily in the most apical two thirds of the cytoplasm, whereas apical PGTIs were restricted to the top ~4 μm of the cytoplasm. In polarized cells, neither apical nor basolateral PGTIs fused with the basal membrane. Instead, fusion of basolateral PGTIs was concentrated in upper regions of the lateral membrane. Apical PGTIs were not observed fusing with either the basal or lateral membrane in polarized cells, suggesting that these carriers fused directly with the apical membrane. In contrast, disruption of microtubules with nocodazole promoted fusion of apical PGTIs with the basal membrane and depolarization of apical Syntaxin 3. We show that micro-injection of a function-blocking antibody against Syntaxin 3 inhibits delivery of an apical marker in polarized, untreated MDCK cells, as well as its fusion with the basal membrane when microtubules were depolymerized. Our results implicate microtubules in maintaining the apical distribution of Syntaxin 3, and thus in prohibiting fusion of apical PGTIs with the basolateral membrane. This study represents the first live-cell analysis of the three-dimensional distribution of post-Golgi transport intermediates and their fusion with restricted domains of the

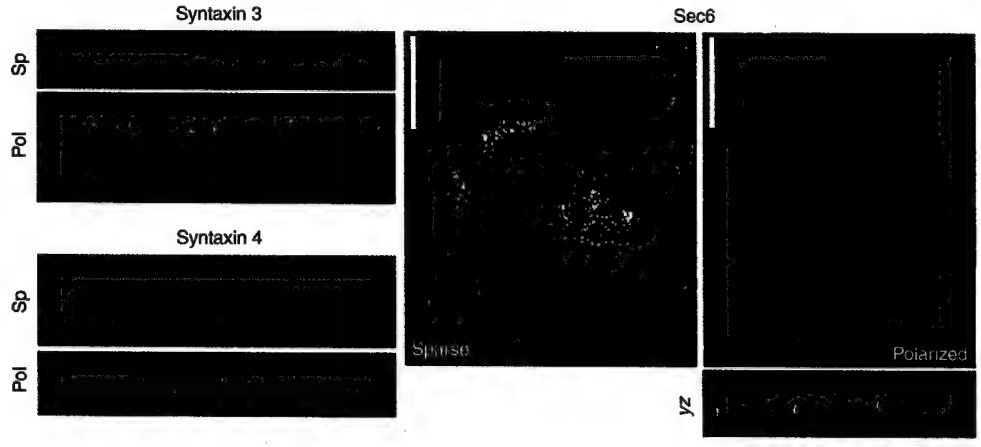

Figure 2 **Localization of Syntaxins 3 and 4 and Sec6 in MDCK cells.** The steady state, surface distribution of Syntaxins 3 and 4 (green) in sparse and polarized MDCK cells was determined by immunostaining for the extracellular Myc epitope fused to Syntaxins 3 and 4. The tight junction marker, ZO-1 (red) was costained as a reference for cell–cell boundaries. Images of polarized cells are *z* sections through either confocal (syntaxins) or wide-field (Sec6) images taken at sequential focal planes. The distribution of Sec6 at the basal membrane of non-polarized cells was visualized using TIR-FM. In polarized cells, Sec6 (red) was present in the lateral membrane (*xy* view, top) and often colocalized with E-cadherin (green, *yz* view, bottom). DAPI-stained nuclei are shown in blue. Scale bars represent 20 μm.

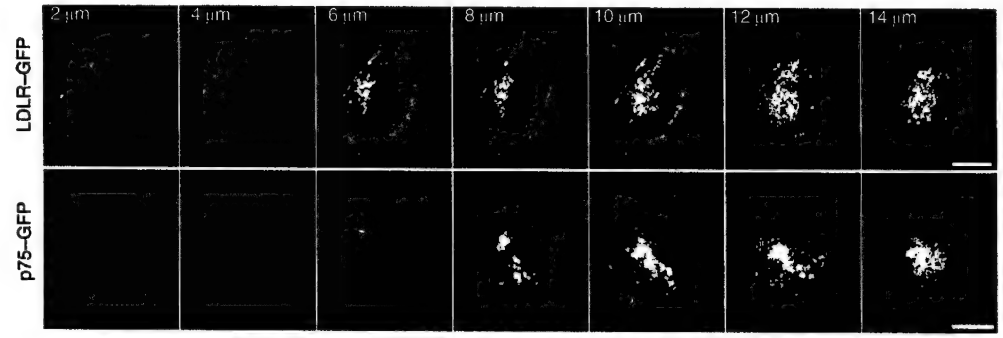

Figure 3 **Post-Golgi carrier movements are restricted within the apical cytoplasm.** The spatial distribution of post-Golgi carriers in polarized cells was determined using confocal time-lapse imaging in sequential *z*-axis planes. Time projections from 1-min recordings made at 2, 4, 6, 8, 10, 12 and 14 μm above the basal membrane are shown in cells expressing LDLR–GFP (34–50 min after release of the Golgi block) or p75–GFP (14–30 min after release of the Golgi block). Time-lapse images were recorded using identical acquisition settings and are displayed using identical display settings. The distribution of basolateral and apical PGTIs shown here was observed in 28 cells injected with LDLR–GFP and 23 cells injected with p75–GFP recorded during two independent experiments. Corresponding time-lapse recordings can be seen in Supplementary Information, Movie 2. Scale bars represent 10 μm.

plasma membrane in polarized epithelial cells.

Results

Apical or basolateral post-Golgi carriers fuse with the basal membrane in non-polarized MDCK cells. Proteins that are restricted to apical or basolateral membranes in polarized MDCK cells are often found on all cell surfaces in non-polarized cells. As at least some apical and basolateral proteins are sorted and packaged into different PGTIs in non-polarized epithelial cells[3], the non-restricted distribution of these markers could potentially be attributed to two processes: first, diffusion of apical and basolateral proteins throughout the cell surface after targeted delivery to presumptive apical and basolateral membranes (before the formation of tight junctions); second, to non-targeted surface delivery of apical and basolateral proteins. To examine these possibilities, we used TIR-FM to assess whether apical and basolateral PGTIs fuse with the plasma membrane domain that makes contact with the coverslip (hereafter referred to as the 'basal' plasma membrane). We expressed the green fluorescent protein (GFP)-tagged apical membrane protein p75 neurotrophin receptor (p75–GFP) and the GFP-tagged basolateral membrane proteins neural cell adhesion molecule (NCAM–GFP) or internalization-defective low-density lipoprotein receptor mutant (LDLR-A18–GFP) by injecting cDNAs into the nucleus of non-polarized or polarized MDCK cells[9]. During a 20 °C incubation, newly synthesized membrane proteins

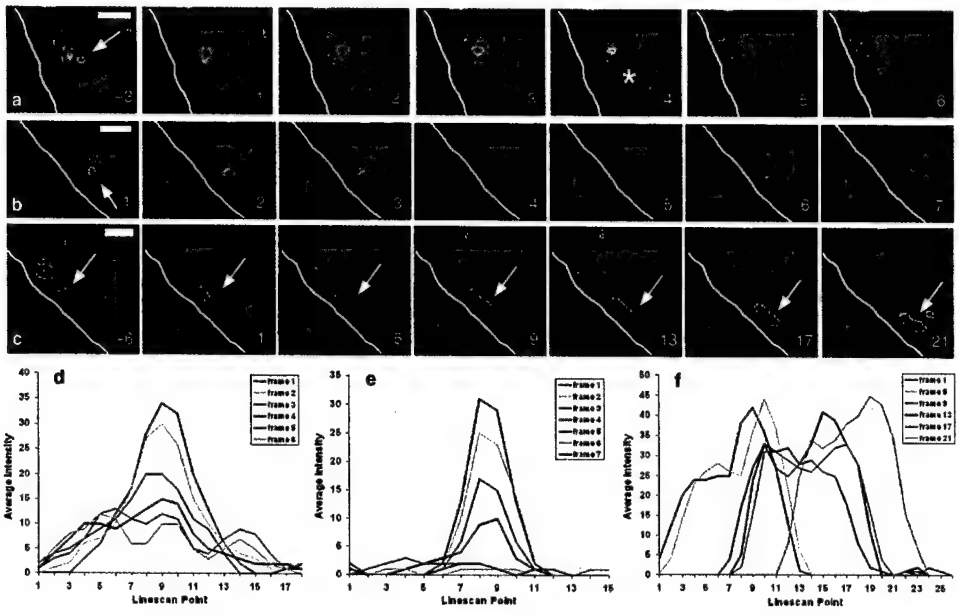

Figure 4 **Fusion of basolateral PGTIs with the lateral membrane in polarized MDCK cells.** PGTIs travelling through the cytoplasm to the plasma membrane exhibited different behaviours after making contact with the lateral membrane, each of which was represented by a different linescan intensity profile. Panels in **a–c** show selected images from time-lapse sequences (acquired between 15 and 53 min after release from the Golgi temperature block), illustrating these behaviours for PGTIs containing LDLR–GFP. White lines demarcate the extracellular boundaries of the plasma membrane with the cytoplasm always to the right of the lines. Arrows denote the PGTI of interest. Corresponding graphs in **d–f** show the measured linescan intensity profiles for each of the PGTIs in **a–c**, respectively. **a** and **d** show a fusing PGTI. The asterisk denotes the image frame at which a spread in carrier fluorescence was first visible. Note, however, that the linescan shows spreading began in the previous frame. **b** and **e** show a PGTI moving out of the plane of focus after contacting the membrane. **c** and **f** show a PGTI moving along the membrane without leaving the focal plane. Frame numbers refer to the time-lapse image plane at the start of each PGTI event. Image frames were enlarged and pseudocoloured for clarification. Scale bars represent 1 μm.

accumulated in a perinuclear compartment (Fig. 1a, wide field), defined as Golgi/TGN by colocalization with newly synthesized galactosyl transferase–cyan fluorescent protein (CFP; data not shown). After release from the temperature block, all three markers acquired a homogeneous distribution in non-polarized cells and distinctive apical or basolateral distributions in polarized cells (Fig. 1a).

Using TIR-FM, PGTIs containing GFP-tagged fusion proteins are detected only when they move into an evanescent field, which in our experiments was within ~120nm of the basal membrane. Previously, we established a quantitative method for detecting *bona fide* fusion of PGTIs with the plasma membrane[20]. In time-lapse TIR-FM recordings (500 frames, ~4 frames s^{-1}) made in non-polarized MDCK cells after release from a Golgi temperature block, we observed fusion of 57 PGTIs containing p75–GFP (Fig. 1a and Supplementary Information, Movie 1), 42 PGTIs containing LDLR-A18–GFP (Fig. 1a) or 27 PGTIs containing NCAM–GFP with the basal membrane (circles demarcate positions of fusion events). Accompanying movies can be found at http://www.boulan-lab.acomhosting.com. Fusing PGTIs displayed both vesicular and tubular morphologies (Fig. 1b) and could often be observed moving along the basal membrane in TIR-FM movies. Images shown in Fig. 1 and Supplementary Information Movies are representative of time-lapse recordings from at least three independent experiments monitoring exocytosis of each of the GFP-tagged cargoes. Fusion of post-Golgi carriers with the plasma membrane began within 5 min after release of the Golgi temperature block and continued for 60–70 min (NCAM–GFP) or for up to 2 h (LDLR-A18–GFP or p75–GFP). In all cases, the cessation of plasma membrane fusion correlated directly with the emptying of GFP markers from the Golgi, as detected by wide-field illumination. These results demonstrate that the uniform surface distribution of apical and basolateral markers is caused by non-targeted membrane delivery before MDCK polarization. The observed difference in rates of Golgi emptying for each of the markers, and the fact that co-expressed apical and basolateral proteins fused to cyan or yellow fluorescent protein were often segregated into different PGTIs (data not shown and ref. 3) further supports the idea that protein sorting in the Golgi occurs in non-polarized MDCK cells. Neither LDLR-A18 (ref. 36), p75 (ref. 37) nor NCAM[38] are efficiently recycled from the plasma membrane into the endosomal system (see Supplementary Information, Fig. S3). Thus, the fusion events we report probably represent direct delivery of Golgi-derived secretory carriers to the plasma membrane.

Fusion of post-Golgi carriers with the basal membrane is abrogated by cell polarization. In contrast to non-polarized cells (in which PGTIs fused with an averaged rate of 0.25–0.5 fusions s^{-1} $cell^{-1}$), in polarized cells, we did not detect fusion of a single apical or basolateral PGTI with the basal membrane (Fig. 1a, polarized, TIR-FM). Despite the lack of detectable fusion events using TIR-FM, wide-field illumination clearly showed that p75–GFP (Fig. 1a, polarized, wide field) accumulated in the apical membrane, while both LDLR-A18–GFP (Fig. 1a, polarized, wide field) and

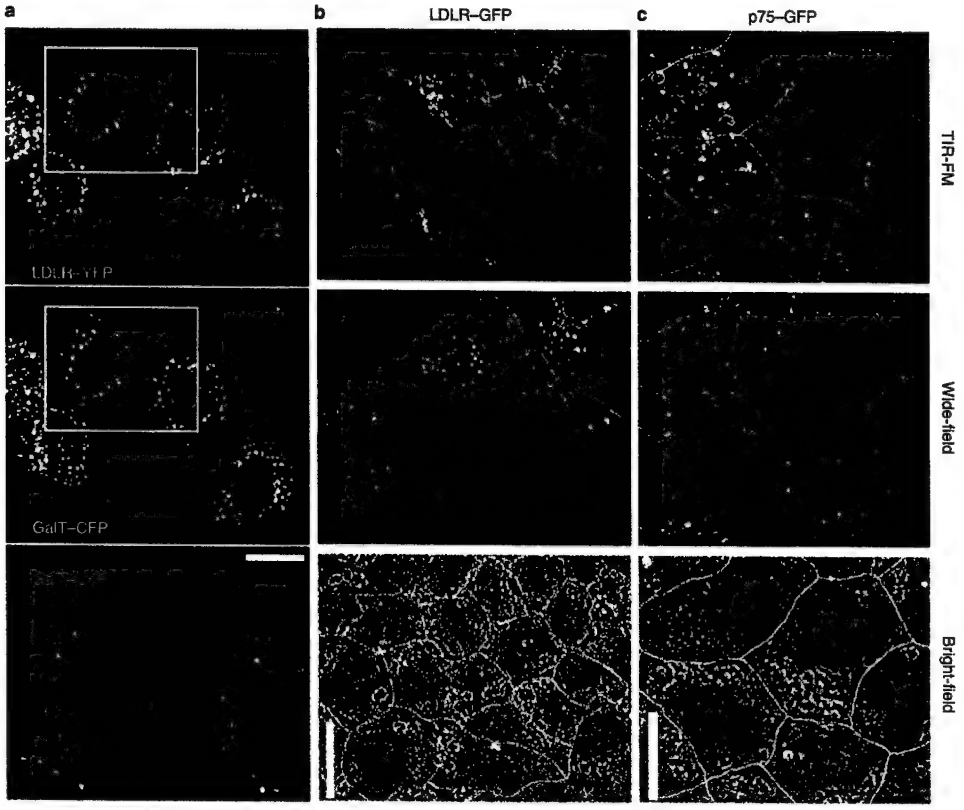

Figure 5 **Microtubule disruption selectively promotes fusion of apical PGTIs with the basal membrane.** TIR-FM was used to monitor fusion of transport intermediates with the plasma membrane in nocodazole-treated, polarized MDCK cells. Nocodazole induces fragmentation and scattering of the Golgi/TGN (as detected by the presence of GalT–CFP in **a**), but does not block accumulation of newly synthesized membrane proteins (LDLR-A18–YFP in **a** and p75–GFP in panel **b**, wide-field) in the Golgi during a 20 °C block. Colocalization of GalT–CFP and LDLR-A18–YFP after incubation at 20 °C is demonstrated in the colour overlay; the LDLR–YFP image was shifted down and left (2 × 3 pixels) to best illustrate the degree of colocalization. Circles in the TIR-FM image of p75–GFP show where PGTIs containing p75–GFP fused with the basal membrane (see Supplementary Information, Movie 4; 6 min after release of the Golgi block). Wide-field images in **b** and **c** are three-dimensional projections of serial *z*-axis images after release from the Golgi temperature block. No fusion events were detected by TIR-FM in nocodazole-treated cells expressing LDLR–GFP (**b**, 14 min after release of the Golgi block). Cell boundaries were demarcated using bright-field images as a reference (**b**, bright-field). Scale bar represents 15 μm.

NCAM–GFP (data not shown) accumulated in the lateral membrane during the course of our recordings. Interestingly, although we detected no fusion of basolateral PGTIs, TIR-FM identified some basolateral carriers moving in close proximity with the basal membrane. Thus, although some basolateral PGTIs can reach the basal membrane, in polarized cells, this membrane is not fusion competent. These results show that after epithelial cell polarization, fusion of post-Golgi carriers is restricted to regions of the plasma membrane other than the basal domain.

Sites of exocytosis correspond with the distribution of Syntaxin 3 and Syntaxin 4. Next, we examined whether changes in the distribution of the targeting and fusion machinery correlated with abrogation of basal fusion after MDCK polarization. We analysed the surface localization of the t-SNARES, Syntaxin 3 and 4, and the exocyst component, Sec6, in sub-confluent and fully polarized MDCK cells. In sparsely seeded cells, both Syntaxin 3 and 4 localized to all plasma membrane surfaces (Fig. 2, sparse). In polarized cells, however, neither syntaxin was present at the basal membrane. Instead, Syntaxin 3 localized exclusively to the apical membrane, whereas Syntaxin 4 was highly enriched in the lateral membrane (Fig. 2, polarized; also see ref. 33). In non-polarized cells, wide-field illumination revealed that Sec6 localizes to both the cytoplasm and punctate foci distributed throughout the cell periphery (data not shown). These Sec6 foci were present at, or near, the basal membrane, as they could be imaged using TIR-FM (Fig. 2, sparse). In polarized cells, Sec6 localized exclusively along the lateral membrane and partially colocalized with E-cadherin (Fig. 2, polarized and *yz* view of polarized cells). Thus, fusion of apical and basolateral PGTIs to the basal membranes of non-polarized cells correlated with the basal localization of Sec6 and Syntaxins 3 and 4; however, abrogation of fusion to basal membranes in polarized cells correlated with a redistribution of Syntaxins 3 and 4 and Sec6 to apical or lateral membrane domains.

Apical and basolateral PGTIs are concentrated in the apical half of polarized MDCK cells. As neither apical nor basolateral PGTIs fused with the basal membrane of polarized MDCK cells, we wondered where PGTIs fuse after polarization. First, we studied the distribution of PGTIs in polarized cells by making time-lapse

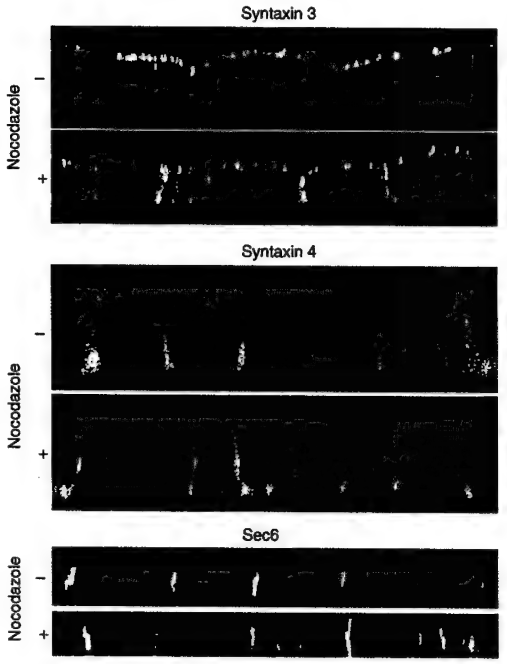

Figure 6 **Disruption of microtubules results in the selective depolarization of Syntaxin 3 in polarized MDCK cells.** Microtubules were depolymerized as described in Fig. 5. Cells stably transfected with Myc-tagged Syntaxins 3 or 4 were surface-labelled with an anti-Myc antibody. Note that Syntaxin 3 immunolocalizes to both apical and basolateral membranes after nocodazole-treatment, whereas the distribution of Syntaxin 4 is unaffected. Immunolabelling of endogenous Sec6 revealed that the distribution of this exocyst component is unaffected by microtubule perturbation.

Table 1 Three-dimensional distribution of lateral membrane fusion in polarized MDCK cells.

	LDLR–GFP				
	Cell 1	Cell 2	Cell 3	Cell 4	Total
μm from cell bottom					
14	0	0	0	0	0
12	4	3	2	2	11
10	2	1	5	3	11
8	3	2	3	1	9
6	4	5	3	0	12
4	0	0	0	0	0
2	0	0	0	0	0
0	0	0	0	0	0
Total	13	11	13	6	43

The number of PGTIs exhibiting an intensity profile indicative of fusion with the lateral membrane at various distances from the cell bottom were counted in four cells expressing the basolateral membrane protein LDLR-A18–GFP. Intensity profiles representative of fusing PGTIs were only observed in time-lapse images acquired at 6, 8, 10 and 12 mm above the cell bottom.

confocal microscopy recordings at 2-μm *z*-axis intervals through polarized cells expressing p75–GFP, NCAM–GFP or LDLR-A18–GFP. Images were acquired at ~3.5 frames s^{-1} for a duration of 1 min at each *z* interval. In all experiments, MDCK cells were grown on glass coverslips and polarized cells reached an average height of 14 μm. The tall stature of polarized MDCK cells in our experiments directly reflects measuring cell height in living, rather than fixed, cells. Our recordings showed that trafficking PGTIs containing LDLR-A18–GFP (Fig. 3; also see Supplementary Information, Movie 2) or NCAM–GFP (data not shown) were concentrated in the cytoplasm, between 6–12 μm above the basal plasma membrane. In contrast, whereas Golgi membranes containing p75–GFP were observed between 8–12 μm above the basal membrane, PGTIs containing p75–GFP were most frequently observed between 10–12 μm above the basal membrane (Fig. 3, also see Supplementary Information, Movie 2). These apical PGTIs were mainly excluded from all other regions of the cytoplasm. Thus, PGTIs containing basolateral proteins had broader distributions than PGTIs containing apical proteins, which were restricted to a narrow band under the apical surface.

Basolateral, but not apical, PGTIs fuse with the lateral membrane. The different distribution of apical and basolateral PGTIs in polarized cells suggested that they might fuse with different domains of the plasma membrane. We utilized time-lapse confocal microscopy, as described above, to evaluate if, and where, apical or basolateral carriers fuse with the lateral membrane. We analysed changes in the total fluorescence intensity over time of small (5 × 5 pixels), consecutive regions drawn throughout the entire lateral membrane at each *z* interval imaged. Approximately 60 individual membrane regions were analysed per cell at each focal plane. When PGTIs entered a membrane region of interest (ROI), there was always an increase in the total fluorescence intensity at that ROI. In cells expressing LDLR-A18–GFP, an average of 17 ± 12 of the 60 membrane ROIs per focal plane (at focal planes 2–12 μm above the cell bottom) exhibited a transient increase in total fluorescence over time. Similarly, in cells expressing p75–GFP, an average of 15 ± 9 membrane ROIs per focal plane (at focal planes 8–12 μm above the cell bottom) exhibited a transient increase in total fluorescence over time. As apical PGTIs were almost entirely excluded from the bottom half of the cytoplasm (see above), we detected very few changes in fluorescence intensity at membrane ROIs in focal planes 2–6 μm from the cell bottom. A subsequent decrease in fluorescence intensity at the same membrane ROI could be attributed to one of four possible events: first, fusion of the PGTI with the membrane; second, movement of the PGTI out of the focal plane (Δ-*z*); third, movement of the PGTI away from the ROI in the plane of focus (Δ-*xy*); fourth, either a combination of fusion with movement out of the focal plane or movement in both *xy* and *z* axes.

To discriminate between these possibilities, each membrane ROI displaying a transient increase in fluorescence intensity clearly above the noise was screened by linescan analysis (see Methods). Analysis of PGTIs ($n = 235$) moving near the plasma membrane revealed linescan profiles characteristic of all four behaviours described above. Analysis of PGTIs moving in the cytoplasm near the cell centre ($n = 20$) revealed profiles characteristic of carriers either moving out of the focal plane, moving in the plane of focus without fusing or moving in both the *xy* and *z* axes (see Supplementary Information, Fig. S1c and S1c′), but none were characteristic of PGTIs fusing with the plasma membrane. Only linescan profiles exhibiting a decrease in total intensity, concomitant with an increase in the width of fluorescence intensity along the line being measured at the membrane, were counted as fusion events in our analysis. This profile probably represents fusion of a PGTI with the plasma membrane and subsequent diffusion of its

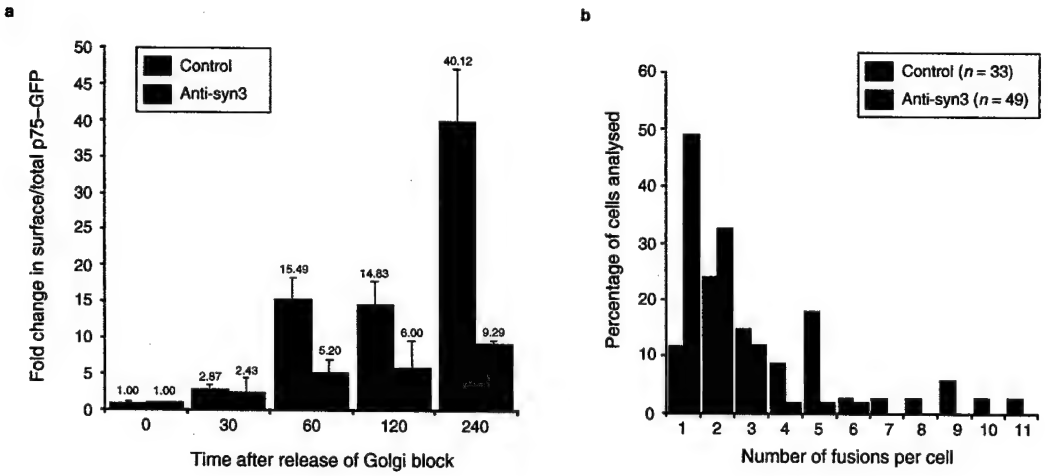

Figure 7 **Micro-injected Syntaxin 3 antibody inhibits fusion of apical PGTIs with the basal membrane in nocodazole-treated, polarized cells.** Untreated (**a**) or nocodazole-treated (**b**) cells were co-injected with p75–GFP cDNA and either a control antibody or an anti-Syntaxin 3 antibody. **a**, Delivery of p75–GFP to the apical membrane of control polarized cells was analysed by measuring the relative amount of surface-immunolabelled p75–GFP to total p75–GFP over time. The graph shows the fold change in surface:total GFP in cells micro-injected with control antibody or an anti-Syntaxin 3 antibody after release from the Golgi temperature block. Error bars represent the standard deviation of results from two independent experiments. **b**, Fusion of PGTIs containing p75–GFP with the basal membrane was monitored by TIR-FM between 15 and 50 min after release from the Golgi temperature block. Fusion events were counted in 33 (control antibody) and 49 (Syntaxin 3 antibody) cells imaged in 1500-frame time-lapse recordings. Images were acquired at 5 frames s^{-1}. The graph shows the percentage of cells in which 1–11 fusion events were detected at the basal membrane. Only cells in which we detected at least one fusion event were counted in this analysis. Data were compiled from three independent experiments.

fluorescent cargo (Fig. 4a, d; also see Supplementary Information, Movie 3 and Fig. S1a). An increase in the width of PGTI fluorescence intensity is one of the criteria for quantitatively defining fusion by TIR-FM[20]. These profiles were only observed for PGTIs that contacted the plasma membrane. This indicates that linescan profiles showing an increase in the width of fluorescence intensity exemplify events unique to PGTI–plasma membrane interactions, such as membrane fusion. Thus, only events exhibiting this profile were counted as fusion events in the quantitative analysis shown below.

Using this analysis on cells expressing LDLR-A18–GFP (four cells from two independent experiments), we identified 43 PGTIs whose fluorescence intensity profile indicated that the carrier had fused with the plasma membrane. All of these events occurred at approximately equal frequencies within four confocal planes imaged between 6–12 μm from the basal membrane (Table 1). We observed an additional 67 PGTIs with linescan profiles representative of either simultaneous fusion and movement of the carrier in the *xy* and/or *z* axes or movement of the carrier in both *xy*- and *z*-axes without fusion (see Supplementary Information, Fig. S1b, S1b′). These types of events were observed from 2–12 μm above the basal membrane. In an independent assay, fusion with the lateral membrane could also be identified when the colour of GFP-labelled PGTIs (green) transiently turned yellow as they fused with a DiIC[16]-labelled (red) plasma membrane (see Supplementary Information, Fig. S2 and Movie 5). In contrast, in cells expressing p75–GFP (three cells from two independent experiments), we did not identify any PGTIs that could be considered to be fusing with the lateral membrane. The complete absence of membrane fusion for apical PGTIs could not be attributed to a reduced number of PGTIs coming into contact with the membrane, as cells expressing either p75–GFP or LDLR-A18–GFP contained a similar number of membrane regions exhibiting a transient change in total fluorescence intensity (see above). In addition, comparable numbers of PGTIs containing p75–GFP were observed moving through the apical cytoplasm (see Supplementary Information, Movie 2). Nor could it be attributed to a change in PGTI properties that rendered them undetectable, as measurements of apical carrier size, shape and cargo capacity were not significantly different in non-polarized and polarized cells (G.K. and E.R.B., unpublished observations).

In summary, the results of the experiments described above suggest that PGTIs carrying basolateral membrane proteins fuse selectively with the lateral plasma membrane. PGTIs containing an apical marker were not observed to fuse with the lateral membrane, suggesting that they fuse directly with the apical membrane.

Targeted fusion of apical, but not basolateral, PGTIs in polarized MDCK cells requires microtubules. The mechanism by which disruption of microtubules preferentially perturbs the asymmetric distribution of apical membrane proteins is not known. To investigate whether microtubules are involved in determining plasma membrane fusion sites of apical or basolateral PGTIs, we examined whether PGTIs fused with the basal membrane of polarized cells when microtubules were completely depolymerized. To depolymerize all microtubules, we incubated cells on ice in the presence of 20 μM nocodazole for 60 min before micro-injection. Cells were continuously incubated in 10 μM nocodazole for the duration of experiments to prevent re-assembly of microtubules. As previously described[39,40], nocodazole treatment resulted in fragmentation of the Golgi apparatus into numerous GalT–CFP-positive Golgi mini-stacks that were dispersed throughout the cell (Fig. 5a). This treatment affected neither expression nor Golgi accumulation of the GFP-tagged reporter proteins (Fig. 5a; colocalization of LDLR-A18–YFP with GalT–CFP). After incubation at 20 °C, Golgi mini-stacks containing either apical or basolateral GFP-tagged membrane proteins were visible in close proximity to the basal membrane by TIR-FM (Figs 5b, c). This is in

marked contrast to polarized cells with an intact microtubule array, in which the Golgi localizes to a supra-nuclear position and cannot be detected by TIR-FM (compare with Fig. 1). Additionally, in nocodazole-treated cells that were co-injected with p75–CFP and LDLR-A18–YFP, we found that apical and basolateral markers colocalized in Golgi mini-stacks during the 20 °C block, but emptied from the Golgi at different rates after release of block (data not shown). This indicates that the protein sorting activity of the Golgi/TGN is maintained in the absence of microtubules.

After release of the Golgi temperature block in nocodazole-treated cells, neither LDLR–GFP (Fig. 5b) nor NCAM–GFP (data not shown) could be detected fusing with the basal plasma membrane. In marked contrast, carriers containing p75–GFP fused with the basal membrane under these conditions (Fig. 5c; also see Supplementary Information, Movie 4, $n = 40$ fusions per 1000 frames). As both apical and basolateral carriers were detected by TIR-FM after nocodazole treatment, but only carriers containing p75–GFP fused with the basal membrane, our results show that exocytosis at the basal membrane is not caused by the proximity of redistributed Golgi elements with the basal cell surface. Rather, they show that sorting of apical and basolateral membrane proteins still occurs within scattered Golgi elements and that the basal membrane becomes fusion competent specifically for apical, but not basolateral, PGTIs after disruption of microtubules. The role of microtubules in targeted exocytosis of apical cargo could either be direct, by targeting delivery of apical PGTIs to the correct membrane domain, or indirect, by regulating the distribution of components of the targeting and fusion machinery for apical exocytosis.

Microtubule disruption results in a non-polarized distribution of Syntaxin 3. To elucidate the mechanism by which nocodazole selectively induces fusion of PGTIs containing p75–GFP with the basal membrane in polarized cells, we tested whether the localization of components of apical and basolateral tethering and fusion machineries were altered by disruption of microtubules. Nocodazole treatment resulted in a redistribution of Syntaxin 3 from the apical surface to both apical and basolateral membranes, but did not alter the distribution of Syntaxin 4 or Sec6 (compare Fig. 2 and Fig. 6, polarized cells). Nocodazole treatment does not disrupt the barrier function of tight junctions in MDCK cells[19], nor did it perturb the apicolateral distribution of zonula occludens 1 (ZO-1), a marker for the tight junction (data not shown). These results suggest that redistribution of Syntaxin 3 may be critical in facilitating exocytosis of apical cargo at the basal membrane after microtubule disruption.

To test whether Syntaxin 3 is permissive for fusion of apical PGTIs with the plasma membrane, we co-injected untreated or nocodazole-treated polarized cells with p75–GFP cDNA and either an antibody raised against the cytoplasmic domain of Syntaxin 3 or a control antibody. Delivery of p75–GFP to the apical membrane of cells with an intact microtubule array was assayed by measuring the ratio of cell-surface immunolabelled p75 (see Methods) to total p75–GFP in polarized cells at varying times after release of the Golgi block. In two independent experiments, micro-injection of Syntaxin 3 antibodies resulted in a 77 ± 3% reduction in the ratio of surface:total p75–GFP at the apical membrane 4 h after release from the Golgi, compared with cells micro-injected with control antibody (Fig. 7a). These data indicate that in MDCK cells, our anti-Syntaxin 3 antibody has function-blocking properties with respect to Syntaxin 3-mediated delivery of apical cargo to the plasma membrane. In nocodazole-treated cells, we evaluated the effect of Syntaxin 3 inhibition by comparing the number of fusion events observed by TIR-FM in single cells injected with control or Syntaxin 3 antibodies. In data combined from three independent experiments, we detected four or more fusion events in only 6% of the cells injected with anti-Syntaxin 3 antibodies, as compared with 49% of cells injected with control antibodies (Fig. 7b). These results show that Syntaxin 3 contributes directly to creating a plasma membrane environment permissive for fusion of apical PGTIs *in vivo*. Furthermore, they suggest that microtubules facilitate apical delivery of plasma membrane proteins by promoting a restricted apical distribution of Syntaxin 3.

Discussion

Advances in time-lapse fluorescence microscopy and the use of GFP-tagged chimaeras have facilitated the study of intracellular membrane trafficking along the biosynthetic pathway in non-polarized cells[3,8,9,20,41,42]. In this study, we used live-cell imaging techniques to study the trafficking and fusion of PGTIs with the cell surface in polarized MDCK cells. Our results provide fresh insights into how epithelial cells organize their exocytic machinery during the establishment of polarity.

Using TIR-FM, we show that PGTIs carrying apical or basolateral cargo can fuse with the basal membrane of non-polarized MDCK cells. These data are in agreement with results obtained in non-polarized PtK_2 epithelial cells[3]. Our results provide direct evidence that the uniform plasma membrane distribution of at least some apical and basolateral membrane proteins in non-polarized MDCK cells is caused by non-targeted delivery of PGTIs, rather than by targeted delivery and subsequent membrane diffusion in the absence of tight junctions. Additionally, we made the observation that exocytosis of both apical and basolateral membrane proteins at the basal plasma membrane is completely abrogated after MDCK cells polarize. As wide-field illumination revealed that apical and basolateral proteins accumulated in the correct plasma membrane domain, the loss of basal fusion indicated activation of a polarization-dependent mechanism for redirecting PGTIs to different regions of the cell surface. Indeed, sequential *z*-axis recordings of post-Golgi trafficking revealed a spatial segregation of apical and basolateral carriers emerging from the Golgi complex; apical PGTIs were localized primarily in the uppermost 4 μm of the cytoplasm, whereas basolateral PGTIs were broadly distributed throughout central regions of the cytoplasm. The restricted distribution of apical PGTIs may be attributed to an association with the sub-apical microtubule array. In contrast, the wider distribution of basolateral PGTIs could reflect their emergence from an apically localized Golgi complex and association with more broadly distributed cytoskeletal elements.

Using time-lapse confocal microscopy, we were able to quantitatively analyse whether basolaterally targeted PGTIs containing either LDLR–GFP or NCAM–GFP fused with the lateral membrane. Fluorescence intensity profiles characteristic of fusing PGTIs were only observed in central and apical domains of the lateral membrane. This is consistent with the observation that basolateral PGTIs were concentrated in central and apical regions of the cytoplasm. Although a variety of biochemical assays have demonstrated a direct pathway from the Golgi to the basolateral membrane[43–45], they inherently cannot discriminate whether exocytosis occurs throughout the basolateral membrane or at specific regions of this membrane. In contrast, our microscopy-based assays clearly demonstrate that basolateral carriers are targeted exclusively to the lateral domain of the basolateral membrane for exocytosis. To our knowledge, these experiments are the first direct demonstration of targeted exocytosis in polarized epithelial cells.

We did not observe fluorescence intensity profiles characteristic of fusing carriers at either the basal or lateral membrane in polarized cells expressing the apical marker, p75–GFP. The lack of detectable fusion events for apical PGTIs, despite their abundance in the cytoplasm and the accumulation of p75–GFP at the apical surface, suggests that they fuse directly with the apical membrane. This interpretation is consistent with domain-selective, surface labelling data showing that newly synthesized ^{35}S-methionine-labelled p75–GFP is delivered directly to the apical membrane in polarized MDCK cells[9]. Although PGTIs containing p75–GFP do not fuse with the lateral membrane, PGTIs carrying other apical

proteins may be capable of lateral membrane fusion in polarized cells. In the future, it will be interesting to address this using cells expressing proteins delivered to the apical membrane via the indirect, transcytotic route, as well as in cells expressing apical proteins dependent on inclusion into lipid rafts for their delivery to the apical surface.

Abrogation of exocytic events at the basal plasma membrane and redirection to the lateral membrane after polarization correlated with changes in the distribution of molecular components of the apical and basolateral fusion machineries. Basal fusion of PGTIs occurred in non-polarized cells when Syntaxins 3 and 4 were present at the basal membrane but was never observed in polarized cells where both syntaxins were absent from the basal membrane. These results suggest that Syntaxins 3 and 4 must be present in target membranes for fusion of apical and basolateral PGTIs to occur. Syntaxin 3-dependent delivery of apical proteins was confirmed by the measured inhibition in delivery of p75–GFP to the apical or basal membrane in untreated or nocodazole-treated cells, respectively, when cells were injected with an antibody against the cytoplasmic domain of Syntaxin 3. Syntaxin 4-dependent fusion of basolateral PGTIs was suggested by the restricted lateral localization of both Syntaxin 4 and fusion of basolateral PGTIs. These data are consistent with the concept that t-SNAREs are necessary for fusion of PGTIs, but do not rule out the possibility that additional factors, such as tethering proteins, are also involved in domain-specific targeting of some PGTIs[46–49]. One of these additional factors is the exocyst, which localizes along the lateral membrane in our cells and was recently demonstrated to have an important role in basolateral membrane trafficking in MDCK cells[31,32]. The imperfect codistribution of basolateral PGTIs fusing at the lateral membrane with Syntaxin 4 and Sec6 might be attributed to the fact that fusion events were monitored in living cells, whereas Syntaxin 4 and Sec6 were localized in fixed cells by immunocytochemistry.

Finally, we found that in polarized cells, apical PGTIs regained the ability to fuse with the basal membrane after depolymerization of microtubules. This mis-targeting of p75–GFP to the basal membrane correlated with mis-localization of Syntaxin 3 at the basal membrane in response to treatment with microtubule antagonists. It has previously been shown that antibodies against Syntaxin 3 inhibit delivery of influenza haemagglutinin (HA) to the apical surface in permeabilized MDCK cells[35]. Similarly, we found that micro-injected Syntaxin 3 antibodies inhibited delivery of p75–GFP to the apical surface in intact cells (Fig. 7a). Strikingly, nocodazole-induced fusion of apical PGTIs with the basal membrane was also partially inhibited by injected Syntaxin 3 antibodies, suggesting that mis-localization of Syntaxin 3 causes the basal membrane to become fusion-competent for apical PGTIs after disruption of microtubules. The incomplete inhibition of basal fusion by Syntaxin 3 antibodies could reflect either incomplete inhibition by the antibody or the participation of another factor(s) in mediating fusion of apical PGTIs with the membrane under these conditions. In contrast, microtubule depolymerization did not promote fusion of PGTIs containing either LDLR–GFP or NCAM–GFP with the basal membrane, nor did it result in redistribution of Syntaxin 4 or exocyst components to the basal membrane. The mechanism by which t-SNAREs are targeted to different membrane domains in polarized cells is unclear. Our finding that the localization of Syntaxin 3, but not Syntaxin 4, is sensitive to microtubule depolymerization demonstrates that t-SNARE distributions are differentially controlled by microtubules *in vivo*. These results provide mechanistic insight into previous findings showing that microtubules are preferentially involved in controlling the apical targeting of membrane proteins in epithelial cells[18,19,21–28]. □

Methods

Cell culture and micro-injection

MDCK cells were maintained in DMEM (Invitrogen, Carlsbad, CA) supplemented with 10% foetal bovine serum (FBS) in a 37 °C incubator humidified with 5% CO_2. For analysis of non-polarized cells, MDCK cultures were seeded at a density of ~13,000 cells cm^{-2} onto heat-sterilized 25 mm round coverslips and grown for 36 h before micro-injection. For polarized cell analyses, cells were seeded at a density of ~130,000 cells cm^{-2} and grown for 4–5 days to ensure the formation of a fully polarized monolayer before micro-injection. Cells were pressure micro-injected intranuclearly with cDNAs prepared in HKCl micro-injection buffer (10 mM Hepes, 140 mM potassium chloride at pH 7.4); 5 μg ml^{-1} for p75–GFP, 20 μg ml^{-1} for NCAM–GFP and 15 μg ml^{-1} for LDLR-A18–GFP, using back-loaded glass capillaries and a Narishige micromanipulator (Narishige, Greenvale, NY). Rabbit polyclonal antibodies raised against a GST fusion protein of the full-length carboxy-terminal cytoplasmic tail of rat Syntaxin3 have been described previously[50]. The anti-Syntaxin 3 antibody was purified from rabbit serum, as previously described[9]. Control and Syntaxin 3 antibodies were concentrated by vacuum dialysis in HKCl injection buffer and micro-injected at a final concentration of 11 mg ml^{-1}. Injected antibody could be detected in cells after fixation and staining with fluorescently conjugated anti-rabbit antibody (Jackson ImmunoResearch, West Grove, PA). After injection, cells were maintained at 37 °C in a humidified CO_2 environment for 60 min to allow for expression of injected cDNAs. Newly synthesized protein was accumulated in the TGN by incubating cells at 20 °C in bicarbonate-free DMEM supplemented with 5% FBS, 20 mM Hepes and 100 μg ml^{-1} cycloheximide (Sigma, St Louis, MO). Before release of the 20 °C block no significant amount of LDLR-A18–GFP, NCAM–GFP or p75–GFP could be detected at the cell surface, as determined by surface immunolabelling of unpermeabilized paraformaldehyde-fixed cells. Cells were transferred to recording medium (Hanks Balanced Salt Solution, without phenol-red, supplemented with 20 mM HEPES, 1% FBS, 4.5 g l^{-1} glucose, essential and non-essential amino acids and 100 μg ml^{-1} cycloheximide) and the transport and fusion of post-Golgi carriers was monitored by time-lapse fluorescence microscopy after shifting to the permissive temperature for transport out of the Golgi (32 °C).

Microtubule depolymerization

Before micro-injection, cells were incubated in bicarbonate-free DMEM supplemented with 5% FBS and 20 mM Hepes on ice for 30 min to depolymerize the cold-labile, nocodazole-resistant microtubule population. Nocodazole (Sigma) was added to a final concentration of 20 μM and the cells were incubated for another 30 min on ice. This treatment completely depolymerized all microtubules (data not shown). cDNAs were then micro-injected and cells were treated as described above, except that they were maintained in 10 μM nocodazole for the remainder of each experiment to prevent re-assembly of the microtubule cytoskeleton.

DiIC^{16} plasma membrane labelling

Cells were micro-injected as described. Fluorescently labelled DiIC^{16} (Molecular Probes, Eugene OR) was added (50 μM final concentration) to bicarbonate-free DMEM without serum, supplemented with 20 mM Hepes and 100 μg ml^{-1} cycloheximide. DiIC^{16}-containing medium was added to the cells during the final 30 min of the Golgi temperature block. Cells were then washed three times with recording medium before dual-wavelength, confocal time-lapse imaging.

Plasmid construction

The cDNA encoding full-length NCAM in pBKCMV was a gift from J. Bruses (Memorial Sloan Kettering Cancer Center, New York, NY). PCR was used to introduce a *KpnI* site at the NCAM 5′ end. The resulting PCR product was subcloned into pBKCMV-NCAM to create full-length NCAM without a stop codon. This construct was subcloned into the *SalI* and *KpnI* sites of pEGFP-N1 (Clontech, Palo Alto, CA) to generate NCAM-pEGFP-N1. The cDNA encoding LDLR-A18 (ref. 36) in pCB6 was provided by Karl Matter (University College of London, London, UK). PCR was used to introduce an *xmaI* site at the 5¢ end. The resulting PCR product was subcloned into pBluescript-LDLR-A18, creating a full length LDLR-A18 without a stop codon. This construct was subcloned into the *KpnI* and *xmaI* sites of pEGFP-N1, to generate LDLR-A18–GFP. The construction of p75–GFP cDNA has been described previously[9]. cDNAs for human Syntaxins 3 and 4 were cloned into a modified pcDNA4/TO vector (Invitrogen) to add two C-terminal Myc epitope tags in tandem and one hexa-histidine tag to the C termini. MDCK cells were stably transfected and individual clones were used for this study. The additional epitope tags did not interfere with the correct polarized targeting of the Syntaxins and allowed detection at the plasma membrane by surface immunolabelling.

Indirect immunofluorescence

For Syntaxin 3 and 4 surface staining, MDCK cells transfected with tetracycline-inducible, Myc-tagged Syntaxin 3 or 4 were washed three times in ice-cold phosphate-buffered saline containing calcium (1 mM) and magnesium (1 mM) (PBS-CM), placed on ice and incubated with an anti-Myc monoclonal antibody (9E10 ascites, Santa Cruz Biotechnology, Santa Cruz, CA) for 2 h. Cells were washed in PBS-CM and fixed in freshly prepared 3% paraformaldehyde for 20 min on ice. Cells were permeabilized in PBS-CM with 0.1% Triton X-100 for 10 min at room temperature. The tight junction marker, ZO-1, was immunolabelled by incubating cells for 30 min at room temperature with a rat monoclonal antibody (Chemicon, Temecula, CA). Cells were subsequently labelled with appropriate fluorescently conjugated secondary antibodies (Jackson ImmunoResearch). For Sec6 immunostaining, cells were fixed in −20 °C methanol for 3 min or in 3% paraformaldehyde on ice for 15 min before permeabilization in 0.1 M Tris-HCl at pH 7.5 containing 0.05% SDS for 10 min at room temperature. Samples were then stained with a mouse monoclonal antibody against rSec6 (StressGen, Victoria, BC).

Quantification of p75–GFP at the cell surface

Groups of polarized cells were injected with p75–GFP cDNA and anti-Syntaxin 3 or control antibody. Cells were incubated for 1 h at 37 °C to allow expression of p75–GFP and then p75–GFP was accumulated in the Golgi by incubation at 20 °C for 2.5 h. Cells were shifted to 37 °C and fixed 0, 30, 60, 120 and 240 min after release of the Golgi temperature block in 2% paraformaldehyde at room temperature for 2 min. p75–GFP at the cell surface was immunolabelled with a monoclonal antibody that recognizes an extracellular epitope of p75, as described previously[9]. Cells were subsequently labelled with Cy3-conjugated anti-mouse antibodies. Images were acquired using a Nikon TE-300 microscope and a back-illuminated, cooled, charge-coupled-device camera (CCD 512X512-EBFT, Princeton

Instruments). Images of p75–GFP and anti-p75-injected cells were acquired using identical acquisition settings and exposure times for all samples in a single experiment. The integrated fluorescence intensities in GFP and anti-p75 images was measured and the ratio of anti-p75:p75–GFP intensities was calculated for each group of injected cells. The integrated fluorescence of 40–60 injected cells was measured at each time point.

Total internal reflection fluorescence microscopy (TIR-FM).

The prism-less TIR-FM was set up on an Olympus microscope (IX-70, Olympus America Inc.) as previously described[20] using a high numerical aperture lens (Apochromat 60×, NA 1.45, Olympus), resulting in an evanescent field with a decay length between 70 and 120 nm. In all TIR-FM recordings, we acquired 500-frame time-lapse sequences at ~4 frames s^{-1} (222-ms exposures), except as noted in Table 2. Images were acquired without binning, using a 12-bit cooled CCD (ORCA I, C4742-95, Hamamatsu) with 6.7-μm pixels. The camera was controlled by in-house software written in Labview 5.1 using the IMAQ Vision package (National Instruments, Austin, TX). Analysis of carrier fusion was performed as described[20]. Briefly, carrier fusion is defined by a simultaneous increase in both the total PGTI fluorescence intensity and the area occupied by carrier fluorescence as the carrier flattens into the plasma membrane and the cargo diffuses laterally. These criteria make it possible to distinguish fusing carriers from those moving near the plasma membrane or those that lyse.

Time-lapse confocal microscopy

After micro-injection and a 20 °C Golgi block, cells were transferred to a thermal-controlled recording chamber mounted on a Zeiss Axiovert 100 microscope (Carl Zeiss, Oberkochen, Germany) equipped with an UltraView spinning disc confocal head (Perkin Elmer, Shelton, CT). Spinning disc confocal recordings were made at the Rockefeller University Bioimaging Resource Center. The confocal depth was 1 μm and GFP was illuminated using the 488-nm argon laser. Images were collected using a 63× objective and the ORCA-ER, cooled CCD with 6.7-μm pixels (Hamamatsu, Bridgewater, NJ) with 2 × 2 binning. All imaging hardware was controlled by a workstation running MetaMorph imaging software (Universal Imaging, West Chester, PA). Time-lapse sequences were acquired at ~3.5 frames s^{-1} (200-ms exposures). Sequential time-lapse recordings were made at 2-μm *z*-intervals, starting at the bottom of the cell. Recording duration at each *z*-interval was 1 min. Post-acquisition analysis and processing of confocal images was performed using MetaMorph.

Lateral membrane fusion analysis

Adjacent 5 × 5 pixel regions were drawn along the entire lateral membrane of injected cells at each focal plane. The total fluorescence intensities in each region were measured for all frames. Regions of interest displaying transient increases in intensity above the noise level were subsequently screened for fusion by measuring the average fluorescence intensity at individual points on short lines drawn along the plasma membrane (linescan analysis). Before linescan analysis, all the frames from the time-lapse were averaged and the resulting averaged image was subtracted from each frame of the time-lapse. Subtraction of the averaged image resulted in elimination of the fluorescence signal contributed by non-moving structures (that is, the plasma membrane) enabling us to analyse selectively the fluorescence contributed by moving PGTIs. Linescan widths varied slightly from region to region and are displayed in the *x*-axis of graphs shown in Fig. 4. All image analysis was performed using MetaMorph. Several types of linescan profiles were observed: first, a decrease in total intensity concomitant with an increase in the width of fluorescence intensity along the line being measured at the membrane is representative of PGTI fusion with the plasma membrane and subsequent diffusion of its fluorescent cargo (Fig. 4a, d); second, a decrease in total intensity without an increase in the width of fluorescence intensity along the membrane. This profile was considered to be representative of carriers moving out of the plane of focus (Fig. 4b, e); third, a translocation of fluorescence along adjacent membrane regions without a significant change in either the total intensity or the width of fluorescence intensity. This profile clearly exemplifies PGTIs moving in the focal plane along the membrane (Fig. 4c, f); fourth, a combination of the profiles described above. For example, some PGTIs moved along adjacent membrane regions concomitant with a decrease in their total fluorescence intensity (see Supplementary Information, Figs S1b, S1b'). The linescan profile generated from such PGTIs could represent either simultaneous fusion and movement of the carrier in the *xy* and/or *z* axes or movement of the carrier in both *xy*- and *z*-axes without fusion. As we could not unambiguously differentiate between these two possible activities, they were not counted as fusion events. Only those carriers whose total fluorescence intensity decreased concomitant with an increase in the width of fluorescence intensity over time were considered to be fusing with the lateral membrane.

RECEIVED 1 APRIL 2002; REVISED 21 AUGUST 2002; ACCEPTED 5 DECEMBER 2002; PUBLISHED 27 JANUARY 2003.

1. Rodriguez-Boulan, E. & Nelson, W. J. Morphogenesis of the polarized epithelial cell phenotype. *Science* **245**, 718–725 (1989).
2. Simons, K. & Wandinger-Ness, A. Polarized sorting in epithelia. *Cell* **62**, 207–210 (1990).
3. Keller, P., Toomre, D., Diaz, E., White, J. & Simons, K. Multicolour imaging of post-Golgi sorting and trafficking in live cells. *Nature Cell Biol.* **3**, 140–149 (2001).
4. Rodriguez-Boulan, E. & Gonzalez, A. Glycans in post-Golgi apical targeting: sorting signals or structural props? *Trends Cell Biol.* **9**, 291–294 (1999).
5. Chuang, J. Z. & Sung, C. H. The cytoplasmic tail of rhodopsin acts as a novel apical sorting signal in polarized MDCK cells. *J. Cell Biol.* **142**, 1245–1256 (1998).
6. Le Gall, A., Yeaman, C., Muesch, A. & Rodriguez-Boulan, E. Epithelial cell polarity: new perspectives. *Sem. Nephrol.* **15**, 272–284 (1995).
7. Ikonen, E. & Simons, K. Protein and lipid sorting from the *trans*-Golgi network to the plasma membrane in polarized cells. *Semin Cell Dev Biol* **9**, 503–509 (1998).
8. Toomre, D., Keller, P., White, J., Olivo, J. C. & Simons, K. Dual-color visualization of *trans*-Golgi network to plasma membrane traffic along microtubules in living cells. *J. Cell Sci.* **112**, 21–33 (1999).
9. Kreitzer, G., Marmorstein, A., Okamoto, P., Vallee, R. & Rodriguez-Boulan, E. Kinesin and dynamin are required for post-Golgi *trans*port of a plasma-membrane protein. *Nature Cell Biol.* **2**, 125–127 (2000).
10. Bonifacino, J. S. & Dell'Angelica, E. C. Molecular bases for the recognition of tyrosine-based sorting signals. *J. Cell Biol.* **145**, 923–926 (1999).
11. Ohno, H. *et al.* The medium subunits of adaptor complexes recognize distinct but overlapping sets of tyrosine-based sorting signals. *J. Biol. Chem.* **273**, 25915–25921 (1998).
12. Kirchhausen, T. Adaptors for clathrin-mediated traffic. *Annu. Rev. Cell Dev. Biol.* **15**, 705–732 (1999).
13. Kirchhausen, T., Bonifacino, J. S. & Riezman, H. Linking cargo to vesicle formation: receptor tail interactions with coat proteins. *Curr. Opin. Cell Biol.* **9**, 488–495 (1997).
14. Noda, Y. *et al.* KIFC3, a microtubule minus end-directed motor for the apical *trans*port of annexin XIIIb-associated Triton-insoluble membranes. *J. Cell Biol.* **155**, 77–88 (2001).
15. Nakagawa, T. *et al.* A novel motor, KIF13A, *trans*ports mannose-6-phosphate receptor to plasma membrane through direct interaction with AP-1 complex. *Cell* **103**, 569–581 (2000).
16. Setou, M., Nakagawa, T., Seog, D. H. & Hirokawa, N. Kinesin superfamily motor protein KIF17 and mLin-10 in NMDA receptor-containing vesicle *trans*port. *Science* **288**, 1796–1802 (2000).
17. Bacallao, R. *et al.* The subcellular organization of Madin-Darby Canine Kidney cells during the formation of a polarized epithelium. *J. Cell Biol.* **109**, 2817–2832 (1989).
18. Gilbert, T., Le Bivic, A., Quaroni, A. & Rodriguez-Boulan, E. Microtubular organization and its involvement in the biogenetic pathways of plasma membrane proteins in Caco-2 intestinal epithelial cells. *J.Cell Biol.* **113**, 275–288 (1991).
19. Grindstaff, K. K., Bacallao, R. L. & Nelson, W. J. Apiconuclear organization of microtubules does not specify protein delivery from the *trans*-Golgi network to different membrane domains in polarized epithelial cells. *Mol. Biol. Cell* **9**, 685–699 (1998).
20. Schmoranzer, J., Goulian, M., Axelrod, D. & Simon, S. M. Imaging constitutive exocytosis with total internal reflection fluorescence microscopy. *J. Cell Biol.* **149**, 23–32 (2000).
21. Achler, C., Filmer, D., Merte, C. & Drenckhahn, D. Role of microtubules in polarized delivery of apical membrane proteins to the brush border of the intestinal epithelium. *J.Cell Biol.* **109**, 179–189 (1989).
22. Breitfeld, P. P., Mckinnon, W. C. & Mostov, K. E. Effect of nocodazole on vesicular traffic to the apical and basolateral surfaces of polarized Madin-Darby canine kidney cells. *J. Cell. Biol.* **111**, 2365–2373 (1990).
23. Rindler, M. J., Ivanov, I. E. & Sabatini, D. D. Microtubule-acting drugs lead to the nonpolarized delivery of the influenza hemagglutinin to the cell surface of polarized Madin-Darby canine kidney cells. *J. Cell Biol.* **104**, 231–241 (1987).
24. Matter, K., Bucher, K. & Hauri, H. P. Microtubule perturbation retards both the direct and the indirect apical pathway but does not affect sorting of plasma membrane proteins in intestinal epithelial cells (Caco-2). *EMBO J.* **9**, 3163–3170 (1990).
25. Lafont, F., Burkhardt, J. & Simons, K. Involvement of microtubule motors in basolateral and apical transport in kidney cells. *Nature* **372**, 801–803 (1994).
26. Hugon, J. S., Bennett, G., Pothier, P. & Ngoma, Z. Loss of microtubules and alteration of glycoprotein migration in organ cultures of mouse intestine exposed to nocodazole or colchicine. *Cell Tissue Res.* **248**, 653–662 (1987).
27. Saunders, C. & Limbird, L. E. Disruption of microtubules reveals two independent apical targeting mechanisms for G-protein-coupled receptors in polarized renal epithelial cells. *J. Biol. Chem.* **272**, 19035–19045 (1997).
28. Eilers, U., Klumperman, J. & Hauri, H. P. Nocodazole, a microtubule-active drug, interferes with apical protein delivery in cultured intestinal epithelial cells (Caco-2). *J. Cell Biol.* **108**, 13–22 (1989).
29. De Almeida, J. B. & Stow, J. L. Disruption of microtubules alters polarity of basement membrane proteoglycan secretion in epithelial cells. *Am. J. Physiol.* **261**, C691–C700 (1991).
30. Boll, W., Partin, J. S., Katz, A. I., Caplan, M. J. & Jamieson, J. D. Distinct secretory pathways for basolateral targeting of membrane and secretory proteins in polarized epithelial cells. *Proc. Natl Acad. Sci. USA* **88**, 8592–8596 (1991).
31. Grindstaff, K. *et al.* Sec6/8 Complex is recruited to cell-cell contacts and specifies transport vesicle delivery to the basal–lateral membrane in epithelial cells. *Cell Press* **93**, 731–740 (1998).
32. Lipschutz, J. H. *et al.* Exocyst is involved in cystogenesis and tubulogenesis and acts by modulating synthesis and delivery of basolateral plasma membrane and secretory proteins. *Mol. Biol. Cell* **11**, 4259–4275 (2000).
33. Low, S. H. *et al.* Differential localization of Syntaxin isoforms in polarized Madin-Darby canine kidney cells. *Mol. Biol. Cell* **7**, 2007–2018 (1996).
34. Low, S. H. *et al.* The SNARE machinery is involved in apical plasma membrane trafficking in MDCK Cells. *J. Cell Biol.* **141**, 1503–1513 (1998).
35. Lafont, F. *et al.* Raft association of SNAP receptors acting in apical trafficking in Madin-Darby canine kidney cells. *Proc. Natl Acad. Sci. USA* **96**, 3734–3738 (1999).
36. Matter, K., Hunziker, W. & Mellman, I. Basolateral sorting of LDL receptor in MDCK cells: The cytoplasmic domain contains two tyrosine-dependent targeting determinants. *Cell* **71**, 741–753 (1992).
37. Le Bivic, A. *et al.* An internal deletion in the cytoplasmic tail reverses the apical localization of human NGF receptor in transfected MDCK cells. *J. Cell Biol.* **115**, 607–618 (1991).
38. Le Gall, A. H., Powell, S. K., Yeaman, C. A. & Rodriguez-Boulan, E. The neural cell adhesion molecule expresses a tyrosine-independent basolateral sorting signal. *J. Biol. Chem.* **272**, 4559–4567 (1997).
39. Cole, N. B., Sciaky, N., Marotta, A., Song, J. & Lippincott-Schwartz, J. Golgi dispersal during microtubule disruption: regeneration of Golgi stacks at peripheral endoplasmic reticulum exit sites. *Mol. Biol. Cell* **7**, 631–50 (1996).
40. Storrie, B. *et al.* Recycling of Golgi-resident glycosyltransferases through the ER reveals a novel pathway and provides an explanation for nocodazole-induced Golgi scattering. *J. Cell Biol.* **143**, 1505–1521 (1998).
41. Wacker, I. *et al.* Microtubule-dependent transport of secretory vesicles visualized in real time with a GFP-tagged secretory protein. *J. Cell Sci.* **110**, 1453–1463 (1997).
42. Hirschberg, K. *et al.* Kinetic analysis of secretory protein traffic and characterization of Golgi to plasma membrane transport intermediates in living cells. *J. Cell Biol.* **143**, 1485–1503 (1998).
43. Rindler, M. J., Ivanov, I. E., Plesken, H., Rodriguez-Boulan, E. & Sabatini, D. D. Viral glycoproteins destined for apical or basolateral plasma membrane domains traverse the same Golgi apparatus during their intracellular transport in doubly infected Madin-Darby canine kidney cells. *J. Cell Biol.* **98**, 1304–1319 (1984).

44. Le Bivic, A., Sambuy, Y., Mostov, K. & Rodriguez-Boulan, E. Vectorial targeting of an endogenous apical membrane sialoglycoprotein and uvomorulin in MDCK cells. *J. Cell Biol.* **110**, 1533–1539 (1990).
45. Pfeiffer, S., Fuller, S. D. & Simons, K. Intracellular sorting and basolateral appearance of the G protein of vesicular stomatitis virus in Madin-Darby canine kidney cells. *J. Cell Biol.* **101**, 470–476 (1985).
46. Pfeffer, S. R. Transport-vesicle targeting: tethers before SNAREs. *Nature Cell Biol.* **1**, E17–E22 (1999).
47. Waters, M. G. & Pfeffer, S. R. Membrane tethering in intracellular transport. *Curr. Opin. Cell Biol.* **11**, 453–459 (1999).
48. Lowe, M. Membrane transport: tethers and TRAPPs. *Curr. Biol.* **10**, R407–R409 (2000).
49. Hazuka, C. D. *et al.* The Sec6/8 complex is located at neurite outgrowth and axonal synapse-assembly domains. *J. Neurosci.* **19**, 1324–1334 (1999).
50. Low, S. H. *et al.* Intracellular redirection of plasma membrane trafficking after loss of epithelial cell polarity. *Mol. Biol. Cell* **11**, 3045–3060 (2000).

ACKNOWLEDGEMENTS
This work was supported in part by a grant from the National Institutes of Health (GM34107) and by a Jules and Doris Stein professorship of the Research to Prevent Blindness Foundation (to E.R.-B.) and by an NIH National Research Service Award (EY06886, to G.K.). J.S. and S.M.S. acknowledge support from the National Science Foundation (BES0110070 and BES0119468, to S.M.S.). T.W. acknowledges support from the NIH (DK62338), the Department of Defense Prostate Cancer Research Program and the American Heart Association.
Supplementary Information accompanies the paper on www.nature.com/naturecellbiology.
Correspondence and requests for material should be addressed to E.R.B. or G.K.

COMPETING FINANCIAL INTERESTS
The authors declare that they have no competing financial interests.

Available online at www.sciencedirect.com
SCIENCE DIRECT®
Methods 30 (2003) 191–197
METHODS
www.elsevier.com/locate/ymeth

SNAREs and epithelial cells

Thomas Weimbs,[a,b,*] Seng Hui Low,[a] Xin Li,[a] and Geri Kreitzer[c]

[a] *Department of Cell Biology, Lerner Research Institute, NC10, The Cleveland Clinic, 9500 Euclid Avenue, Cleveland, OH 44195, USA*
[b] *Glickman Urological Institute, The Cleveland Clinic, 9500 Euclid Avenue, Cleveland, OH 44195, USA*
[c] *Margaret M. Dyson Vision Research Institute, Weill Medical College of Cornell University, New York, NY, USA*

Accepted 5 February 2003

Abstract

SNARE proteins control the membrane fusion events of membrane trafficking pathways. Work in epithelial cells has shown that polarized trafficking to the apical and basolateral plasma membrane domains requires different sets of SNAREs, suggesting a mechanism that contributes to the overall specificity of polarized trafficking and, perhaps, the formation and maintenance of polarity itself. This article describes methods that have been designed and adapted specifically for the investigation of SNAREs in epithelial cells. The knowledge of the subcellular localization of a SNARE of interest is essential to understand its function. Unfortunately, the endogenous expression levels of SNAREs are often low which makes detection challenging. We provide guidelines for determination of the localization of SNAREs by immunofluorescence microscopy including methods for signal amplification, antigen retrieval, and suppression of antibody cross-reactivity. To define which trafficking pathway a SNARE of interest is involved in, one needs to specifically inhibit its function. We provide guidelines for SNARE inhibition by overexpression of the SNARE of interest. An alternative is to introduce inhibitors of SNARE function, such as antibodies or clostridial toxins, into cells. Two methods are presented to make this possible. The first allows the monitoring of effects on trafficking pathways by biochemical assays, and is based on plasma membrane permeabilization using the bacterial toxin streptolysin-O. The second is suitable for single-cell observations and is based on microinjection.

Keywords: SNARE; Syntaxin; SNAP; streptolysin-O; Microinjection; Epithelial polarity; Immunofluorescence microscopy

1. Introduction

The SNARE machinery controls membrane fusion events in all membrane trafficking pathways investigated to date [1,2]. SNAREs are relatively small, membrane-anchored proteins that belong to distinct protein families which are related to each other by the presence of one or two conserved coiled-coil domains [3,4]. These so-called "SNARE motifs" mediate the binding interactions of SNARE proteins to each other. The resulting SNARE complexes generally consist of four coiled-coil domains contributed by SNAREs residing in the target membrane (t-SNAREs) and vesicle membrane (v-SNAREs). Recent experiments have shown that only matching combinations of v- and t-SNAREs lead to successful fusion [5,6], indicating that SNAREs not only mechanistically accomplish membrane fusion but also contribute to the specificity of this process. In support of this, different SNARE proteins are generally localized to specific organelles and are involved only in specific trafficking pathways.

Investigation of SNARE function in epithelial cells has indicated that the polarized distribution of t-SNAREs, most notably the apical-specific syntaxin 3 and the basolateral-specific syntaxin 4, is highly conserved among epithelial cell types and is likely to be crucial for the establishment and maintenance of epithelial polarity [7–11]. This article describes and discusses techniques that have proven highly valuable for the investigation of expression, subcellular localization, and function of SNAREs in epithelial cells. While these methods have been specifically adapted and optimized for this purpose, many of them are applicable to the study of other proteins and cell systems as well.

* Corresponding author. Fax: 1-216-444-9404.
E-mail address: weimbst@lerner.ccf.org (T. Weimbs).

1046-2023/03/$ - see front matter © 2003 Elsevier Science (USA). All rights reserved.
doi:10.1016/S1046-2023(03)00025-2

2. Immunolocalization of SNAREs

The best initial approach to aid in the identification of the trafficking pathway in which a t-SNARE is involved is to determine its steady-state localization. In general, t-SNAREs appear to mediate fusion events to the organelle/domain in which they reside most of the time. For example, at steady state the majority of syntaxin 3 is found at the apical plasma membrane of epithelial cells [8,9,12]. Consequently, it functions in trafficking pathways that are directed to this domain [10,13]. Although it has not formally been excluded it appears very unlikely that syntaxin 3 (or any other t-SNARE) also functions at another location that is "invisible" at steady state. The case of v-SNAREs is more complicated because they are generally thought to cycle between the donor compartment from which the respective transport vesicles are formed and the target membrane.

The steady-state localization of a SNARE can be determined either by detecting the endogenously expressed protein or after expression of an exogenous protein. The endogenous expression levels of most SNAREs are relatively low (with the exception of neuronal SNAREs in neurons) which can make detection a challenge. Below are descriptions of our methods for enhancing signals in immunofluorescence experiments using cultured cells or tissue sections.

2.1. Immunofluorescence staining with signal amplification by anti-fluorescein tertiary antibody

This method uses a primary rabbit antibody against a SNARE protein, followed by a fluorescein-labeled donkey anti-rabbit IgG secondary antibody. To enhance the signal, a rabbit antibody is then used that recognizes fluorescein and is coupled to the fluorophore Alexa-488 (Molecular Probes, Eugene, OR, USA, Catalog No. A-11090). Since the spectral properties of Alexa-488 are nearly identical to those of fluorescein, the result is an amplification of the fluorescein signal. In our experience, this increases the signal approximately fivefold.

1. Culture MDCK cells on 12-mm Transwell filters in MEM containing 10% FBS. Allow the cells to polarize for at least 3 days, changing the medium every other day.
2. Rinse cells briefly three times with PBS containing 1 mM $CaCl_2$ and 1 mM $MgCl_2$ (PBS^+).
3. Fix with 4% paraformaldehyde in PBS^+ for 20 min at room temperature. During fixation, place the cells on an orbital shaker at very low speed (alternatively, cells can be fixed in cold methanol at −20 °C for 10 min).
4. Quench any remaining fixative with 75 mM NH_4Cl and 20 mM glycine (both from a 1 M stock) in PBS at room temperature for 10 min with shaking (in the case of the methanol fixation, omit the quenching step).
5. After two brief rinses in PBS, block the cells and permeabilize in Block Solution (PBS containing 3% BSA and 0.2% Triton X-100) at 37 °C for 30 min.
6. Centrufuge primary antibody diluted in Block Solution at 12,000*g* for 15 min to pellet any aggregates.
7. Carefully cut out the membrane of the Transwell mount and place it on Parafilm on a 30-μl drop of the antibody. Place another 30 μl of the diluted antibody on top of the filter. Incubate in a humid chamber at 37 °C for 2 h.
8. Transfer the membrane back to a 12-well dish and wash 4 × 5 min in Wash Solution (PBS with 0.05% Triton X-100 and 0.7% fish skin gelatin (Catalog No. G-7765, Sigma, St. Louis, MO, USA).
9. Dilute the secondary antibody conjugated with fluorescein in Wash Solution and centrifuge again for 15 min to pellet out any aggregates; apply it to the membrane as described for the primary antibody. Incubate for 1 h at 37 °C in a humid chamber.
10. Wash the membrane 4 × 5 min in Wash Solution. Dilute the Alexa-488-conjugated anti-fluorescein antibody in Wash Solution and apply it to the membrane after centrifugation as described previously. Allow the antibody to incubate for 1 h at 37 °C.
11. Remove excess antibody by washing 4 × 5 min in Wash Solution and 2 × 3 min in PBS containing 0.1% Triton X-100, followed by two rinses in PBS.
12. Mount the membrane cell side up. It is ready for viewing under the microscope.

2.2. Antigen retrieval by pressure cooking

In our experience, immunofluorescence staining of SNAREs in sections of fixed tissues often results in weak signals. This may be due to the fact that SNAREs appear to spend most of the time in complexes with other SNAREs or regulatory proteins. Fixation with protein-crosslinking fixatives, like formaldehyde, may then mask many epitopes. This could theoretically lead to localization artifacts because a subpopulation of a SNARE may be "invisible" by immunostaining. Several methods are used to unmask epitopes in tissue sections, including digestion with proteolytic enzymes; denaturation with urea, SDS, or guanidine hydrochloride; and heat treatment. In our hands, heat treatment using a pressure cooker leads to the most reproducible signal enhancement while preserving tissue morphology. Paraffin sections of tissues from animals perfusion-fixed with 4% paraformaldehyde in PBS^+ have worked best for us.

1. Deparaffinize and rehydrate sections on slides as usual (leave slides wet until ready for pressure cooking).
2. Make 2 liters of 10 mM Na-citrate buffer, pH 6.0, by diluting from a 1 M stock.
3. Put the citrate buffer in a large stainless-steel household pressure cooker (must not be aluminum as it reacts with the citrate). With the lid only loosely on the cooker, heat until boiling.
4. Place slides in a glass or steel slide holder and put into boiling citrate buffer.
5. Close lid tightly. Place the weight on the pressure cooker's valve.
6. Continue to heat until weight starts to wobble.
7. Heat for one more minute.
8. Remove cooker from heater; place under running cold water tap.
9. Once pressure is down, open lid and flood cooker with running cold tap water.
10. Remove slides and proceed with immunostaining as usual.

2.3. Suppression of antibody cross-reactivity

Immunolocalization experiments with endogenous proteins suffer from the inherent problem that usually no negative control is available (in contrast to experiments with transfected cells in which the nontransfected cells can serve as the negative control). Omitting the primary antibody controls only for autofluorescence, background by the secondary antibody, etc., but does not establish the specificity of the primary antibody. Competition with the antigen is better but does still not exclude cross-reactivity of the primary antibody. Polyclonal antibodies have to be affinity-purified against the antigen. Unpurified antisera almost always lead to artifactual staining results.

Many SNAREs are closely related to each other, especially in the "SNARE" motifs [3], which can lead to problems of antibody cross-reactivity. For example, we found that polyclonal antibodies raised against GST fusion proteins of any of the mammalian plasma membrane t-SNAREs syntaxins 2, 3, and 4 cross-react slightly with the other two syntaxins even after affinity purification. A simple method to overcome this problem is competitive inhibition using lysates of bacteria that express the related syntaxin–GST fusion proteins (e.g., immunostaining for syntaxin 2 would be carried out in the presence of syntaxin 3 and 4 lysates). Because the nonspecific antibodies may be against both native and denatured antigen, we add a mixture of denatured and nondenatured lysates to the antibody solution before staining.

1. Grow *Escherichia coli* expressing GST–syntaxins under the appropriate conditions. Prepare a total cell lysate using a standard lysozyme protocol. Bacteria from a 1-liter culture will lead to approximately 25 ml of lysate.
2. Add 250 µl SDS lysis buffer (0.5% SDS, 100 mM NaCl, 50 mM triethanolamine-Cl, pH 8.1, 5 mM EDTA) to 250 µl of bacterial lysate.
3. Boil the above solution for 10 min.
4. Add 250 µl Triton dilution buffer (2.5% Triton X-100, 50 mM triethanolamine-Cl, 100 mM NaCl, 5 mM EDTA).
5. Mix the above solution, add 250 µl of nondenatured bacterial lysate, and store at −80 °C in aliquots.
6. Add the above mixture at 4% to the primary anti-syntaxin antibody dilution during immunofluorescence staining.

3. Inhibition of SNARE function

A major strategy for defining the function of SNAREs is to specifically inhibit the function of an individual SNARE protein and measure the effects on the kinetics or fidelity of membrane trafficking pathways, the targeting of cargo proteins, or parameters of epithelial cell polarity. The difficulty lies in the fact that no ideal and simple method is available to inhibit epithelial SNAREs efficiently and specifically. Nature has provided us with the clostridial neurotoxins—tetanus and botulinum toxins—which are highly specific metalloproteases that cleave and inactivate several SNARE proteins [14]. However, most of these toxins cleave only neuronal SNAREs such as syntaxin 1, SNAP-25, and synaptobrevin, which are not normally expressed in epithelial cells. To make matters worse, clostridial neurotoxins can attach to and enter neurons but not non-neuronal cells. It is therefore necessary to introduce these toxins by other means. The same is the case for other inhibitory reagents such as antibodies and recombinant fragments of SNAREs. Two methods, use of permeabilized cells and microinjection, for introducing these membrane impermeable inhibitors into epithelial cells are described below. An alternative strategy is to express dominant-negative inhibitors by gene transfer.

3.1. Dominant-negative inhibition by overexpression of SNAREs

It has been observed in several systems that the overexpression of a wild-type syntaxin causes inhibition of the trafficking pathway in which the syntaxin is normally involved. Examples are syntaxin 3 in MDCK cells [10], syntaxin 5 in BHK-21 cells [15], and syntaxin 4 in mast cells [16]. It is not clear why the observed inhibition occurs but a plausible hypothesis is that the overexpression of one SNARE results in a stoichiometric imbalance with the other SNAREs involved in the

same pathway. This may lead to the formation of nonproductive, incomplete SNARE complexes and may cause one of the other required SNAREs (or a regulatory factor) to become limiting. In any case, the effect appears to be quite specific as other trafficking pathways generally remain unaffected. However, successful inhibition requires relatively high levels of overexpression. For example, overexpression of syntaxin 3 (~10× over endogenous levels) by stable transfection in MDCK cells resulted in partial inhibition of biosynthetic trafficking to the apical membrane, as well as apical recycling, however, similar overexpression of syntaxin 4 had no measurable effect on any pathway [10].

For this reason, an expression system should be chosen that results in high-level expression but can ideally also be regulated. Dasher and Balch used a vaccinia virus system that allows constitutive high-level expression [15]. However, it is useful only for relatively short-term expression and may therefore be unsuitable to investigate long-term parameters such as development of epithelial cell polarity. The same is the case with the usual transient transfection approaches. A promising alternative is expression by stable transfection using a regulatable system such as those using the tetracycline repressor or transactivator. Also useful are adenoviral vectors that express the gene of interest under tetracycline control. The ability to regulate expression of the SNARE may be essential because inhibition of any trafficking pathway may be potentially toxic.

In all cases it is important to verify that the overexpressed SNARE is still correctly targeted. Mistargeting of the SNARE of interest may compromise the specificity of the desired inhibition. Since too strong overexpression of any protein may result in its mislocalization, it is again desirable to be able to regulate the expression level.

Dominant-negative inhibition can also be achieved by expression of truncated SNAREs. There have been no systematic studies aimed at identifying domains of SNAREs that may be most potent and/or specific inhibitors. But is it generally believed that a non-membrane-anchored truncation mutant will form complexes with its cognate SNAREs that are nonproductive due to the lack of proper membrane attachment. A potential caveat is that non-membrane-anchored SNAREs generally localize throughout the cytoplasm. Since SNARE–SNARE interactions, at least in vitro, are relatively promiscuous [17], the potential exists that a non-membrane-anchored SNARE may be a less specific inhibitor than the same full-length SNARE when overexpressed.

Successful examples are the expression of the cytoplasmic domain of syntaxin 4 in adipocytes (inhibits GLUT4 translocation [18]) and the expression of the cytoplasmic domain of syntaxin 5 in BHK-21 cells (inhibits ER-to-Golgi transport [15]). In both cases, vaccinia virus expression systems were used for relatively short-term experiments (~3–6 h postinfection). We have found that expression of non-membrane-anchored mutants of syntaxin 2 and endobrevin/VAMP-8 using a replication-deficient, tetracycline-regulatable adenovirus system very effectively inhibited the function of the respective SNAREs in MDCK cells [27]. In this case, the cells could be monitored for periods up to 24 h postinfection. As an important control, the observed inhibitory effects could be eliminated by tetracycline-suppression.

3.2. Introduction of SNARE inhibitors by cell permeabilization using streptolysin-O

Streptolysin-O (SLO) is a bacterial protein toxin that can bind to and integrate into plasma membranes of mammalian cells due to its affinity for cholesterol [19]. Once integrated, SLO oligomerizes and forms large pores of up to 35 nm in diameter. These pores are too small to allow membrane-bound organelles to escape; however, macromolecules can be introduced into these permeabilized cells. To subsequently study membrane trafficking events it is necessary to resupply cytoplasmic proteins and ATP (which are lost after permeabilization). Under appropriate conditions, many cell functions including polarized membrane traffic can be reconstituted. If an inhibitory reagent, such as an antibody, recombinant protein, or peptide, is included, the involvement of the protein of interest can be studied if an appropriate assay is available to monitor the membrane traffic pathway of interest. Such assays are usually pulse–chase experiments. The secretion of a soluble reporter protein into the culture medium can then be monitored. Alternatively, the arrival at the plasma membrane of a reporter membrane protein can be monitored by surface immunoprecipitation or surface biotinylation. Using MDCK cells, several laboratories have successfully employed experimental protocols based on work by Gravotta et al. [20] and Pimplikar et al. [21]. Membrane traffic pathways such as biosynthetic apical and basolateral trafficking, transcytosis, recycling, and endocytosis have been reconstituted [10,13,22–25].

Below is our protocol for the permeabilization of polarized MDCK cells cultured on Transwell filters combined with an assay of the surface delivery of the polymeric immunoglobulin receptor by metabolic labeling and surface immunoprecipitation. This protocol can be modified for other trafficking pathways. This protocol has been used to introduce intact IgG antibodies and recombinant botulinum toxin light chains [10].

The following points should be noted: (1) Permeabilizing the basolateral plasma membrane generally leads to more reproducible results than permeabilizing the

apical membrane. We found that apical SLO permeabilization leads to membrane shedding into the apical medium. (2) In our experience, the source of the SLO is critical. All commercially available SLO preparations that were tested were highly problematic. In contrast, recombinant SLO purchased from the Institute of Medical Microbiology, Mainz University (Dr. S. Bhakdi, sbhakdi@mail.uni-mainz.de), led to efficient permeabilization and highly reproducible results. (3) A reducing environment must be provided for reconstitution of cell functions after permeabilization. This is commonly achieved by inclusion of DTT in all buffers. However, since DTT is membrane permeable it can potentially reduce disulfide bonds present in secretory proteins and luminal domains of membrane proteins, thereby disrupting their secretion or function. A better alternative is reduced gluthathione which we use at 5 mM. Glutatione is also less likely to reduce antibodies that are to be introduced into cells. (4) The amount of SLO required for efficient permeabilization has to be determined empirically. This can be done by performing a mock experiment according to the protocol described below using varying concentrations of SLO. Release of the cytoplasmic protein lactate dehydrogenase (LDH) can then be measured using an enzymatic assay kit (Sigma Diagnostics No. 500). Release of 70–80% of the LDH into the medium indicates efficient permeabilization. (5) The source of cytosol to be used for reconstitution can be critical. We have had the best results with cytosol prepared from HeLa cells grown in suspension culture. Rat liver and rat brain cytosols were somewhat less efficient. However, each membrane trafficking step may have different requirements which should be determined experimentally.

3.2.1. Materials

0.5 M EGTA stock: Suspend 19 g EGTA in ~60 ml water, adjust pH with KOH to 7.4 (during which the EGTA will dissolve), make up volume to 100 ml, filter through disposable cell culture sterile filtration unit, and store at 4 °C.

0.5 M glutathione stock: Dissolve 3.073 g reduced glutathione in ~17 ml water, adjust pH to 7.4, make up volume to 20 ml, filter through 0.45-μm syringe filter, and store 1-ml aliquots at −80 °C.

0.1 M K–Ca–EGTA buffer: Dissolve 1 g $CaCO_3$ and 3.8 g EGTA in ~70 ml water until everything is dissolved (may take up to 1 h), adjust pH to 7.4 with KOH, make up volume to 100 ml, filter through disposable cell culture sterile filtration unit, and store at 4 °C.

KOAc-minus buffer: Combine 115 mM potassium acetate, 20 mM Hepes, and 2.5 mM magnesium acetate, adjust pH to 7.4 with KOH, filter through disposable cell culture sterile filtration unit, and store at 4 °C.

KOAc-plus buffer: Combine 115 mM potassium acetate, 20 mM Hepes, 0.5 mM magnesium acetate, and 0.9 mM $CaCl_2$, adjust pH to 7.4 with KOH, filter through disposable cell culture sterile filtration unit, and store at 4 °C.

KTM buffer: To 50 ml KOAc-minus buffer add 0.5 ml 5 mM glutathione stock (5 mM final), 0.2 ml EGTA stock (2 mM final), 0.1 ml K–Ca–EGTA buffer; use final buffer only fresh.

Starving medium for metabolic labeling with [^{35}S]cysteine or [^{35}S]methionine: Dissolve powdered DME medium (without cysteine and methionine, Sigma No. D-0422) and add 1/100th vol of 100× Pen/Strep (penicillin/streptomycin); 1/50th vol of 1 M Na-Hepes, pH 7.3; 0.35 g/liter $NaHCO_3$; and 0.584 g/liter L-glutamine. For cysteine-deficient medium add 30 mg/liter methionine or for methionine-deficient medium add 48 mg/liter cystine. Filter through disposable cell culture sterile filtration unit, and store at 4 °C, keep sterile.

MEM etc: Dissolve powdered MEM medium (Sigma M-4642) in water and add 1/50th vol of 1 M Hepes–NaOH, pH 7.3; 1/100th vol of 100× Pen/Strep; 6 g/liter bovine serum albumin; and 0.35 g/liter $NaHCO_3$. Adjust pH to 7.35–7.4 with HCl or NaOH, and store frozen at −20 °C.

ATP-regenerating system: Prepare these three stock solutions: (a) 800 mM creatine phosphate in water; (b) 100 mM ATP in 10 mM Hepes pH 7; (c) 5 mg/ml creatine kinase (Roche No. 127566) in water. Store all three solutions in single-use aliquots (e.g., 50 μl) at −80 °C.

3.2.2. Method

All washes are done in 12-well culture plates.

Cells: Seed MDCK type II cells onto 12-mm Transwell filters (0.4 μm) and culture for 3–4 days.

Metabolic labeling: Wash cells twice with prewarmed Starving Medium and starve for 15 min in a humid chamber placed in a 37 °C water bath; metabolically label for 10 min by placing individual Transwell filters onto 25-μl drops of Starving Medium including 40–50 μCi [^{35}S]cysteine or [^{35}S]methionine (specific activity 1000 Ci/mmol) on Parafilm inside a humid chamber at 37 °C.

TGN accumulation of newly synthesized membrane proteins: Wash twice with MEM-etc precooled to 17 °C; chase/accumulate for 2 h at 17 °C with MEM-etc in a humid chamber placed in a 17 °C water bath.

SLO binding: (Everything is done on the surface of a metal plate placed on ice.) Wash both sides of the Transwell filter twice with KOAc-plus buffer and once with KTM buffer; place filter onto a 20-μl drop of SLO (100 μg/ml stock) diluted with KOAc-minus buffer + 5 mM glutathione; incubate 10 min on ice; wash three times with KTM buffer.

Permeabilization: Replace with 0.5 ml fresh KTM buffer precooled to 17 °C; at this point the desired inhibitor can already be included (e.g., antibody or clostridial neurotoxins); incubate 45 min at 17 °C

(during this time cell permeabilization will occur and the cytosol will be washed out of the cells).

Reconstitution of transport: Add to the basolateral side of filter the following (prewarmed to 37 °C): 200 µl HeLa cytosol, 15 µl ATP, 15 µl creatine kinase, 15 µl creatine phosphate, and the desired inhibitor (e.g., antibody or clostridial neurotoxins). Make volume up to 500 µl with KTM buffer. Add to apical side of filter 500 µl of prewarmed KTM buffer; incubate at 37 °C in a humid chamber for desired period. This is followed by the appropriate method for detection of the protein of interest that has reached the apical or basolateral surface such as surface immunoprecipitation or biotinylation. For an example, see Low et al. [10].

3.3. Introduction of SNARE antibodies by microinjection

The SLO permeabilization method described above is useful for biochemical assays of membrane traffic pathways that require that the SNARE inhibitor is introduced into the majority of the cells in a population. If effects on trafficking pathways are to be analyzed microscopically on an individual cell basis, microinjection may be preferable. Several points should be considered. (1) It is helpful to know how much of the targeted protein is present in the cells. This information will guide the initial estimation of the antibody concentration required to inhibit a protein of interest. Otherwise, one can prepare a concentrated antibody stock and titrate down to the lowest concentration needed to detect effects. (2) Cells generally tolerate injection of no more than 10% of the total cell volume. Five to ten percent is generally used. (3) Antibody stocks for microinjection must be prepared in physiological buffers that do not, alone, affect cellular processes. We routinely prepare antibodies for injection in a Hepes–KCl buffer, which also appears to prevent aggregation of antibody during long-term storage. Do not use Tris-based buffers! Tris has been shown to inhibit endocytosis, and microinjection of even the smallest amount usually results in rapid cell death. (4) Cells must be cultured on glass coverslips rather than filters since filters are not transparent to transmitted light and thus cells cannot be visualized during injection. MDCK cells grown on glass form distinct apical (with microvilli) and basolateral membranes, form tight and adherent junctions, and support polarized transport of apical and basolateral markers to the plasma membrane. Thus, like filter-grown cells, MDCK cells cultured on glass can fully polarize and are suitable for studies of polarized trafficking pathways.

3.3.1. Methods

3.3.1.1. Preparing antibodies for microinjection.

1. Both, IgG fractions prepared using standard protein A purification and affinity-purified antibodies are suitable for microinjection. Antibodies should be dialyzed against Microinjection Buffer (10 mM Hepes, 140 mM KCl, pH 7.4). Determine the antibody concentration by measuring the absorbance at 280 nm in a spectrophotometer. An A_{280} of 1.4 = 1 mg/ml IgG.
2. Concentrate the purified antibody. We have found that 8–12 mg/ml injection stock of syntaxin 3 IgG is effective in inhibiting the appearance of apical membrane proteins at the apical surface of MDCK and FRT epithelial cells. We routinely use vacuum dialysis but other methods such as ultrafiltration work as well. After concentration, determine the antibody concentration by diluting a small aliquot and measuring the absorbance at 280 nm using a microcuvette.
3. Store the antibody in single-use, 5- to 10-µl aliquots at −20 °C (−80 °C for long-term storage). Repeated freezing and thawing of purified antibodies often results in protein aggregation and loss of activity.
4. Just prior to microinjection, thaw antibody stock on ice and spin at 14,000 rpm in a microfuge for 5–10 min at 4 °C to pellet any aggregated protein. Transfer antibody to a new tube and keep on ice.

3.3.1.2. Preparing the cells. Cells are cultured on glass coverslips for microinjection experiments. We routinely place 7–20 coverslips (depending on the size of the glass) into a single 10-cm culture dish before adding the cells. MDCK type II cells are plated at high density, resulting in ~80% confluence after attachment. Cells are subsequently cultured for 3–5 days until a fully polarized monolayer has formed. Medium is changed on the first day after plating.

3.3.1.3. Injection.

1. Transfer coverslips to individual culture dishes with fresh medium.
2. If you are performing a time course, it is important that you rigorously control the amount of time spent injecting cells on each coverslip. We generally limit injection times to 5 min per coverslip and then transfer the cells back to the incubator. Use multiple coverslips to increase the number of injected cells at each time point.

3.3.1.4. Example: effect of microinjected anti-syntaxin 3 IgG on protein delivery to the apical membrane. A reporter protein was expressed in polarized MDCK cells in order to monitor apical trafficking. We used the GFP-tagged apical membrane protein p75-neurotrophin receptor (p75-GFP) which was expressed by nuclear microinjection of the cDNA. Subsequently, either anti-syntaxin 3 IgG or nonspecific IgG was introduced by cytoplasmic microinjection. A simplification is to co-inject both the cDNA and the antibody at the same time, which is possible because nuclear injections always lead to a significant cytoplasmic delivery.

One hour after microinjection, the cells were incubated at 20 °C to accumulate newly synthesized p75-GFP in the Golgi apparatus (see Kreitzer et al. [26] for a more complete description of protein expression using microinjection). Once p75-GFP had accumulated in the Golgi, cells were shifted to 37 °C to permit exit from the Golgi, and were fixed at 30-min intervals. This assay relies on the ability to differentiate between intracellular and surface-associated membrane proteins. Thus, cells were briefly fixed in paraformaldehyde (2 min at room temperature) without subsequent permeabilization so that p75-GFP at the cell surface could be selectively immunolabeled. The appearance of p75-GFP at the apical surface was determined by immunostaining with an anti-p75 ectodomain antibody after fixation. The effects of microinjected antibodies on delivery of p75 to the apical membrane were then determined by measuring the ratio, over time, of surface:total p75-GFP fluorescence (immunostained p75:direct GFP fluorescence) in the presence of control or syntaxin 3 antibodies [28].

Acknowledgments

Work in T.W.'s laboratory was supported by NIH-DK62338, a Jerry and Martha Jarrett Grant for Research on Polycystic Kidney Disease, a grant from the Department of Defense Prostate Cancer Research Program (DAMD17-02-1-0039), and a Beginning Grant-in-Aid from the American Heart Association. S.H.L. was supported by a Scientist Development Grant from the American Heart Association. G.K. was supported in part by NIH EX06886.

References

[1] Y.A. Chen, R.H. Scheller, Nat. Rev. Mol. Cell. Biol. 2 (2001) 98–106.
[2] R. Jahn, T.C. Sudhof, Annu. Rev. Biochem. 68 (1999) 863–911.
[3] T. Weimbs, S.H. Low, S.J. Chapin, K.E. Mostov, P. Bucher, K. Hofmann, Proc. Natl. Acad. Sci. USA 94 (1997) 3046–3051.
[4] T. Weimbs, K.E. Mostov, S.H. Low, K. Hofmann, Trends Cell Biol. 8 (1998) 260–262.
[5] J.A. McNew, F. Parlati, R. Fukuda, R.J. Johnston, K. Paz, F. Paumet, T.H. Sollner, J.E. Rothman, Nature 407 (2000) 153–159.
[6] S.J. Scales,, Y.A. Chen, B.Y. Yoo, S.M. Patel, Y.C. Doung, R.H. Scheller, Neuron 26 (2000) 457–464.
[7] H.Y. Gaisano, M. Ghai, P.N. Malkus, L. Sheu, A. Bouquillon, M.K. Bennett, W.S. Trimble, Mol. Biol. Cell 7 (1996) 2019–2027.
[8] X. Li, S.H. Low, M. Miura, T. Weimbs, Am. J. Physiol. Renal Physiol. 283 (2002) F1111–F1122.
[9] S.H. Low, S.J. Chapin, T. Weimbs, L.G. Kömüves, M.K. Bennett, K.E. Mostov, Mol. Biol. Cell 7 (1996) 2007–2018.
[10] S.H. Low, S.J. Chapin, C. Wimmer, S.W. Whiteheart, L.K. Kömüves, K.E. Mostov, T. Weimbs, J. Cell Biol. 141 (1998) 1503–1513.
[11] S.H. Low, L.Y. Marmorstein, M. Miura, X. Li, N. Kudo, A.D. Marmorstein, T. Weimbs, J. Cell Sci. 115 (2002) 4545–4553.
[12] S.H. Low, M. Miura, P.A. Roche, A.C. Valdez, K.E. Mostov, T. Weimbs, Mol. Biol. Cell 11 (2000) 3045–3060.
[13] F. Lafont, P. Verkade, T. Galli, C. Wimmer, D. Louvard, K. Simons, Proc. Natl. Acad. Sci. USA 96 (1999) 3734–3738.
[14] G. Schiavo, M. Matteoli, C. Montecucco, Physiol. Rev. 80 (2000) 717–766.
[15] C. Dascher, W.E. Balch, J. Biol. Chem. 271 (1996) 15866–15869.
[16] F. Paumet, J. Le Mao, S. Martin, T. Galli, B. David, U. Blank, M. Roa, J. Immunol. 164 (2000) 5850–5857.
[17] B. Yang, L. Gonzalez Jr., R. Prekeris, M. Steegmaier, R.J. Advani, R.H. Scheller, J. Biol. Chem. 274 (1999) 5649–5653.
[18] A.L. Olson, J.B. Knight, J.E. Pessin, Mol. Cell. Biol 17 (1997) 2425–2435.
[19] S. Bhakdi, H. Bayley, A. Valeva, I. Walev, B. Walker, M. Kehoe, M. Palmer, Arch. Microbiol. 165 (1996) 73–79.
[20] D. Gravotta, M. Adesnik, D.D. Sabatini, J. Cell Biol. 111 (1990) 2893–2908.
[21] S.W. Pimplikar, E. Ikonen, K. Simons, J. Cell Biol. 125 (1994) 1025–1035.
[22] G. Apodaca, M.H. Cardone, S.W. Whiteheart, B.R. DasGupta, K.E. Mostov, EMBO J. 15 (1996) 1471–1481.
[23] O. Garred, S.K. Rodal, B. van Deurs, K. Sandvig, Traffic 2 (2001) 26–36.
[24] K.K. Grindstaff, C. Yeaman, N. Anandasabapathy, S.C. Hsu, E. Rodriguez-Boulan, R.H. Scheller, W.J. Nelson, Cell 93 (1998) 731–740.
[25] S.M. Leung, D. Chen, B.R. DasGupta, S.W. Whiteheart, G. Apodaca, J. Biol. Chem. 273 (1998) 17732–17741.
[26] G. Kreitzer, A. Marmorstein, P. Okamoto, R. Vallee, E. Rodriguez-Boulan, Nat. Cell Biol. 2 (2000) 125–127.
[27] S.H. Low, X. Li, M. Miura, N. Kudo, B. Quinones, T. Weimbs, Dev. Cell, in press.
[28] G. Kreitzer, J. Schmoranzer, S.H. Low, X. Li, Y. Gan, T. Weimbs, S.M. Simon, E. Rodriguez-Boulan, Nat. Cell Biol. 5 (2003) 126–136.